

# Mechanisms of the gas-phase decomposition of C-nitro compounds inferred from quantum chemical calculations †

G M Khrapkovskii, A G Shamov, E V Nikolaeva, D V Chachkov

## Contents

I. Introduction	903
II. The mechanism of the thermal decomposition of nitroalkanes	904
III. The mechanism of the thermal decomposition of nitroalkenes	915
IV. Mechanisms of the gas-phase monomolecular decomposition of nitrobenzene and its derivatives	933
V. Conclusion	941

**Abstract.** Data on the mechanisms of the gas-phase monomolecular decomposition of nitroalkanes, nitroalkenes and nitroarenes obtained with the use of state-of-the-art quantum chemical methods are systematically surveyed. Considerable attention is focused on the discussion of the multistep decompositions of nitro compounds into elementary experimentally observed products. Peculiarities of the competition of various mechanisms and the influence of the molecular structure on the changes in the Arrhenius parameters of the primary reaction step are addressed. The bibliography includes 125 references.

## I. Introduction

Studies of the kinetics and reaction mechanisms of thermal decomposition is an important branch of research in chemistry of nitro compounds.<sup>1–3</sup> The results of investigations of the gas-phase decomposition of nitro compounds serve as a major source of data on bond dissociation energies ( $D$ ) in organic molecules and the enthalpies of formation of organic radicals. At present, detailed data on kinetic patterns for thermal decomposition of various classes of nitro compounds is available.<sup>2–5</sup> Thermal decompositions of nitroalkanes, nitroalkenes and nitroarenes are investigated in most details. More than a hundred of their reactions, just in the gas phase, have been studied. Arrhenius parameters of the initial steps of the decomposition have been determined and mechanisms accounting for the experimentally

observed products have been suggested.<sup>3,5–8</sup> At the same time, the discussion of the results of experimental studies on thermodestruction kinetics in the framework of one or another mechanism of the primary step faces considerable difficulties,<sup>2,3</sup> the main problem being the contribution of several parallel processes to the experimentally measured rate constant. If the rate constants of elementary reactions are similar, correct interpretation of the experiment outcomes is significantly complicated.

In view of the aforesaid, the importance of independent assessment of the rate constants of elementary steps of the chemical reactions involved in the thermal decomposition of nitro compounds is beyond any doubt. Such estimates can be obtained with the use of state-of-the-art quantum chemical methods, which have widely been employed in recent years for studying the thermal decomposition reactions of nitro compounds. The results inferred allowed a substantial increase in the number of mechanisms that can be considered and, in some cases, permitted more accurate interpretations of the experimental observations. Of particular interest is the use of quantum chemical calculations for examining the key problem of the thermal stability of nitro compounds, *viz.*, the influence of the molecular structures on the changes in the activation energy ( $E_a$ ) and the pre-exponential factor ( $A$ ) corresponding to the primary step of thermal decomposition and on the competition of different mechanisms in a series of compounds. Quantum chemical studies on the molecular structures and mechanisms of the thermal decomposition of C-, N- and O-nitro compounds are extremely abundant, which results from a great scientific and practical interest in this kind of investigations. In addition, the molecules of nitro compounds are convenient subjects for theoretical examination: due to the small sizes of these molecules, diverse quantum chemical calculations, including most powerful *ab initio* methods, can be applied.<sup>9,10</sup>

The present review discusses the results of quantum chemical studies on the mechanisms of the gas-phase

G M Khrapkovskii, A G Shamov, E V Nikolaeva, D V Chachkov Kazan State Technological University, ul. K Marksa 72, 420015 Kazan, Russian Federation. Fax (7-843) 236 76 02  
Kazan Scientific Centre of the Russian Academy of Sciences, ul. Lobachevskogo 2, 420111 Kazan, Russian Federation.  
Fax (7-843) 231 90 06, tel. (7-843) 231 41 52,  
e-mail: khrapkovskii@kstu.ru (G M Khrapkovskii),  
shamov@kstu.ru (A G Shamov), katrin@kstu.ru (E V Nikolaeva),  
e-mail: chachkov@kstu.ru (D V Chachkov)

Received 23 March 2009

*Uspekhi Khimii* 78 (10) 980–1021 (2009); translated by A F Nasonov

† The review is dedicated to the 100th birthday of Corresponding Member of the USSR Academy of Sciences S S Novikov.

decomposition of nitroalkanes, nitroalkenes and nitroar- enes. Theoretical studies on the molecular structures and vibrational spectra of *C*-nitro compounds are also cited, however, only if necessary, in connection with the use of these data for the evaluation of activation enthalpies and entropies of the reactions. Theoretical works devoted to reaction mechanisms of thermal decomposition in condensed media are not covered, since these problems require special and in-depth examination. Papers published in recent 10–15 years are primarily analyzed; among earlier publications, only a few fundamental theoretical investigations are mentioned, and the necessary references to experimental data used are provided. Theoretical studies on the mechanisms of the thermodecomposition of *C*-nitro compounds published before 1995 (mainly, using semi-empirical methods) have been reviewed.<sup>11, 12</sup>

## II. The mechanism of the thermal decomposition of nitroalkanes

The kinetics of the gas-phase decomposition of nitroalkanes was studied in most details: more than 80 reactions were explored and the corresponding Arrhenius parameters for the primary reaction step were determined.<sup>3</sup> The accuracy of the determination of the activation energy is very high, the error does not exceed 4–8 kJ mol<sup>−1</sup> (Ref. 3). The experimental findings are categorized by two basic mechanisms of the primary reaction step, *viz.*, a radical mechanism with a homolytic cleavage of the C–NO<sub>2</sub> bond and a molecular mechanism with elimination of HNO<sub>2</sub>. Nitromethane, *gem*-dinitro- and 1,1,1-trinitroalkanes, their halogenated derivatives as well as some  $\alpha,\alpha$ -dihalomononitroalkanes in the gaseous state dissociate according to the radical mechanism. The molecular mechanism is typical of the gas-phase decomposition of the majority of mononitroalkanes and some their halogenated derivatives at relatively low temperatures (600–750 K).<sup>1, 3</sup>

### 1. The gas-phase decomposition of nitroalkanes by the radical mechanism

The most critical problem of the mechanism of the gas-phase decomposition of nitroalkanes that has not been solved in full measure until now, pertains to the absence of data on the structures of transition states (TS) of the reactions. Data on the values of the rate constants for the recombination reactions of radicals formed upon homolytic dissociation of a C–NO<sub>2</sub> bond, which were obtained<sup>3, 13</sup> for several simplest nitroalkanes, make it possible to classify the TS of this radical reaction as semi-rigid. However, attempts to reliably determine the value of the critical distance of the C–NO<sub>2</sub> bond that corresponds to the TS were not crowned with success. The published data on localization of the TS of the radical gas-phase decomposition obtained by various quantum chemical methods, mostly semi-empirical, are not confirmed by *ab initio* calculations.<sup>9, 10</sup> A decade ago it was demonstrated for the first time that there is no maximum on the reaction pathway for the cleavage of the C–N bond in nitromethane and the enthalpy (energy) of activation coincides with the enthalpy of the reaction.<sup>14</sup> It was thus inferred that the barrier to the radical recombination is absent (*i.e.*, equal to zero). The calculations were carried out using a variety of *ab initio* methods including the Density Functional Theory (DFT) approach.

The values of  $D(\text{C}–\text{N})$  and the activation energy of the reaction consistent with the experiment were calculated by the hybrid density functional B3LYP with different basis sets including 6-31G(d), which allows for polarization functions only on heavy atoms. It was established that the radicals pre-spaced 400–500 pm apart should be moved closer to one another to the distance corresponding to the formation of a molecule in order to achieve a correct asymptotic behaviour of the process. An essential peculiarity of the employed technique is a preliminary mixing of the highest occupied and lowest unoccupied orbitals. Figure 1 shows curves obtained for the reactions of radical decomposition of nitromethane and nitroethane.<sup>14, 15</sup>

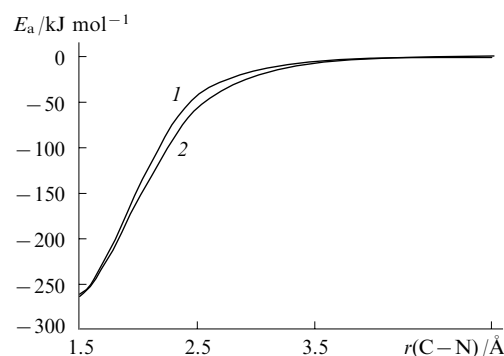


**Figure 1.** The change in the activation energy upon contraction of the C–N bond in nitromethane (1) and nitroethane (2) [B3LYP/6-31G(d)].<sup>14, 15</sup>

Subsequently, analogous data were obtained for some other nitro compounds as well as for the homolytic dissociation reactions of C–C and C–H bonds in hydrocarbons.<sup>16</sup> It should be noted that state-of-the-art quantum chemical calculations prove that some radical decomposition reactions of organic compounds have barriers to radical recombination.<sup>17</sup>

The absence of a barrier to recombination in radical decomposition reactions of nitro compounds theoretically substantiates the comparison of kinetic estimates of  $D(\text{C}–\text{N})$  obtained by using Eqn (1) with the quantum chemical and thermochemical assessments according to Eqn (2):

$$D(\text{C}–\text{N}) = E_a - RT, \quad (1)$$

where  $E_a$  is an experimental value of the activation energy of a radical gas-phase decomposition with a homolytic cleavage of the C–NO<sub>2</sub> bond,  $T$  is an average temperature in the range in which the experiment was carried out,  $R$  is the universal gas constant;

$$D(\text{C}–\text{N}) = \Delta H_{\text{R}}^\circ + \Delta H_{\text{NO}_2^\bullet}^\circ - \Delta H_{\text{R–NO}_2}^\circ, \quad (2)$$

where  $\Delta H_{\text{R}}^\circ$ ,  $\Delta H_{\text{NO}_2^\bullet}^\circ$ ,  $\Delta H_{\text{R–NO}_2}^\circ$  are the enthalpies of formation of the products and the starting compound in reaction (3), respectively:



If there is a barrier to radical recombination, the enthalpy (energy) of activation differs from the enthalpy of

the reaction by the magnitude of the corresponding barrier. The absence of a barrier to recombination considerably simplifies the theoretical estimation of the activation enthalpy (energy) of the reaction based on Eqns (1) and (2), albeit significantly complicates the calculation of the activation entropy and pre-exponential factor of the radical dissociation.

According to the canonical variational transition state theory (CVTST),<sup>18</sup> if the barrier is absent from a section on the potential energy surface (PES) along the reaction coordinate, a point on the PES section along the reaction coordinate where the maximum activation energy is achieved, is accepted as the TS. This approach was employed<sup>10</sup> for the radical decomposition of trinitromethane.

Experimental studies of a large number of the radical decomposition reactions of alkanes revealed basic regularities of the influence of the molecular structure on the activation energy of a reaction, which were discussed in most details in a review.<sup>3</sup> In particular, it was noted that the value of  $D(\text{C}-\text{N})$  is affected by the inductive, steric and resonance effects of substituents. A decrease in the activation energy occurs in most cases upon the introduction of bulky electronegative substituents ( $\text{NO}_2$ , Cl, Br, I). Alkyl groups and fluorine atoms virtually have no effect on the strength of the  $\text{C}-\text{NO}_2$  bond. Another peculiarity of the gas-phase radical decomposition of nitroalkanes is that the values of  $D(\text{C}-\text{N})$  for *gem*-dinitro, 1,1,1-trinitro and halonitro derivatives of methane, propane and *n*-butane are close. For the corresponding mononitroalkanes, the values of  $D(\text{C}-\text{N})$  are somewhat different, which can be associated with errors in their experimental determination, since the reactions of mononitroalkanes are complicated by the competitive elimination of  $\text{HNO}_2$ .

Studies on the basic regularities of changes in the length of the  $\text{C}-\text{N}$  bond [ $r(\text{C}-\text{N})$ ] by quantum chemical methods (experimental observations on the geometries of free molecules are available only for a comparatively small number of nitroalkanes<sup>19</sup>) demonstrated that a decrease in the strength of the  $\text{C}-\text{N}$  bond in the majority of cases is accompanied by its elongation.<sup>11, 15, 19</sup> It was established by semi-empirical quantum mechanical methods that for many nitroalkanes the following relationship linking the activation energy of thermal decomposition and the change in the length of the  $\text{C}-\text{N}$  bond [ $\Delta r(\text{C}-\text{N})$ ] relative to the first representative of a series (nitromethane, nitroethane, 1-nitropropane, 1-nitrobutane) holds true:

$$\log E_a = 2.34 - 0.0158 \Delta r(\text{C}-\text{N}), \quad (4)$$

where  $E_a$  is measured in  $\text{kJ mol}^{-1}$ ,  $r$  is in pm (the correlation coefficient is 0.967).

An analogous linear dependence interconnects the activation energy and the change in the ionization potential ( $\Delta I$ ) of molecules compared with the first representative of the series:<sup>11</sup>

$$\log E_a = 2.36 - 0.175 \Delta I \quad (5)$$

(the correlation coefficient is 0.955).

As has already been stated, the most significant change in the activation energy of gas-phase radical decomposition and the value of  $D(\text{C}-\text{N})$  occurs upon the substitution of bulky halogen atoms (Cl, Br, I) and the  $\text{NO}_2$  group for hydrogen atoms in nitroalkanes. In this case, the calculation

forecasts a considerable increase in  $\Delta r(\text{C}-\text{N})$ . The influence of steric strain on the length and strength of the  $\text{C}-\text{N}$  bond can most evidently be observed by the example of the conformers of polynitroalkanes and halopolynitroalkanes that differ in energy.<sup>19</sup> For quantitative evaluation of this effect,<sup>11, 20</sup> the steric strain factor  $\alpha$  was used:

$$\alpha = \frac{E_s}{\Delta H_{\text{at}}^{\circ}}, \quad (6)$$

where  $E_s$  is the strain energy (the total energy of the interactions of non-bonded atoms);  $\Delta H_{\text{at}}^{\circ}$  is the enthalpy of atomization of a nitro compound. Both values are easily computed by molecular mechanics methods. For methane, propane and butane nitro and halo derivatives, an increase in the factor  $\alpha$  is accompanied in most instances by a decrease in the activation energy of radical gas-phase decomposition, and the value of  $E_a$  can be determined by the equation

$$\log E_a = 2.380 - 0.065 \Delta \alpha \quad (7)$$

(the correlation coefficient is 0.962).

The root-mean-square deviation of the calculated and experimental values of  $E_a$  derived from Eqn (7) does not exceed  $6 \text{ kJ mol}^{-1}$ .

The dependences considered above hold certain interest for studying the influence of various structural factors on the change in the  $D(\text{C}-\text{N})$  value and activation energy of gas-phase decomposition in the nitroalkane series. In a number of cases, they allow the assessment of the reliability of experimental data obtained by different authors.<sup>11</sup> However, their potential should not be overestimated. The exploration of nitroalkanes by using state-of-the-art *ab initio* methods enables substantial revisions of the above-mentioned correlations.<sup>9, 15</sup>

Confirming a link between changes in the values of  $D(\text{C}-\text{N})$  and  $r(\text{C}-\text{N})$  in the nitroalkane series (with the exception of fluoronitroalkanes<sup>15</sup>) on the whole, the *ab initio* and DFT methods suggest that semi-empirical methods overestimate the repulsion of non-bonded atoms with the accumulation of bulky substituents in a molecule. It should also be noted that in some cases the use of semi-empirical methods can lead to erroneous conclusions. Thus it was pointed out<sup>11</sup> that the correlation

$$\log E_a = 2.360 - 0.0277 \Delta r(\text{C}-\text{H}) \quad (8)$$

was observed for polynitroalkanes according to MINDO/3 (the correlation coefficient was 0.984). Later, an investigation by state-of-the-art *ab initio* and DFT methods showed that this dependence had been an artefact. Actually, the increase in the number of nitro groups in molecules results in a reduction rather than an increase in  $r(\text{C}-\text{H})$ .<sup>15</sup>

Geometric parameters of free molecules of nitroalkanes calculated by modern quantum chemistry methods are in good agreement with experimental data. In regard to the importance of these data to discussing the influence of molecular structures on the changes in  $D(\text{C}-\text{N})$  and the Arrhenius parameters of the radical decomposition reactions of nitroalkanes ( $E_a$  and  $\log A$ ) in a series of compounds, we will dwell on this problem. Numerous results demonstrate the reliability of the assessment of the geometric parameters of free molecules of nitro compounds.

**Table 1.** The structure of a nitromethane molecule (bond lengths are in pm, angles are in degrees).<sup>19</sup>

Parameter	Calculation by B3LYP with various basis sets							Experiment
	6-31G(d)	6-311G(d,p)	cc-pvtz	6-311++G(d,p)	6-311++G(3df,3pd)	6-311++G(df,p)	6-311++G(2dp)	
C–H <sup>1</sup>	109.1	109.0	108.8	109.0	108.7	109.0	108.9	108.9
C–H <sup>2</sup>	108.8	108.6	108.4	108.6	108.4	108.6	108.5	108.9
C–H <sup>3</sup>	109.1	108.6	108.4	108.6	108.4	108.6	108.5	108.9
C–N	150.0	150.3	149.9	150.3	149.8	150.1	149.8	148.9
N–O <sup>1</sup>	122.6	122.0	121.8	122.1	121.8	122.0	122.1	122.4
N–O <sup>2</sup>	122.7	122.0	121.8	122.1	121.8	122.0	122.1	122.4
C–N–O <sup>1</sup>	117.7	117.0	117.1	117.2	117.1	117.2	117.2	117.4
O <sup>1</sup> –N–O <sup>2</sup>	126.0	126.0	125.8	117.2	125.7	125.6	125.7	125.3
H <sup>1</sup> –C–N	108.4	106.7	106.7	106.5	106.5	106.6	106.5	107.5
H <sup>2</sup> –C–N	107.2	108.0	108.1	108.0	108.1	108.1	108.1	107.5
H <sup>3</sup> –C–N	107.1	108.0	108.1	108.0	108.1	108.1	108.1	107.5
H <sup>1</sup> –C–H <sup>2</sup>	112.2	112.9	112.9	113.0	113.0	112.9	113.0	107.5
H <sup>1</sup> –C–H <sup>3</sup>	112.0	110.6	110.4	110.5	110.4	110.5	110.4	107.5
H <sup>2</sup> –C–H <sup>3</sup>	109.7	110.5	110.4	110.5	110.4	110.5	110.4	107.5

**Note.** In the equilibrium conformation of the molecule, one of the CHN planes is perpendicular to the CNO<sub>2</sub> plane.

The corresponding data for nitromethane listed in Table 1 can be quoted.<sup>19</sup>

The presented results show that all the basis sets within the framework of the hybrid DFT B3LYP level of theory provide consistent estimates of geometric parameters that are in good agreement with the experiment. For bond lengths, the variation of calculated estimates does not exceed several tenth of a picometer, and for angles they are  $<1^\circ$ , *i.e.*, the observed differences are at the level of experimental determination errors. For other nitroalkanes, the situation is similar. Hence, the results of calculation, if necessary, can complement, and in a number of cases (for instance, for nitroethane<sup>20</sup>), even refine experimental data.

Modern quantum chemical methods permit reliable estimates of the enthalpies of formation of nitroalkanes and the energy of dissociation of the C–N bond.<sup>15, 21, 22</sup> The best results in calculation of the dissociation energies in the mononitroalkane series are obtained with the methods G2 and G3 as well as B3LYP in various basis sets.<sup>9, 22</sup> These methods afford important additional data for examining basic regularities of the influence of molecular structures on the value of  $D(\text{C–N})$  and activation energy of the radical decomposition of nitroalkanes.

For polynitroalkanes bearing several nitro groups at the same carbon atom, the estimates of the dissociation energies obtained by DFT methods are significantly inferior. They are systematically underestimated, the more nitro groups are at a carbon atom the more they are underestimated. For example, for trinitromethane the difference between the experimental (kinetic) and calculated [at the B3LYP/6-31G(d) and B3LYP/6-311++G(df,p) levels] values of  $D(\text{C–N})$  is more than 20 kJ mol<sup>–1</sup>, for tetranitromethane this difference is elevated to 27–28 kJ mol<sup>–1</sup>. Only the G2, G3 and QCISD methods give satisfactory estimates of  $D(\text{C–N})$  in the series nitro-, dinitro-, trinitro- and tetranitromethane.<sup>9</sup> Hence, for studying the radical decompositions of polynitroalkanes the use of high-level methods (for instance, QCISD with various basis function sets) as well as composite methods (G3B3, CBS-QB3) is expedient. For the isomers that contain the same number of nitro groups, the energy difference is predicted with a good accuracy not only by the composite methods G2 and G3, but also by various

DFT methods, which allows the latter to be employed for studying the competition of different mechanisms of thermodestruction.<sup>9, 19, 21</sup>

Theoretical studies showed that significant changes in the major geometric parameters of the C–NO<sub>2</sub> groups, including  $r(\text{C–N})$ , in the mononitroalkane series are observed (Table 2).<sup>15, 22, 23</sup> In nitromethane, according to the calculations, the bond length  $r(\text{C–N})$  is 1.2 pm shorter than in nitroethane. At the same time, the corresponding values for nitroethane, 1-nitropropane, 1-nitrobutane, 1-nitropentane virtually coincide.

By the example of nitrobutanes and nitropropanes, the influence of isomerism on the geometry of the C–NO<sub>2</sub> group can be traced. The lengths of the C–N bonds in 2-nitrobutane and 2-nitropropane, which are the same according to the calculations, substantially exceed those for the compounds with primary nitro groups. For 2-methyl-2-nitropropane, the calculation predicts the longest  $r(\text{C–N})$ , whereas for 2-methyl-1-nitropropane it is the smallest of all the isomers.<sup>15</sup> For mononitroalkanes, elongation of the C–N bond is accompanied by a reduction in its dissociation energy, and in those cases where the bond lengths coincide, the bonds are also similar in their strengths. It should be noted that for the *gem*-dinitroalkanes and 1,1,1-trinitroalkanes studied (dinitromethane, fluorodinitromethane, difluorodinitromethane, 1,1-dinitroethane, 1,1-dinitropropane, 1,1-dinitrobutane, trinitromethane, fluorotrinitromethane, 1,1,1-trinitroethane, 1,1,1-trinitropropane, 1,1,1-trinitrobutane) the value of  $\Delta r(\text{C–N})$  virtually does not change;<sup>11, 15</sup> this fact can be juxtaposed with the constancy of the activation energies of the gas-phase decomposition of these compounds.

Essential additional material for the analysis of the influence of chemical structure on changes in the geometric parameters and enthalpies of formation of molecules and the values of  $D(\text{C–N})$  is provided by the investigations of halonitromethanes and halonitroethanes (see Table 2).<sup>15, 22, 23</sup> Replacement of hydrogens by fluorine atoms in the nitromethane molecule results in elongation of the C–N bond and affects relatively little the value of  $D(\text{C–N})$ . Thus the introduction of the first and the third F atoms (*i.e.*, the transition from nitromethane to fluoronitro-

**Table 2.** The length of the C–N bond and dissociation energy  $D(\text{C}–\text{N})$  upon homolytic cleavage of the C–N bond calculated at the B3LYP/6-31G(d) level.<sup>15, 22, 23</sup>

Compound	$r(\text{C}–\text{N})/\text{pm}$	$D(\text{C}–\text{N})/\text{kJ mol}^{-1}$	Compound	$r(\text{C}–\text{N})/\text{pm}$	$D(\text{C}–\text{N})/\text{kJ mol}^{-1}$
$\text{CH}_3\text{NO}_2$	149.9	236.1	$\text{CH}_3\text{CHClNO}_2$	153.1	196.7
$\text{CH}_2\text{FNO}_2$	152.1	230.1	$\text{CH}_3\text{CCl}_2\text{NO}_2$	157.4	162.0
$\text{CHF}_2\text{NO}_2$	154.0	218.9	$\text{CH}_2\text{ClCH}_2\text{NO}_2$	151.5	216.3
$\text{CF}_3\text{NO}_2$	155.0	215.5	$\text{CCl}_3\text{CH}_2\text{NO}_2$	151.5	192.0
$\text{CH}_2\text{ClNO}_2$	152.6	200.5	$\text{CCl}_3\text{CCl}_2\text{NO}_2$	161.8	118.0
$\text{CHCl}_2\text{NO}_2$	154.5	166.1	$\text{CH}_3\text{CHBrNO}_2$	152.3	203.8
$\text{CCl}_3\text{NO}_2$	161.3	133.1	$\text{CH}_3\text{CFClNO}_2$	156.3	194.2
$\text{CHFCINO}_2$	154.1	195.8	$\text{CH}_3\text{CH}_2\text{CH}_2\text{NO}_2$	151.1	235.6
$\text{CF}_2\text{ClNO}_2$	156.3	192.5	$\text{CH}_3\text{CHNO}_2\text{CH}_3$	152.4	230.1
$\text{CFCl}_2\text{NO}_2$	158.3	167.0	$\text{CH}_3\text{CH}_2\text{CHFNO}_2$	153.1	229.7
$\text{CH}_2\text{BrNO}_2$	152.4	205.5	$\text{CH}_3\text{CH}_2\text{CHClNO}_2$	153.6	198.8
$\text{CH}_3\text{CH}_2\text{NO}_2$	151.2	236.0	$\text{CH}_3\text{CCl}(\text{NO}_2)\text{CH}_3$	156.2	189.1
$\text{CH}_3\text{CHFNO}_2$	153.3	227.2	$\text{CH}_3\text{CH}_2\text{CHBrNO}_2$	152.9	204.6
$\text{CH}_3\text{CF}_2\text{NO}_2$	155.9	218.8	$\text{CH}_3\text{CBr}(\text{NO}_2)\text{CH}_3$	155.6	194.6
$\text{CH}_2\text{FCH}_2\text{NO}_2$	151.4	230.6	$\text{CH}_3(\text{CH}_2)_3\text{NO}_2$	151.1	236.4
$\text{CHF}_2\text{CH}_2\text{NO}_2$	150.4	226.0	$\text{CH}_3\text{CH}_2\text{CH}(\text{NO}_2)\text{CH}_3$	152.3	231.4
$\text{CF}_3\text{CH}_2\text{NO}_2$	150.7	210.9	$(\text{CH}_3)_2\text{CHCH}_2\text{NO}_2$	150.7	238.1
$\text{CF}_3\text{CF}_2\text{NO}_2$	155.4	198.0	$(\text{CH}_3)_3\text{CNO}_2$	154.9	220.9

methane and from difluoronitromethane to trifluoronitromethane) reduces the value of  $D(\text{C}–\text{N})$  merely by 4 and 6  $\text{kJ mol}^{-1}$ , respectively, while the decrease in the enthalpy of formation of a compound upon introduction of a fluorine atom in the molecule is virtually completely offset by a similar decrease in the enthalpy of formation of fluoromethyl radicals. For the introduction of the second F atom (*i.e.*, in order to move from fluoronitromethane to difluoronitromethane), the calculation forecasts a relatively larger decrease in the value of  $D(\text{C}–\text{N})$  (by 11.2  $\text{kJ mol}^{-1}$ ), which pertains to additional stabilization of the difluoromethyl radical.

Upon replacement of hydrogen atoms by chlorine atoms, a substantial increase in the enthalpies of formation of the compounds is observed, whereas for the radicals these values change insignificantly. As a result, noticeable reduction of the value of  $D(\text{C}–\text{N})$  occurs in the series: nitromethane, chloronitromethane, dichloronitromethane and trichloronitromethane.<sup>21</sup>

In mixed chlorofluoronitromethanes, the dissociation energy of the C–N bond is governed by the presence of chlorine atoms in molecules and radicals. For instance, the value of  $D(\text{C}–\text{N})$  in dichlorofluoronitromethane, according to calculations, is somewhat higher (by 0.8  $\text{kJ mol}^{-1}$ ) than in dichloronitromethane. This is a convincing example of the fact that in the presence of bulky substituents (two chlorine atoms) the influence of a fluorine atom on the value of  $D(\text{C}–\text{N})$  is virtually completely negated.

Qualitatively concordant outcomes were also obtained<sup>22</sup> for fluoronitroethanes. In the presence of chlorine atoms, the influence of substitution of fluorine for hydrogen in nitroethanes is weakly manifested. These findings point to a limited applicability of the statement that fluorine atoms in the  $\alpha$ -position have practically no influence on the value of  $D(\text{C}–\text{N})$  and the energy of activation of radical decomposition, which was inferred from the analysis of experimental data.<sup>3</sup> This is valid for polynitroalkanes, whereas in the case of mononitro compounds it is not satisfied in most cases.

Experimental data<sup>3–5</sup> enable examination of the influence of the molecular structure on the pre-exponential

factor of a reaction of the gas-phase decomposition of nitroalkanes. A detailed analysis allowed one to reveal three major contributors to an increase in the pre-exponential factor in comparison with the ‘normal’ ( $\Delta S = 0$ ,  $A \sim 10^{13} \text{ s}^{-1}$ ) value:

- 1) a decrease in the frequency of bending vibrations associated with the C–N bond;
- 2) release of internal rotation about the C–N bond;
- 3) a decrease in the frequency of the twisting vibrations (down to free rotation) of groups adjacent to the reaction centre (in the nitroalkane series, such groups can be exemplified by alkyl substituents and  $\text{NO}_2$ ).

All the experimental regularities concerning the changes in  $\log A$  in a series of related compounds are explained fairly convincingly with consideration of these factors.<sup>3, 5</sup>

At present, there is a body of calculated low-frequency vibrations and barriers to rotation of functional groups in nitroalkanes,<sup>23, 24</sup> which generally confirm the accuracy of the qualitative analysis of the influence of substituents discussed above. The calculations of the vibration frequencies and barriers to rotation of fragments that model the TS of radical decomposition reaction are also consistent with this analysis.<sup>15</sup> A weak spot of such calculations is the absence of convincing criteria for the determination of the critical distance, geometry and vibration frequencies of a TS. In this connection, of significant interest is the study<sup>10</sup> in which the region of the existence of the TS for the reaction of the gas-phase radical decomposition of trinitromethane was determined at  $r(\text{C}–\text{N}) \approx 280 \text{ pm}$ . The existence of a TS was confirmed by the presence of a maximum on the Gibbs energy curve. In the work cited, the rate constants for a number of the primary and secondary steps of the decomposition of trinitromethane were calculated in a wide temperature range (300–2000 K). The calculated values of the Arrhenius parameters are in good agreement with the available experimental data. The methodological part of this study that pertains to the choice of quantum chemical methods and performance of calculations was executed very thoroughly. Yet certain doubts about the reliability of the method for locating the TS remain. It is known that a maximum obtained on an energy curve upon

scanning any geometric parameter and optimizing the others does not coincide with the transition state of a reaction. For instance, in our calculations<sup>14,15</sup> on scanning the length of the C–N bond in nitromethane from 400 pm to the equilibrium value of  $r(\text{C}–\text{N})$  a minimum and a small barrier in the region of 300 pm were revealed on the energy curve, whereas a descent from the same point along the reaction coordinate showed a monotonic decrease in the energy along the reaction pathway.

There are no arguments that favour the fact that the reported procedure<sup>10,18</sup> should result in the detection of a saddle point on the Gibbs energy surface (GES). The results obtained should be considered as an upper estimate of the GES barrier value.

Other radical decomposition reactions of nitroalkanes have not been studied by CVTST. The problem of the determination of the TS structures of radical decomposition reactions and rigorous theoretical calculation of the Arrhenius parameters of these reactions needs additional investigation.

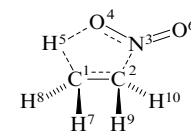
An important and insufficiently studied issue of the mechanism of the radical decomposition of nitroalkanes is also the quantitative theoretical evaluation of the further development of the reaction. For nitromethane, 1,1,1-trinitroethane<sup>3</sup> and a number of other nitroalkanes there are detailed multi-step schemes accounting for all the kinetic peculiarities of the reactions and the products observed at different stages of decomposition. However, these data

should be verified by independent theoretical estimates of the rate constants for the elementary reactions. Without these calculations, the mechanism of the radical gas-phase decomposition of nitroalkanes cannot be regarded as conclusively established.

## 2. The gas-phase elimination of nitrous acid from nitroalkanes

The elimination reaction of  $\text{HNO}_2$  through a planar five-membered transition state is one of the processes of the thermal decomposition of nitro compounds that was studied in most details both theoretically and experimentally. For the first time, the mechanism of this reaction was theoretically explored about 30 years ago at the MINDO/3 level.<sup>25,26</sup> The results obtained allowed a conclusion to be made that is essential for insights into major regularities in the influence of substituents on the enthalpy (energy) of activation of the reaction that the transition state, contrary to conceptions accepted earlier,<sup>3</sup> is non-polar, *i.e.*, the dipole moment of the TS is lower than that of the original molecules (nitroethane, 1-nitropropane and a number of other nitroalkanes containing no halogen atoms). Later this conclusion was justified by *ab initio* and DFT calculations<sup>12,27–29</sup> that permitted attaining good agreement between experimental and calculated values of the activation energy. The theoretical study of the  $\text{HNO}_2$  elimination was carried out especially thoroughly for nitroethane (Table 3).<sup>15</sup> The values of the activation enthalpy of the

**Table 3.** Major geometric parameters of the transition state and the activation enthalpy for the elimination of  $\text{HNO}_2$  from nitroethane according to different quantum chemical methods.<sup>15</sup>



Method	Distances /pm					Angles /deg			$\Delta H_{298}^\ddagger$ /kJ mol <sup>−1</sup>
	C <sup>1</sup> C <sup>2</sup>	C <sup>2</sup> N <sup>3</sup>	N <sup>3</sup> O <sup>4</sup>	O <sup>4</sup> H <sup>5</sup>	C <sup>1</sup> H <sup>5</sup>	C <sup>1</sup> C <sup>2</sup> N <sup>3</sup>	C <sup>2</sup> N <sup>3</sup> O <sup>4</sup>	C <sup>2</sup> C <sup>1</sup> H <sup>5</sup>	
PM3	139.9	159.6	133.6	105.1	157.4	105.6	110.1	90.0	264.0
MINDO3	141.7	173.6	129.0	110.0	157.7	100.1	111.8	94.0	235.6
HF/3-21G	139.5	206.7	131.2	127.5	137.0	97.2	103.9	94.4	196.2
HF/6-31G(d)	139.1	213.1	123.9	127.6	135.4	96.2	102.8	92.6	259.8
HF/6-311 + + G(df,p)	139.0	210.4	122.8	127.1	134.9	97.1	102.8	91.4	243.9
HF/6-311 + + G(3df,3pd)	138.8	209.9	122.8	126.9	135.4	97.4	102.9	91.1	244.8
BLYP/6-31G(d)	139.9	231.0	131.6	127.7	138.7	93.8	99.3	94.5	161.5
BLYP/6-311 + + G(df,p)	139.5	230.7	130.1	130.0	136.1	94.0	99.1	94.4	147.7
B3LYP/3-21G	139.2	217.3	136.6	125.8	140.3	96.2	101.6	94.6	150.2
B3LYP/6-31G(d)	139.0	221.7	128.4	125.6	138.7	95.3	100.7	93.3	190.0
B3LYP/D95(d)	139.9	219.2	128.9	125.1	139.1	95.9	101.0	92.7	188.3
B3LYP/6-31 + G(d,p)	139.3	222.2	127.7	127.7	136.3	95.2	100.6	93.3	177.4
B3LYP/6-311 + + G(df,p)	138.7	220.8	127.0	127.2	136.6	95.7	100.6	92.9	174.9
B3LYP/6-311 + + G(3df,3pd)	138.6	219.9	126.8	127.2	136.7	96.0	100.7	92.6	175.3
B3LYP/D95 + + (3df,3pd)	138.8	219.9	127.0	127.1	136.6	95.9	100.8	92.6	174.9
MP2/6-31G(d)	138.8	211.9	129.1	124.5	139.6	96.5	103.3	93.0	225.5
MP2(fc)/6-31 + G(d,p)	139.1	211.5	128.8	124.9	137.3	96.4	102.9	92.5	213.0
MP2/6-311 + + G(df,p)	138.8	206.0	127.1	120.5	141.3	98.1	103.4	90.6	210.0
MP2(fc)/6-311 + + G(3df,3pd)	138.6	205.9	127.3	121.8	140.5	98.5	103.3	90.3	203.8
MP3(fc)/3-21G	140.4	204.6	134.2	126.9	140.3	98.0	104.8	93.7	192.9
MP3/6-31G(d)	139.1	208.7	126.8	125.7	138.2	97.1	103.8	92.7	235.1
MP4(full)/6-31G(d)	139.5	218.5	130.8	126.4	137.5	94.7	102.3	94.5	214.2
QCISD/6-31G(d)	139.7	218.8	129.2	128.5	135.3	94.7	102.1	94.5	219.2
QCISD(T)/6-31G(d)	140.0	219.0	130.1	128.0	136.4	94.7	102.2	94.6	212.5

reaction that were obtained by a number of *ab initio* and DFT methods are in good agreement with experimental values of the activation energy of the gas-phase decomposition of nitroethane ( $188.3 \text{ kJ mol}^{-1}$ ).<sup>3</sup>

First-principles and semi-empirical methods provide somewhat distinct pictures of the TS structure and reaction mechanism. According to MINDO/3 and PM3, in the TS the C–H bond formed by the hydrogen atom involved in the reaction is elongated most strongly. All the other methods used predict that in the TS it is the length of the almost cleaved C–N bond that changes most strongly. Taking into account that semi-empirical methods considerably overestimate the enthalpy (energy) of a reaction, while *ab initio* and DFT methods provide estimates that on the whole are in good agreement with experimental findings, one can suppose that the predictions of TS structures by the latter methods are more reliable. Since the B3LYP level of theory with various basis sets gives sufficiently accurate results, further study of the influence of substituents was carried out<sup>28,29</sup> using B3LYP/6-31G(d). The most important data obtained are listed in Table 4.

The analysis of major changes in the geometric parameters of the reaction centre in the transition state in comparison with the starting molecules (see Table 2–4) provides an expansion of the changes in the activation enthalpy in the nitroalkane series. Thus for n-nitroalkanes, a decrease in activation enthalpy can be related to the reduction in the value of  $r(\text{C}–\text{H})$  and  $r(\text{N}–\text{O})$  in the TS. For example, these values are smaller for the reactions of 1-nitropropane and 1-nitrobutane than those for nitroethane by 2.8 and 0.4 pm, respectively. Considering the differences in the bond strengths, these changes surpass the relatively stronger elongation of the C–N bonds for the indicated compounds, hence their activation enthalpies are lower than for nitroethane. Interestingly, both the geo-

metric parameters of the starting molecules and the TS and also the barriers to elimination reactions of  $\text{HNO}_2$  for 1-nitropropane, 1-nitrobutane and 1-nitropentane virtually coincide. Let us note that for many nitroalkanes studied the changes in the activation enthalpy and the dissociation energy of the C–N bond occur concordantly (Fig. 2).

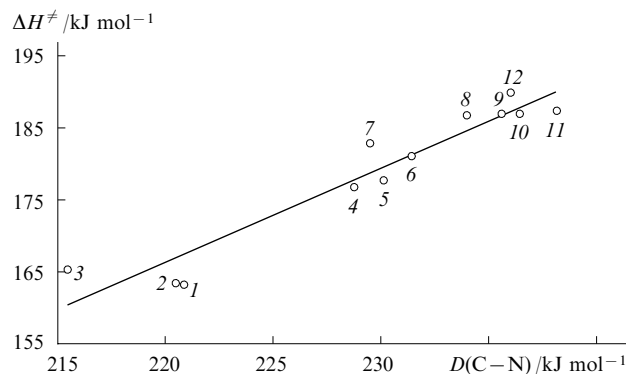


**Figure 2.** Correlation between  $\Delta H^\ddagger$  and  $D(\text{C}–\text{N})$  for nitroalkanes (the correlation coefficient is 0.954).<sup>14,15</sup>

(1)  $(\text{CH}_3)_3\text{CNO}_2$ , (2)  $(\text{CH}_3)_2\text{C}(\text{NO}_2)\text{CH}_2\text{CH}_3$ , (3)  $(\text{CH}_3)_2\text{C}(\text{NO}_2)\text{CH}(\text{CH}_3)_2$ , (4)  $\text{CH}_3\text{CH}(\text{NO}_2)\text{CH}_2\text{C}_3\text{H}_7$ , (5)  $\text{CH}_3\text{CH}(\text{NO}_2)\text{CH}_3$ , (6)  $\text{CH}_3\text{CH}(\text{NO}_2)\text{CH}_2\text{CH}_3$ , (7)  $\text{CH}_2(\text{NO}_2)\text{CH}_2\text{CH}(\text{CH}_3)_2$ , (8)  $\text{C}_5\text{H}_{12}\cdot\text{CH}_2\text{NO}_2$ , (9)  $\text{C}_2\text{H}_5\text{CH}_2\text{NO}_2$ , (10)  $\text{C}_3\text{H}_7\text{CH}_2\text{NO}_2$ , (11)  $\text{CH}_2(\text{NO}_2)\cdot\text{CH}(\text{CH}_3)_2$ , (12)  $\text{CH}_3\text{CH}_2\text{NO}_2$ .

If  $\text{NO}_2$  groups at the secondary or tertiary carbon atoms are involved in the reaction, the decrease in the activation enthalpy occurs monotonically in a series of compounds with an increase in the length of the double bond  $\text{C}=\text{C}$  that is formed in the TS. Clearly, the larger the length of this

**Table 4.** Geometric parameters of the transition state and the activation enthalpies for the elimination of  $\text{HNO}_2$  from some nitroalkanes [by the B3LYP/6-31G(d) method,  $T = 600 \text{ K}$ ] (for atom numbering, see Table 3).<sup>28,29</sup>

Compound	Distances /pm					Angle $\text{C}^1\text{C}^2\text{N}^3$ /deg	$E_a/\text{kJ mol}^{-1}$	
	$\text{C}^1\text{C}^2$	$\text{C}^2\text{N}^3$	$\text{N}^3\text{O}^4$	$\text{O}^4\text{H}^5$	$\text{C}^1\text{H}^5$		calculation <sup>a</sup>	experiment
Nitroethane	139.0	221.7	128.4	125.6	138.7	95.3	195.0	188.5
Nitropropane	139.3	223.5	128.1	128.4	135.9	95.5	192.0	188.1
Nitrobutane	139.3	223.5	128.1	128.4	135.9	95.5	192.1	181.8
Nitropentane	139.3	223.6	128.1	128.6	136.1	95.6	191.9	181.8
Nitrohexane	139.2	223.7	128.2	128.6	136.1	95.6	191.8	181.4
2-Methyl-1-nitropropane	139.6	224.4	128.0	130.5	133.9	95.9	192.4	182.7
3-Methyl-1-nitrobutane	139.3	223.8	128.2	128.5	135.9	95.5	187.9	183.9
2-Nitropropane	139.6	229.4	128.5	128.2	135.8	92.6	182.7	182.3
2-Nitrobutane	139.8	230.9	128.4	130.8	133.4	93.0	186.1	181.4
2-Nitrohexane	139.8	231.4	128.5	130.9	133.5	93.0	181.7	183.1
2-Methyl-2-nitropropane	140.3	236.9	128.7	130.6	133.4	90.3	173.2	177.2
2-Methyl-2-nitrobutane	140.8	238.8	128.6	133.0	131.4	90.6	168.3	179.3
3-Methyl-2-nitrobutane	140.5	231.8	128.2	132.8	131.8	93.5	168.4	173.0
2,3-Dimethyl-2-nitrobutane	141.7	240.0	128.6	134.8	130.1	91.2	181.8	179.3
3,3-Dimethyl-2-nitrobutane	139.7	235.5	128.4	129.7	133.8	91.0	170.4	170.5
1,1-Dinitroethane	138.6	220.0	127.6	125.7	137.8	95.4	181.5	196.5
1,2-Dinitroethane	140.3	197.3	129.1	114.5	153.8	100.4	179.0	192.4
1,1-Dinitropropane	139.1	221.4	127.5	128.6	135.0	95.7	179.1	179.9
1,2-Dinitropropane	140.7	199.6	128.9	116.5	150.1	93.6	177.0	171.5
1,3-Dinitropropane	139.9	209.6	127.9	122.6	143.5	95.0	192.0	—

<sup>a</sup>  $E_a(\text{calculation}) = \Delta H^\ddagger + RT$ .

bond the lower the energy expenditure for the transformation of an single C—C bond to a double bond in the TS. The agreement of the calculated and experimental values of activation energies can be regarded as sufficiently good. The average calculation error for the reactions of mononitroalkanes is  $5.6 \text{ kJ mol}^{-1}$  (Ref. 15). For dinitroalkanes, the accuracy of experimental values of the activation energies of the gas-phase elimination of  $\text{HNO}_2$  calculated<sup>6</sup> from the data for the addition reaction of nitrous acid to alkenes is considerably lower. However, even in this case satisfactory agreement of the calculated and experimental values of activation energy is achieved on the whole.

Of significant interest are theoretical estimates of the barriers to  $\text{HNO}_2$  elimination from 1,1-dinitroethane and 1,1-dinitropropane. In this case, the calculation predicts a small (by 13.5 and  $13.9 \text{ kJ mol}^{-1}$ ) decrease in the reaction activation enthalpy as compared to that of nitroethane and nitropropane, respectively. Although the activation energy of radical recombination and the value of  $D(\text{C—N})$  for these compounds decrease to a greater extent (by  $30\text{--}35 \text{ kJ mol}^{-1}$ ),<sup>3</sup> yet, in experimental studies, one cannot completely exclude a possible contribution of the decomposition by the elimination mechanism to the total rate constant. It should be borne in mind that the experimental study of *gem*-dinitroalkanes was conducted at substantially lower temperatures than those employed for studying mononitro compounds.

Certain progress was also reached in calculating the pre-exponential factor of the reaction. For the first time a theoretical evaluation of the  $A$ -factor of the gas-phase elimination of  $\text{HNO}_2$  for nitroethane, 1-nitropropane, 1-nitrobutane was carried out<sup>30</sup> by the semi-empirical method MINDO/3 allowing for the hindered rotation of functional groups adjacent to the reaction centre, based on the symmetric top model. On the whole, the calculations reproduced adequately both the trend of the  $A$ -factor in the series of these compounds (a decrease in  $\log A$  when moving from nitroethane to 1-nitrobutane), and the absolute values of the pre-exponential factor. At the same time, the calculated estimates of  $\log A$  persistently exceed experimental values by  $0.25\text{--}0.3$ . An analysis of the data obtained demonstrated that the rotational components of the statistical sum do not virtually contribute to the  $\log A$  change, which is connected with negligible alterations of the moments of inertia of molecules during their conversions from the ground state to the TS. The statistical sum of internal rotation in the TS for all the compounds is smaller than that in the ground state differing virtually by the same value. From these findings, a conclusion was made that in the TS a 'freezing' of the internal rotation of the  $\text{NO}_2$  group takes place. The major contributor to the change in the reaction  $A$ -factor is the vibrational component, in all the cases its value in the TS is larger than that in the ground state. It is known<sup>24</sup> that the MINDO/3 method produces large errors when calculating vibration frequencies. However, it was shown<sup>31</sup> that frequency contributions to the vibrational statistical sum reflect correctly the real tendency of the reaction  $A$ -factor in the nitroalkane series.

At present, sufficiently comprehensive calculation data on the vibration frequencies<sup>19,24</sup> and rotation barriers of functional groups<sup>15</sup> in nitroalkane molecules are available that agree well with the available (alas, scanty) experimental data. This allowed a more detailed examination of the influence of molecular structures on the changes in the

pre-exponential factor of the gas-phase elimination of  $\text{HNO}_2$  in the nitroalkane series.

An investigation by the hybrid DFT method B3LYP demonstrated that fairly good results for all the experimentally studied nitroalkanes can be obtained on the basis of a simpler model, *viz.*, completely hindered rotation of functional groups in the starting molecules and the TS.<sup>32</sup> Considering a part of rotations is 'frozen' in the TS, this model should overestimate the  $A$ -factor. The calculations confirm that for most reactions this trend is indeed observed, however, and the agreement of calculated and experimental estimates should be regarded overall as fairly good. The computed values of the  $A$ -factor of the  $\text{HNO}_2$  elimination for compounds with  $\text{NO}_2$  groups at the secondary and tertiary carbons are the exceptions. It was established<sup>31</sup> that for all the experimentally studied nitroalkanes estimates that agree well with the experiment can be obtained by using the most general model, *viz.*, the hindered asymmetric rotation of all the functional groups of the reaction centre. Good agreement of the calculated and experimental values of  $\log A$  is illustrated in Fig. 3.

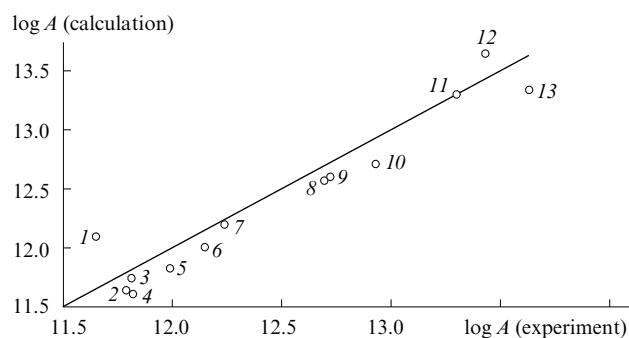


**Figure 3.** Correlation between the calculated (with consideration of asymmetric internal rotation with respect to all bonds adjacent to the reaction centre) and experimental values of  $\log A$  ( $\text{s}^{-1}$ ) for the elimination of  $\text{HNO}_2$  from nitroalkanes ( $T = 600 \text{ K}$ ) (the correlation coefficient is 0.958).<sup>31</sup>

(1)  $\text{CH}_2(\text{NO}_2)\text{CH}(\text{CH}_3)_2$ , (2)  $\text{C}_3\text{H}_7\text{CH}_2\text{NO}_2$ , (3)  $\text{C}_5\text{H}_{12}\text{CH}_2\text{NO}_2$ , (4)  $\text{C}_6\text{H}_9\text{CH}_2\text{NO}_2$ , (5)  $\text{CH}_2(\text{NO}_2)\text{CH}_2\text{CH}(\text{CH}_3)_2$ , (6)  $\text{C}_2\text{H}_5\text{CH}_2\text{NO}_2$ , (7)  $\text{CH}_3\text{CH}_2\text{NO}_2$ , (8)  $\text{CH}_3\text{CH}(\text{NO}_2)\text{CH}_2\text{CH}_3$ , (9)  $\text{CH}_3\text{CH}(\text{NO}_2)\text{CH}_3$ , (10)  $\text{CH}_3\text{CH}(\text{NO}_2)\text{CH}_2\text{C}_3\text{H}_7$ , (11)  $(\text{CH}_3)_2\text{C}(\text{NO}_2)\text{CH}_2\text{CH}_3$ , (12)  $(\text{CH}_3)_2\text{C}(\text{NO}_2)\text{CH}(\text{CH}_3)_2$ , (13)  $(\text{CH}_3)_3\text{CNO}_2$ .

The presented data demonstrate good prospects for the use of state-of-the-art quantum chemical methods for the evaluation of the  $A$ -factor of the gas-phase elimination of  $\text{HNO}_2$ . At the same time, this important and interesting problem requires additional examination.

### 3. Nitro – nitrite rearrangement

The mechanism of the isomerization of the nitro group to the nitrite group in nitro compounds (the nitro – nitrite rearrangement, NNR) is one of the most exciting and controversial mechanisms of thermal decomposition.<sup>32</sup> In the first studies that sum up the research of the thermal destruction of nitro compounds, NNR followed by decomposition of produced nitrites according to various radical and non-radical mechanisms was considered as one of possible alternative processes of the primary step along with the homolytic cleavage of the C—N bond and  $\beta$ -elimination of nitrous acid.<sup>1</sup> The exploration of NNR was



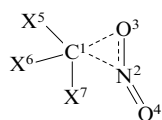
resumed owing to the emergence of results from the experimental investigation of the gas-phase decomposition of nitroalkanes by mass spectrometry and infrared multiphoton dissociation (IRMPD).<sup>33</sup> Of major significance was the quantum chemical study of the TS structure and the NNR mechanism in nitromethane, however the value of the activation enthalpy of the reaction obtained by Dewar *et al.*<sup>34</sup> [199 kJ mol<sup>-1</sup>, which is substantially lower than  $D(\text{C}-\text{N})$  in nitromethane] was soon rebutted by an *ab initio* study of this reaction at the MP2/6-31G(d) level.<sup>35</sup> According to the *ab initio* calculation, the activation enthalpy was more than 100 kJ mol<sup>-1</sup> higher than the estimate reported earlier.<sup>34</sup> Subsequently this reaction was examined by various *ab initio* and DFT methods.<sup>36–43</sup> The major theoretical studies of NNR were analyzed<sup>41</sup> and it was noted that reliable estimates of the reaction activation enthalpy lie in the range 272–277.5 kJ mol<sup>-1</sup> obtained by the B3LYP/6-31G(d) and B3LYP/6-311++(df,p) methods, respectively. The value of 284.7 kJ mol<sup>-1</sup> calculated at the QSCID/6-31G(d) level is recommended as the upper boundary of the

reaction energy barrier. Note that all these values significantly exceed the dissociation energy of the C–N bond in nitromethane; accordingly, the probability of an experimental discovery of NNR is excluded, since its pre-exponential factor ( $\log A \approx 13.0$ ) is substantially lower than that for the radical decomposition in the gaseous state ( $\log A = 14.3$ ). This conclusion is consistent with the one from other theoretical investigations of NNR.<sup>30, 42, 43</sup>

Extensive data on the influence of substituents on the geometric parameters of the transition state and reaction activation enthalpy have been obtained;<sup>32, 41</sup> most essential results are given in Table 5.

According to B3LYP/6-31G(d), the activation enthalpy of NNR for fluoronitromethane is lower than  $D(\text{C}-\text{N})$  for this compound (by 17 kJ mol<sup>-1</sup>), although the pre-exponential factor of NNR ( $\sim 13.0$ ) is substantially lower than that of the radical decomposition of fluoronitromethane. Thus, an entirely new possibility of the competition of these mechanisms opens up. With a decrease in temperature, the process with a lower enthalpy of activation must proceed at

**Table 5.** Geometric parameters of the transition state and starting compound (in parentheses) and the activation enthalpies of the nitro–nitrite rearrangement of nitroalkanes obtained by the B3LYP/6-31G(d) method.



Compound	Distances /pm				Angles /deg			$\Delta H_{298}^\ddagger$ /kJ mol <sup>-1</sup>
	C1N2	N2O3	C1O3	N2O4	O3C1N2	C1N2O3	O3N2O4	
CH <sub>3</sub> NO <sub>2</sub>	194.8	129.8	200.7	120.5	38.3	73.3	118.7	279.1
X <sup>5</sup> = X <sup>6</sup> = X <sup>7</sup> = H	(149.9)	(122.6)	(233.7)	(122.8)	(27.7)	(117.7)	(125.9)	
CH <sub>2</sub> FNO <sub>2</sub>	197.8	129.6	197.9	120.4	38.2	70.9	118.8	210.9
X <sup>5</sup> = X <sup>6</sup> = H, X <sup>7</sup> = F	(152.1)	(121.7)	(235.7)	(122.7)	(27.0)	(118.4)	(127.7)	
CHF <sub>2</sub> NO <sub>2</sub>	196.7	129.2	199.4	120.3	38.1	72.1	119.4	233.9
X <sup>5</sup> = H, X <sup>6</sup> = X <sup>7</sup> = F	(154.0)	(121.8)	(237.0)	(122.4)	(27.0)	(118.0)	(128.2)	
CF <sub>3</sub> NO <sub>2</sub>	192.2	129.3	196.0	119.8	38.9	72.1	119.9	246.4
X <sup>5</sup> = X <sup>6</sup> = X <sup>7</sup> = F	(155.0)	(121.8)	(236.7)	(122.0)	(27.3)	(117.0)	(128.7)	
CH <sub>2</sub> ClNO <sub>2</sub>	195.2	128.3	206.3	120.4	37.1	76.1	119.5	264.9
X <sup>5</sup> = Cl, X <sup>6</sup> = X <sup>7</sup> = H	—	—	—	—	—	—	—	—
CHCl <sub>2</sub> NO <sub>2</sub>	214.9	128.5	218.8	120.8	34.4	74.5	117.5	252.7
X <sup>5</sup> = X <sup>6</sup> = Cl, X <sup>7</sup> = H	(154.5)	(121.7)	(237.3)	(122.4)	(26.9)	(118.0)	(127.8)	
CCl <sub>3</sub> NO <sub>2</sub>	220.8	128.3	221.0	120.9	33.8	73.2	116.6	251.0
X <sup>5</sup> = X <sup>6</sup> = X <sup>7</sup> = Cl	(161.3)	(121.2)	(242.1)	(121.5)	(26.5)	(117.2)	(128.5)	
CHFCINO <sub>2</sub>	203.8	128.4	210.5	120.6	36.1	74.8	119.0	248.1
X <sup>5</sup> = Cl, X <sup>6</sup> = F, X <sup>7</sup> = H	(154.1)	(122.2)	(233.3)	(121.7)	(28.4)	(114.6)	(128.3)	
CF <sub>2</sub> CINO <sub>2</sub>	199.2	129.1	202.4	120.0	37.5	72.6	119.0	248.5
X <sup>5</sup> = Cl, X <sup>6</sup> = X <sup>7</sup> = F	(156.3)	(121.7)	(235.8)	(121.6)	(27.8)	(115.5)	(128.9)	
CFCl <sub>2</sub> NO <sub>2</sub>	208.1	128.9	209.2	120.3	36.0	72.5	117.6	250.6
X <sup>5</sup> = X <sup>6</sup> = Cl, X <sup>7</sup> = F	(158.3)	(121.5)	(238.0)	(121.5)	(27.3)	(115.9)	(128.9)	
CH <sub>2</sub> BrNO <sub>2</sub>	190.6	128.4	203.2	120.4	37.9	76.4	120.0	264.0
X <sup>5</sup> = Br, X <sup>6</sup> = X <sup>7</sup> = H	(152.4)	(121.7)	(238.4)	(122.7)	(26.1)	(120.4)	(127.1)	
CH <sub>3</sub> CH <sub>2</sub> NO <sub>2</sub>	201.9	129.7	207.1	120.9	37.0	73.7	118.2	262.3
X <sup>5</sup> = X <sup>7</sup> = H, X <sup>6</sup> = CH <sub>3</sub>	(151.7)	(122.6)	(236.1)	(122.7)	(27.2)	(27.2)	(125.7)	
CH <sub>3</sub> CHFNO <sub>2</sub>	205.1	128.2	213.1	121.2	35.6	75.6	119.0	239.7
X <sup>5</sup> = F, X <sup>6</sup> = CH <sub>3</sub> , X <sup>7</sup> = H	(153.3)	(121.9)	(236.9)	(122.8)	(26.9)	(118.4)	(127.0)	
CH <sub>3</sub> CF <sub>2</sub> NO <sub>2</sub>	207.9	129.2	208.7	120.8	36.1	72.3	118.1	231.4
X <sup>5</sup> = X <sup>7</sup> = F, X <sup>6</sup> = CH <sub>3</sub>	(155.9)	(121.9)	(238.2)	(122.3)	(27.0)	(117.6)	(127.6)	
CH <sub>3</sub> CHClNO <sub>2</sub>	212.9	128.6	217.6	121.0	34.8	74.6	117.7	251.5
X <sup>5</sup> = Cl, X <sup>6</sup> = CH <sub>3</sub> , X <sup>7</sup> = H	(153.1)	(122.2)	(236.0)	(122.6)	(27.3)	(117.5)	(126.6)	
CH <sub>3</sub> CCl <sub>2</sub> NO <sub>2</sub>	222.0	128.8	221.5	121.0	33.8	72.9	116.6	246.0
X <sup>5</sup> = X <sup>7</sup> = Cl, X <sup>6</sup> = CH <sub>3</sub>	(157.4)	(122.3)	(237.5)	(121.5)	(27.7)	(115.6)	(127.2)	

**Table 6.** Charges on atoms (in electron units) in the transition state of the nitro – nitrite rearrangement of some aliphatic C-nitro compounds [calculated at the B3LYP/6-31G(d) level].

Compound	Atoms			Compound	Atoms		
	C	N	O		C	N	O
CH <sub>3</sub> NO <sub>2</sub>	−0.293	0.300	−0.350	CH <sub>2</sub> ClNO <sub>2</sub>	−0.234	0.330	−0.337
CH <sub>3</sub> FNO <sub>2</sub>	0.160	0.307	−0.368	CH <sub>3</sub> CH <sub>2</sub> NO <sub>2</sub>	−0.124	0.278	−0.369
CHF <sub>2</sub> NO <sub>2</sub>	0.519	0.297	−0.357	CH <sub>2</sub> FCH <sub>2</sub> NO <sub>2</sub>	0.311	0.278	−0.369
CF <sub>3</sub> NO <sub>2</sub>	0.897	0.318	−0.345	CHF <sub>2</sub> CH <sub>2</sub> NO <sub>2</sub>	0.685	0.279	−0.375

a higher rate. As have already been noted above, the calculation of the *A*-factor of radical decomposition reactions is currently a complex problem. At the same time, an analysis of kinetic data for the gas-phase decomposition of polynitroalkanes and fluoronitroalkanes demonstrates that the values of log *A* for compounds bearing the same number of nitro groups are close to one another. Supposing that the values of log *A* for nitromethane and fluoronitromethane are equal [log *A* = 14.3 (s<sup>−1</sup>)], we can expect that NNR will contribute to the effective rate constant for the gas-phase decomposition of fluoronitromethane at 700 K. At 600 K, the contribution of NNR to the effective constant predominates.

According to calculations, the energy barrier of activation for the NNR of nitroethane is considerably smaller (by almost 17 kJ mol<sup>−1</sup>) than for nitromethane. An analysis of charge distributions on atoms in transition states shows a significant reduction in negative charge on the carbon atom in the presence of a methyl substituent; the charges on the oxygen and nitrogen atoms change insignificantly (Table 6).

The described change results in a decrease in the attraction of the oppositely charged C and N atoms and reduces the repulsion of the negatively charged C and O atoms in nitroethane. Apart from this, the C–O bond in the transition state of nitroethane is considerably longer than of nitromethane (207.1 and 200.7 pm, respectively). Evidently, it is these distinctions that account for the additional stabilization of the transition state and reduction in the energy barrier to the reaction of nitroethane in comparison with that of nitromethane.

A study of the NNR of dinitromethane demonstrated that the increase in the number of nitro groups has little influence on the magnitude of the energy barrier: as compared to that of nitromethane, the activation enthalpy lowers by ~7 kJ mol<sup>−1</sup>, which is significantly smaller than the decrease in the energy of dissociation of the C–N bond in this compound.<sup>41</sup> Similar tendencies are observed also for trinitromethane.<sup>10</sup>

For fluoronitromethanes and chloronitromethanes, the activation enthalpies of the considered reaction are substantially lower than that for nitromethane.

The analysis of alterations in bond lengths and bond angles in the transition state does not enable one to explain why it is fluoronitromethane for which the largest reduction in the activation energy is observed.

In the transition states of the NNR of fluoronitromethanes, the carbon and nitrogen atoms are charged positively, while the oxygen atom is charged negatively (see Table 6). At the same time, in the transition state of the NNR of nitromethane (and chloronitromethane) the nitrogen bears a positive charge, while the carbon and oxygen are charged negatively. Therefore, the carbon and oxygen atoms in nitromethane repel each other, while in

fluoronitromethanes they attract. As a result, in the transition state the lengths of the C–O bond monotonically decrease in the series nitromethane, fluoronitromethane, difluoronitromethane, trifluoronitromethane. In this series, the positive charge on the carbon atom increases sharply, whereas the charge on the nitrogen atom alters slightly. Consequently, there are two opposite tendencies: the attraction between carbon and oxygen increases, and simultaneously the repulsion between carbon and nitrogen also increases. In the case of the fluoronitromethane reaction, the repulsion prevails, which leads to greater stabilization of the transition state and a substantial reduction in the enthalpy of activation. In difluoro- and trifluoronitromethane, positive charges on the carbon atom achieve very large values, hence the role of repulsion increases and the reaction barrier of activation is appreciably larger than in fluoronitromethane.

For 1-fluoro-1-nitroethane, the reaction energy barrier diminishes (in comparison with nitroethane) to a considerably lesser extent than that for the reaction of fluoronitromethane. As distinct from the nitromethane derivatives, the minimum value of the barrier is predicted for 1,1-difluoro-1-nitroethane.

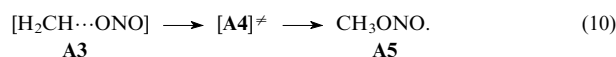
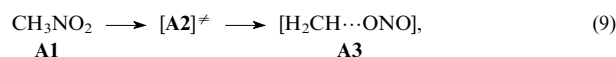
In the chloronitromethane series, the nitro – nitrite rearrangement cannot compete with the radical decomposition. First, with an increase in the number of chlorine atoms the dissociation energy of the C–N bond drops sharply (by 34 kJ mol<sup>−1</sup> in chloronitromethane in comparison with nitromethane<sup>21</sup>), whereas the activation energy of the nitro – nitrite rearrangement is reduced to a considerably lesser degree (by 15 kJ mol<sup>−1</sup>). Second, the value of the pre-exponential factor for radical reactions is higher.

Thus, for nitromethane and the majority of its derivatives the possibility of an experimental discovery of NNR by studying a gas-phase monomolecular decomposition is virtually excluded.

Such a conclusion, however, does not explain quite a low barrier of NNR (215.5–238.5 kJ mol<sup>−1</sup>), obtained by IRMPD,<sup>33</sup> neither does it explain the observed intense peak with *m/z* 30, which correspond to the NO<sup>+</sup> ion, in the mass spectra of nitromethane decomposition products (A1). However, it should be noted that nitrogen oxide can be a product of deeper stages of conversion in the thermal destruction of nitromethane. In this case, its yield says little of the nature of primary reaction steps.

Secondary recombination of the radicals formed upon homolytic dissociation of the C–N bond under the experimental conditions involving the oxygen atom followed by abstraction of NO<sup>•</sup> can be one of possible explanations of the facts listed above.

Another explanation, most interesting from our point of view is the possibility that NNR occurs in two steps through biradical transition states:<sup>44</sup>



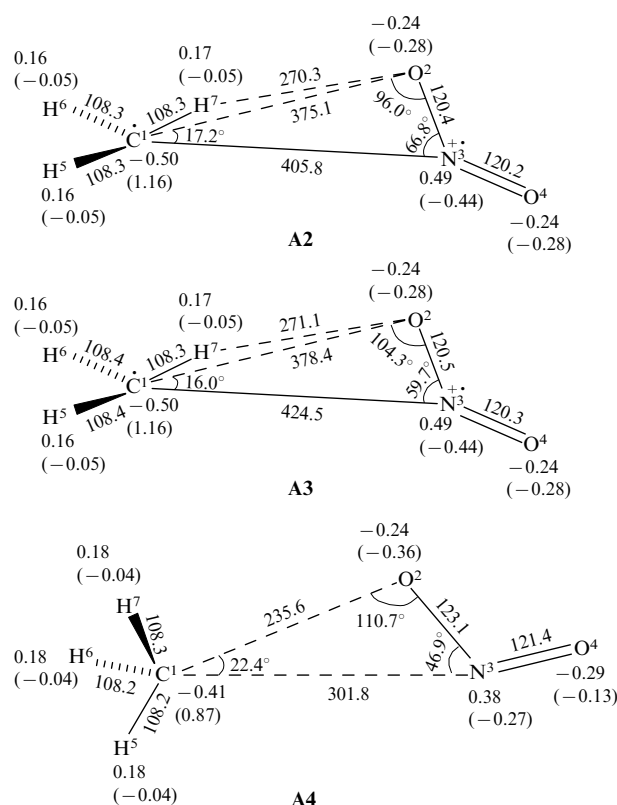
A possibility of such a mechanism was suggested.<sup>45</sup> However, only a transition state region (TSR) could be revealed, neither the TS could not be located nor the proof that this TSR corresponded to the process under study was obtained, which precluded any unambiguous conclusion. As for the presence of the peak with  $m/z$  30 in the mass spectra,<sup>46–49</sup> this can follow from the decomposition of the radical cation rather than nitromethane itself (this possibility is discussed below). A detailed theoretical examination of the mechanism of a two-step biradical nitro–nitrite rearrangement has been carried out.<sup>41, 44</sup>

Figure 4 depicts an energy diagram of nitromethane (A1) decomposition obtained by B3LYP/6-31G(d).

As already mentioned, the process under consideration includes two steps rather than one ( $\text{A1} \rightarrow [\text{A2}]^\ddagger \rightarrow \text{A3} \rightarrow [\text{A4}]^\ddagger \rightarrow \text{A5}$ ), and (in contrast to the hypothesis of secondary processes of individual radical recombinations) the complex  $[\text{CH}_3\cdots\text{NO}_2]$  (A3) is formed in the intermediate step. Dissociation of the complex rather than its formation is the rate-limiting step. In this case, the energy barrier to the rate-limiting step is roughly 22 kJ mol<sup>−1</sup> lower than that to the one-step NNR reaction (see Fig. 4).

The structures of the transition states of elementary steps (9) and (10) of the two-step nitro–nitrite rearrangement as well as charges and spin densities on the atoms are shown in Fig. 5.

It should be noted that the energy of the transition state  $[\text{A2}]^\ddagger$  is just 0.01 kJ mol<sup>−1</sup> higher than that of intermediate A3 (not allowing for the energy of zero-point vibrations). If zero-point vibration corrections are taken into account, the relative enthalpy of formation of complex A3 is somewhat



**Figure 5.** Structures (bond lengths in pm) and charges (in parentheses, spin densities) (in a. u.) on atoms of the singlet biradical transition states of the first (A2) and second (A4) steps as well as intermediate singlet biradical complex A3 of the two-stage nitro–nitrite rearrangement [B3LYP/6-31G(d)].<sup>44</sup>

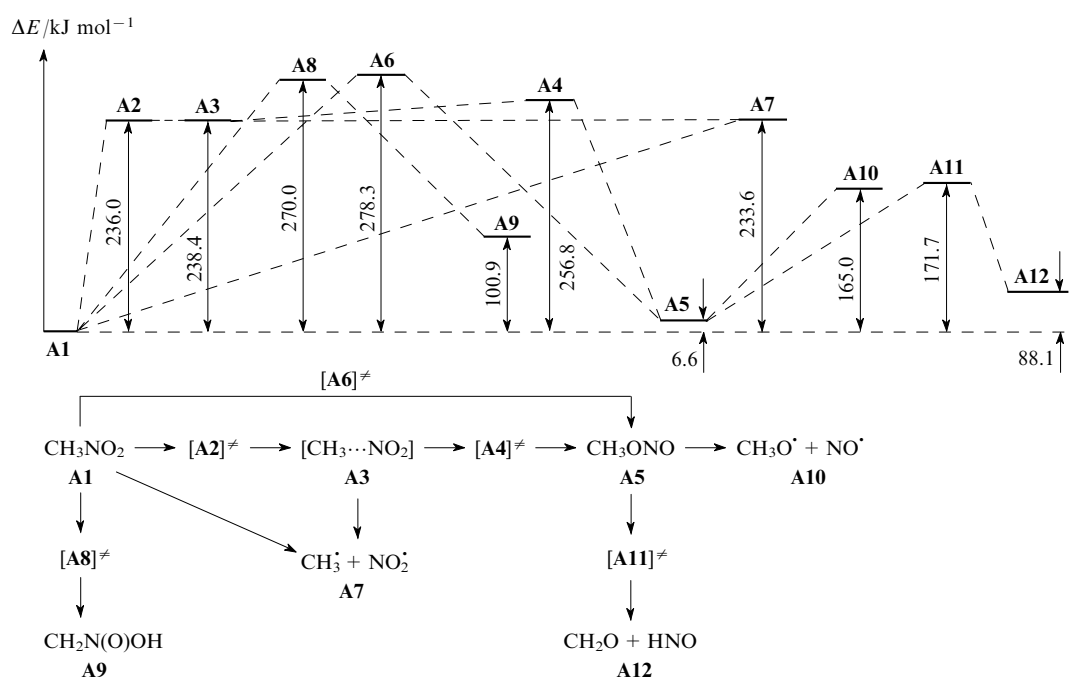


**Figure 4.** The energy diagram of decomposition of nitromethane (A1) obtained by the B3LYP/6-31G(d) method. The enthalpy of formation of nitromethane was taken as zero.<sup>44</sup>

higher (by  $2.5 \text{ kJ mol}^{-1}$ ) than the relative enthalpy of formation of the transition state  $[\mathbf{A2}]^\ddagger$  (see Fig. 4). Such an inversion is due to the small difference in energies and to the fact that the TS has one degree of freedom less than does the local minimum. At the same time, the energy of the intermediate  $\mathbf{A3}$  is  $2.9 \text{ kJ mol}^{-1}$  lower than that of the infinitely remote radicals  $\text{CH}_3^\bullet$  and  $\text{NO}_2^\bullet$  (without zero-point vibration corrections). Note that the interaction of the  $\text{CH}_3^\bullet$  and  $\text{NO}_2^\bullet$  radicals to yield complex  $\mathbf{A3}$  occurs as the activation-free process.

Table 7 lists data on the enthalpies of formation, dipole moments and entropies of reactants, transition states and reaction products of the two-step nitro–nitrite rearrangement.

**Table 7.** Enthalpies of formation, dipole moments and entropies of reactants, transition states and reaction products of the two-step process of the nitro–nitrite rearrangement (see Fig. 4).

Compound or TS	$\Delta H_f$ /kJ mol $^{-1}$	$\mu$ /D	$\Delta S$ /J mol $^{-1}$ K $^{-1}$
$\text{CH}_3\text{NO}_2$ ( <b>A1</b> )	−67.9	3.4747	317.4
$[\mathbf{A2}]^\ddagger$	168.0	0.2438	391.0
$[\text{CH}_3\cdots\text{NO}_2]$ ( <b>A3</b> )	170.5	0.2532	238.4
$[\mathbf{A4}]^\ddagger$	188.8	2.6773	341.7
$\text{CHONO}$ ( <b>A5</b> )	−61.4	2.4772	311.7

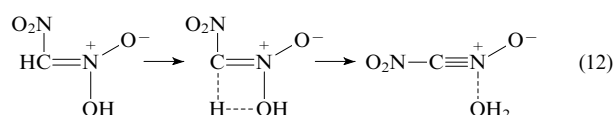
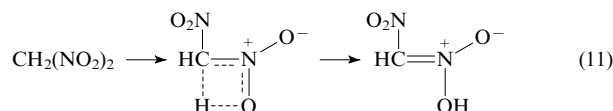
Figure 4 depicts also alternative mechanisms of the primary step of the nitromethane decomposition: one-step NNR ( $\mathbf{A1} \rightarrow [\mathbf{A6}]^\ddagger \rightarrow \mathbf{A5}$ ); homolytic cleavage of the C–N bond ( $\mathbf{A1} \rightarrow \mathbf{A7}$ ); 1,4-sigmatropic shift of a hydrogen atom to afford an *aci*-form ( $\mathbf{A1} \rightarrow [\mathbf{A8}]^\ddagger \rightarrow \mathbf{A9}$ ). In addition, two possible pathways of further development of the nitro–nitrite rearrangement process are indicated: homolytic cleavage of the O–N bond in methyl nitrite ( $\mathbf{A5} \rightarrow \mathbf{A10}$ ) and the formation of formaldehyde and HNO ( $\mathbf{A5} \rightarrow [\mathbf{A11}]^\ddagger \rightarrow \mathbf{A12}$ ).

The activation enthalpy of the methyl nitrite dissociation into the fragments  $\text{CH}_3\text{O}^\bullet$  and  $\text{NO}^\bullet$  is substantially lower (by  $\sim 90 \text{ kJ mol}^{-1}$ ) than that of the rate-limiting step. The reverse process of radical recombination is barrier-free.

Thus, the existence of a new channel of the NNR reaction in nitromethane, which can compete with the radical mechanism of gas-phase decomposition, has been established. Judging by the values of the activation entropy, the pre-exponential factors of the two steps of the NNR are considerably higher than the experimental values of the *A*-factor of the radical decomposition. In this case, a sufficiently uncommon situation in the series of *C*-nitro compounds should be observed: the contribution of NNR must increase with temperature. The mechanism presented above accounts for the experimental results in a natural way.<sup>13</sup> Besides, in published studies on the kinetics of gas-phase decomposition there are also indirect indications of the possibility of this process. Thus, the most extensive survey<sup>3</sup> of experimental data on the thermal decomposition of nitroalkanes notes a difference in the values of the Arrhenius parameters of the gas-phase decomposition of nitromethane that are determined in different temperature ranges.

All the other mechanisms of the gas-phase decomposition of nitroalkanes discussed in the literature cannot apparently compete with the processes considered above: the radical decomposition, elimination of  $\text{HNO}_2$  and NNR.

Of greatest interest is the isomerisation to the *aci*-form, which for the first time was investigated in detail by McKee.<sup>35</sup> A theoretical study of the formation of nitronic acids in polynitroalkanes demonstrated that an increase in the number of  $\text{NO}_2$  groups in the  $\alpha$ -position considerably lowers the activation enthalpy of the reaction. Based on these data, a mechanism of the elimination of water from the *aci*-forms of nitromethane, dinitromethane and other nitroalkanes bearing two hydrogen atoms in the  $\alpha$ -position was proposed.<sup>50</sup>



The suggested mechanism explains a special place of dinitromethane in the nitroalkane series. Dinitromethane is the sole compound in the series that bears two nitro groups in the  $\alpha$ -position (a prerequisite for a significant decrease in the reaction barrier) and two hydrogen atoms enabling the elimination of water molecules. According to calculations by the semi-empirical methods MINDO/3 and PM3,<sup>50</sup> the stage of the formation of the *aci*-form of dinitromethane that limits the overall process has a barrier that is significantly smaller than  $D(\text{C}-\text{N})$ . However, a study by *ab initio* and DFT methods showed that this inference is erroneous, and the mechanism involved cannot materialize in the gas-phase decomposition of nitroalkanes.<sup>51,52</sup> At the same time, a possibility of its occurrence in the liquid-phase decomposition of nitroalkanes cannot be completely excluded, this also applies to dinitromethane as suggested by experimental data.<sup>53</sup>

Considerable part of observations regarding the mechanism of the thermal decomposition of nitroalkanes was inferred from mass spectrometry. However, it should be borne in mind that radical cations produced in the chamber of a mass spectrometer upon electron impact and bearing an excess energy can decompose during the process of recording the mass spectra. Besides, the Maxwell–Boltzmann distribution of kinetic energies, which is typical of thermal processes is absent from the chamber of a mass spectrometer. For this reason, the decomposition channels of molecules and radical cations very often do not coincide, though certain analogies are possible. Therefore, in a number of cases the findings of the experimental examination by mass spectrometry of gas-phase decomposition products in the initial stages of decomposition<sup>46–49</sup> are not consistent with the data from kinetic studies.<sup>3</sup> An extensive theoretical study of the gas-phase decomposition of the nitromethane and nitroethane radical cations has been conducted.<sup>54,55</sup>

Figure 6 presents an energy diagram of decomposition of the nitromethane radical cation (**B1**);<sup>54,55</sup> it is evident that compound **B1** can undergo isomerization through the transition state **B2** to the radical cation **B3** in which the C–N bond is substantially longer (by 35.5 pm). This isomerization lies on the pathways of most energetically favourable channels of decomposition of compound **B1**, *i.e.*, the nitro–nitrite rearrangement ( $\mathbf{B1} \rightarrow [\mathbf{B2}]^\ddagger \rightarrow \mathbf{B3} \rightarrow [\mathbf{B4}]^\ddagger \rightarrow \mathbf{B5}$ ) and cleavage of the C–N bond

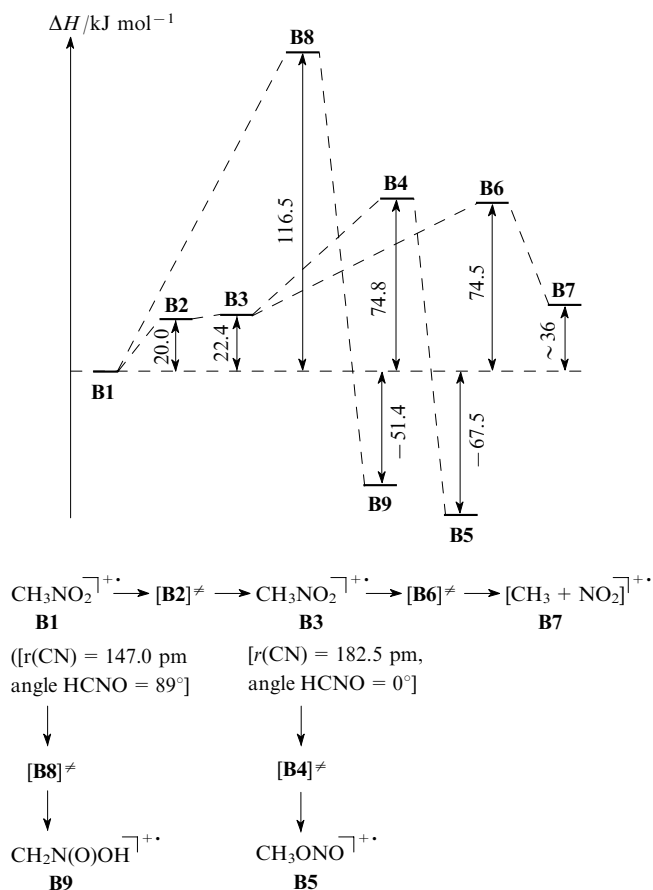


**Figure 6.** The energy diagram of the decomposition of the nitromethane radical cation (**B1**) obtained by the B3LYP/6-31G(d) method (the enthalpy of formation of the nitromethane radical cation was taken as zero).<sup>54,55</sup>

(**B1**  $\rightarrow$  **B2**  $\rightarrow$  **B3**  $\rightarrow$  **B6**  $\rightarrow$  **B7**). 1,4-Sigmatropic shift of a hydrogen atom occurs directly from radical cation **B1** (**B1**  $\rightarrow$  **B8**  $\rightarrow$  **B9**).

The results obtained demonstrate a considerable decrease in activation barriers for a number of the major processes of the gas-phase decomposition of radical cations as compared to those of reactions of a molecule. In particular, the NNR barrier to nitromethane radical cation (**B1**) is more than fivefold lower than that for the molecule **A1** (cf. Figs 4 and 6).

An analysis of changes in the main parameters of the reaction centre of the original compounds and the transition state for the nitro–nitrite rearrangement of nitromethane and its radical cation shows that they do not differ much. For instance, the alterations in the C–N bond length in the course of NNR for molecule **A1** and radical cation **B1** are 45 and 50 pm, respectively. However, in the latter the strength of the C–N bond substantially decreases, which leads to a reduction in the barrier to the nitro–nitrite rearrangement. The theoretical investigation of the nitromethane radical cation decomposition naturally explains the emergence of the  $\text{NO}^+$  ion in the mass spectrum of the gas-phase decomposition products of compound **A1**.<sup>46–49</sup> Consequently, when using mass spectrometry data for examining mechanisms of gas-phase decomposition, the decomposition peculiarities of both molecules and radical cation should be taken into account.

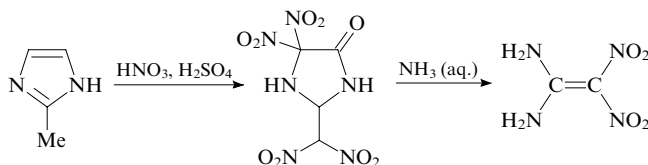
### III. The mechanism of the thermal decomposition of nitroalkenes

#### 1. The monomolecular and bimolecular mechanisms of nitroethylene thermodestruction

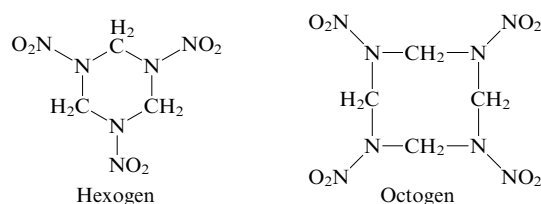
Experimental evidence for the gas-phase decomposition of nitroalkenes (unlike that of nitroalkanes) are extremely sparse.<sup>1,3,56,57</sup> With the exception of several simplest molecules, data on the geometric and thermochemical parameters of compounds and composition of the reaction products in initial stages of decomposition are absent. This altogether appreciably complicates the search for a mechanism of the gas-phase decomposition of nitroalkenes and the examination of the influence of molecular structures on the barriers to the primary steps of thermal decomposition.

For a long time, it was assumed on the basis of similarity of the activation energies and pre-exponential factors of the reactions of nitroalkanes and nitroalkenes with the same number of carbon atoms that nitroethylene (**C1**) and some other  $\alpha$ -nitroalkenes decompose according to the  $\text{HNO}_2$  elimination mechanism.<sup>1,3,56,57</sup> However, for mononitroalkanes this mechanism is verified by extensive data on product compositions, while in the case of nitroethylene no reliable observations on the composition of products in the initial stages of decomposition exist, and this mechanism is a hypothetical one.

The synthesis of 1,1-diamino-2,2-dinitroethylene<sup>58</sup> in 1998 encouraged new theoretical and experimental studies on nitroalkenes.<sup>59,60</sup>



It should be noted that the preparation of this compound was preceded by quantum chemical calculations<sup>61</sup> where attention has been paid to the fact that this compound has the same molecular stoichiometry as hexogen and octogen have, but differs from them in substantially stronger bonds.



Since that moment, the interest in studying the structure and reactivity of nitroalkenes has significantly grown due to their potential exploitation as explosives.

In 1998, based on quantum chemical calculations it was established<sup>62,63</sup> that the barrier to nitrous acid elimination from nitroethylene (Table 8) substantially exceeded the experimentally measured activation energy of the gas-phase decomposition ( $191.9 \text{ kJ mol}^{-1}$ ).<sup>3</sup> These differences reached  $33.5\text{--}50.2 \text{ kJ mol}^{-1}$  (for different basis sets), which is higher than the possible error in estimates of reaction barriers by the density functional method B3LYP/6-311++G(df,p) (the calculation error was assessed by

**Table 8.** Activation enthalpies of processes (13)–(18) calculated by different methods.<sup>62, 63</sup>

Process (equation)	$\Delta H_{298}^\ddagger / \text{kJ mol}^{-1}$			
	B3LYP <sup>a</sup>		QCISD(T)/6-31G(d) <sup>b</sup>	MP4/6-311 + G(d,p) // MP2(FC)/6-31G(d,p) <sup>c</sup>
	6-31G(d)	6-311 + + G(df,p)		
C – N bond cleavage (13)	281.2	268.4	289.5	291.2
The elimination of HO – N=O (14)	243.4	223.9	253.2	232.6
The nitro – nitrite rearrangement (15)	241.5	237.4	244.5	226.8
1,3- <i>H</i> -Sigmatropic shift to an <i>aci</i> -form (16)	257.6	249.2	274.8	256.0
1,4- <i>H</i> -Sigmatropic shift to an <i>aci</i> -form (17)	300.3	280.2	—	—
The formation of 4 <i>H</i> -1,2-oxazete 2-oxide (18)	201.3	203.9	216..5	—

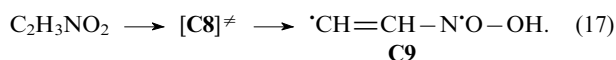
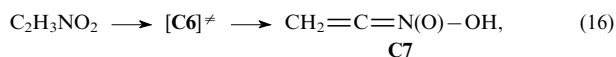
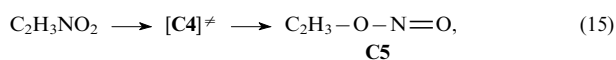
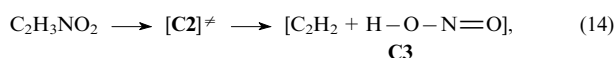
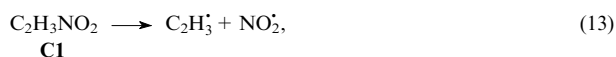
<sup>a</sup> Refs 62, 63, 66 and 67; <sup>b</sup> Refs 54, 67; <sup>c</sup> Ref. 65.

<sup>a</sup> Refs 62, 63, 66 and 67; <sup>b</sup> Refs 54, 67; <sup>c</sup> Ref. 65.

comparison of computed and experimental enthalpies of formation for numerous molecules and radicals<sup>64</sup>).

The magnitude of the barrier to HNO<sub>2</sub> elimination from nitroethylene obtained<sup>65</sup> at the MP4/6-311 + G(d,p)//MP2(FC)/6-31G(d,p) level (see Table 8) exceeds not only the experimental value, but also the estimate by the B3LYP/6-311 + + G(df,p) method.<sup>62, 63, 66, 67</sup>

The studies<sup>62, 63, 65</sup> address also other processes of the nitroethylene decomposition, namely:

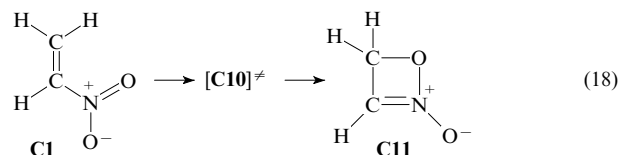


The energetic characteristics of these processes are provided in Table. 8, the structures and overall charges on atoms in the transition states **C2**, **C4**, **C6**, **C8** and reaction products **C3**, **C5**, **C7**, **C9** (13)–(17) are shown in Fig. 7. The same figure includes data on spin density distribution on atoms in the transition state **C8** and product **C9** of process (17), which prove that this process involves a singlet biradical transition state and results in a singlet biradical product.

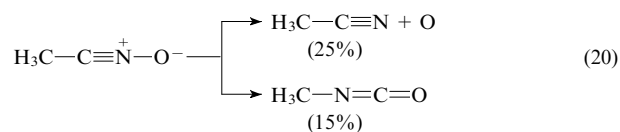
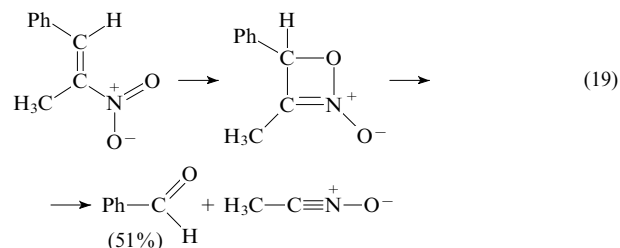
In Fig. 7 and further on, data on calculations by the B3LYP method with the 6-31G(d) basis set are presented. This is a minimum basis set in which molecular geometries are represented well, and differences in the enthalpies of formation of isomers are represented satisfactorily.<sup>64</sup> The principal results of the study of nitroethylene derivatives were obtained with the use of this basis set. Data on the geometries of the starting compounds, transition states and products of reactions (13)–(17) obtained by other methods can be found elsewhere.<sup>54, 62, 63, 65–67</sup>

As seen by inspecting Table 8, the activation enthalpies of all the reactions discussed above are considerably higher than the experimental activation energy of the gas-phase

decomposition of nitroethylene. The formation of a cyclic product, 4*H*-1,2-oxazete 2-oxide (**C11**), is more favourable.



For the first time such a scheme was suggested<sup>68</sup> by examining the high-temperature pyrolysis of β-nitrostyrenes:



The major products of reactions (19) and (20) are PhCHO and CH<sub>3</sub>CN, respectively. It is this fact that served as the ground for considering this mechanism. However, no kinetic or energetic justifications for the possibility of such a process were presented in studies,<sup>68–70</sup> addressing the destruction of *cis*-α,4-dinitrostilbene and 3-*tert*-butyl-4,4-dimethyl-2-nitropent-2-ene.

Although the formation of compound **C11** during thermal decomposition of nitroethylene was not proved experimentally, analogous oxazetes were obtained by the cyclization of substituted nitroethylenes.<sup>71–73</sup>

The calculated barrier to reaction (18) (see Table 8)<sup>54, 62, 63, 66, 67</sup> is close to the experimental estimate (191.9 kJ mol<sup>−1</sup>).<sup>3</sup> The difference is about 8 kJ mol<sup>−1</sup>, which is within possible experimental error. On the other hand, the error of 8–12 kJ mol<sup>−1</sup> is also possible in calculating activation enthalpy, hence the agreement between calculated and experimental values of the reaction

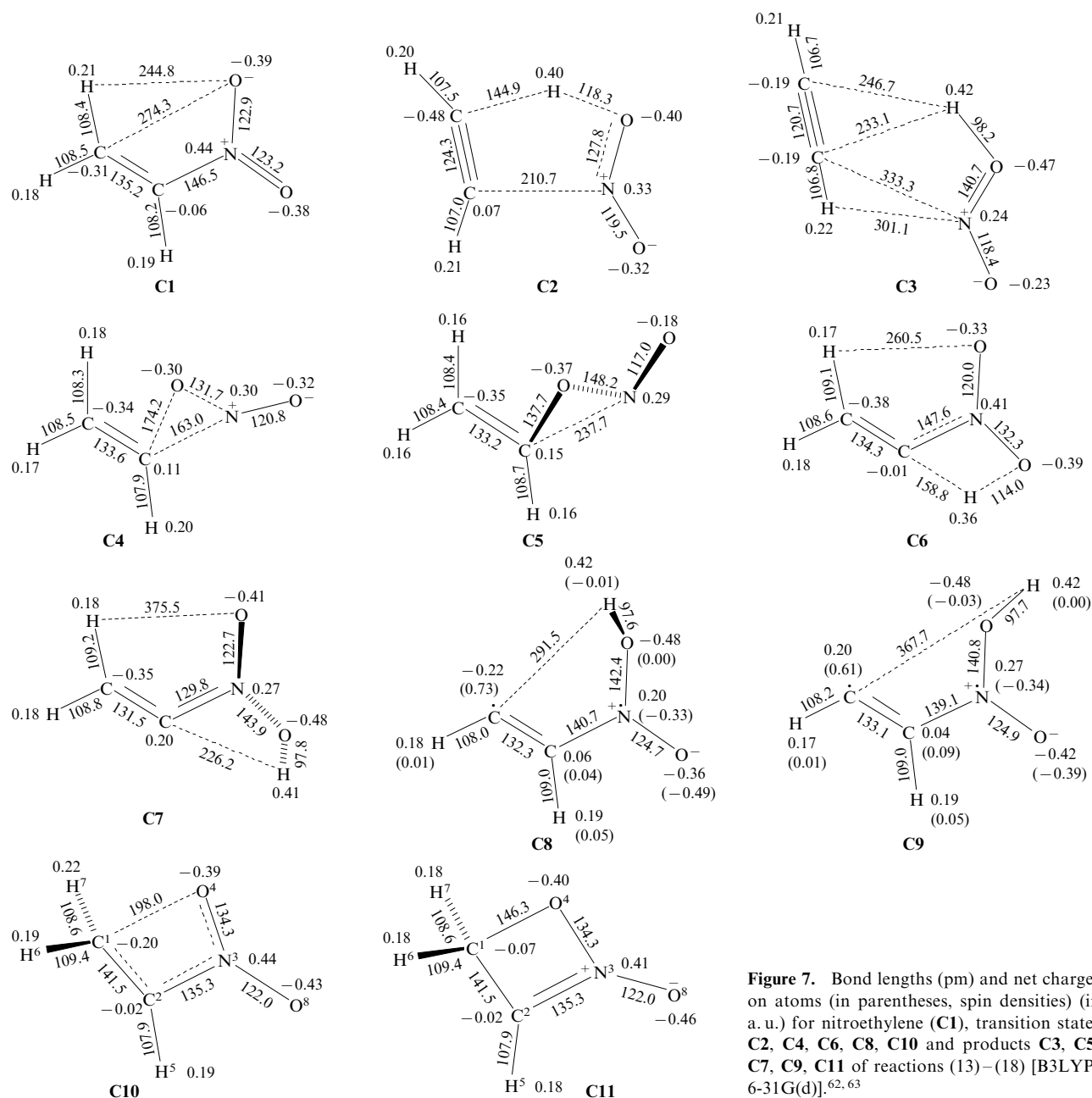


**Figure 7.** Bond lengths (pm) and net charges on atoms (in parentheses, spin densities) (in a. u.) for nitroethylene (**C1**), transition states **C2**, **C4**, **C6**, **C8**, **C10** and products **C3**, **C5**, **C7**, **C9**, **C11** of reactions (13)–(18) [B3LYP/6-31G(d)].<sup>62, 63</sup>

barriers should be accepted as satisfactory. The basis sets 6-31G(d) and 6-311++G(df,p) (B3LYP) give very similar values of the activation enthalpy. The conclusions that rely on the B3LYP calculations are confirmed by results from a study of processes (13)–(18) by the semi-empirical method QCISD(T)/6-31G(d)<sup>54</sup> (see Table 8).

The results of the examination of secondary processes of the decomposition of compound **C11** are summarized in Fig. 8.

The most probable development of the process is the formation of a singlet biradical intermediate **C12** (Fig. 9), which can decompose in three ways. The first of them is associated with a number of conformational transitions (**C12** → **C13** → **C14**) after which the biradical **C14** dissociates into formaldehyde and nitrile oxide (**C15**). The second is connected with the rearrangement to (*Z*)-2-(hydroxyimino)acetaldehyde (**C16**) followed by its decomposition to hydrogen cyanide and formic acid (**C18**). The third pertains

to the rearrangement to 2-nitrosoacetaldehyde (**C19**) followed by decomposition to either carbon monoxide, methyl radical and NO (**C21**), or to hydrogen cyanide, water and CO (**C26**), or to carbon monoxide and ammonia (**C32**).

Note that biradical **C12** rather than a zwitter-ion is formed upon decomposition of 4*H*-1,2-oxazete 2-oxide, which is evidenced by the distributions of charge and spin densities (see Fig. 9) as well as by the dipole moments of the corresponding structures (according to the B3LYP/6-31G(d) method, it is 3.82 D for compound **C11**, 3.34 D for transition state **C33** and 3.38 D for compound **C12**). They unambiguously indicate a high degree of polarization of spin density on the oxygen atom and NO group in the biradical **C12** and a minor redistribution of charges compared with the original structure **C11**.

The formation of cyclic intermediate **C11** upon decomposition of nitroethylene (**C1**) is verified by data from mass spectrometry.<sup>74</sup> The mass spectra of thermal decomposition

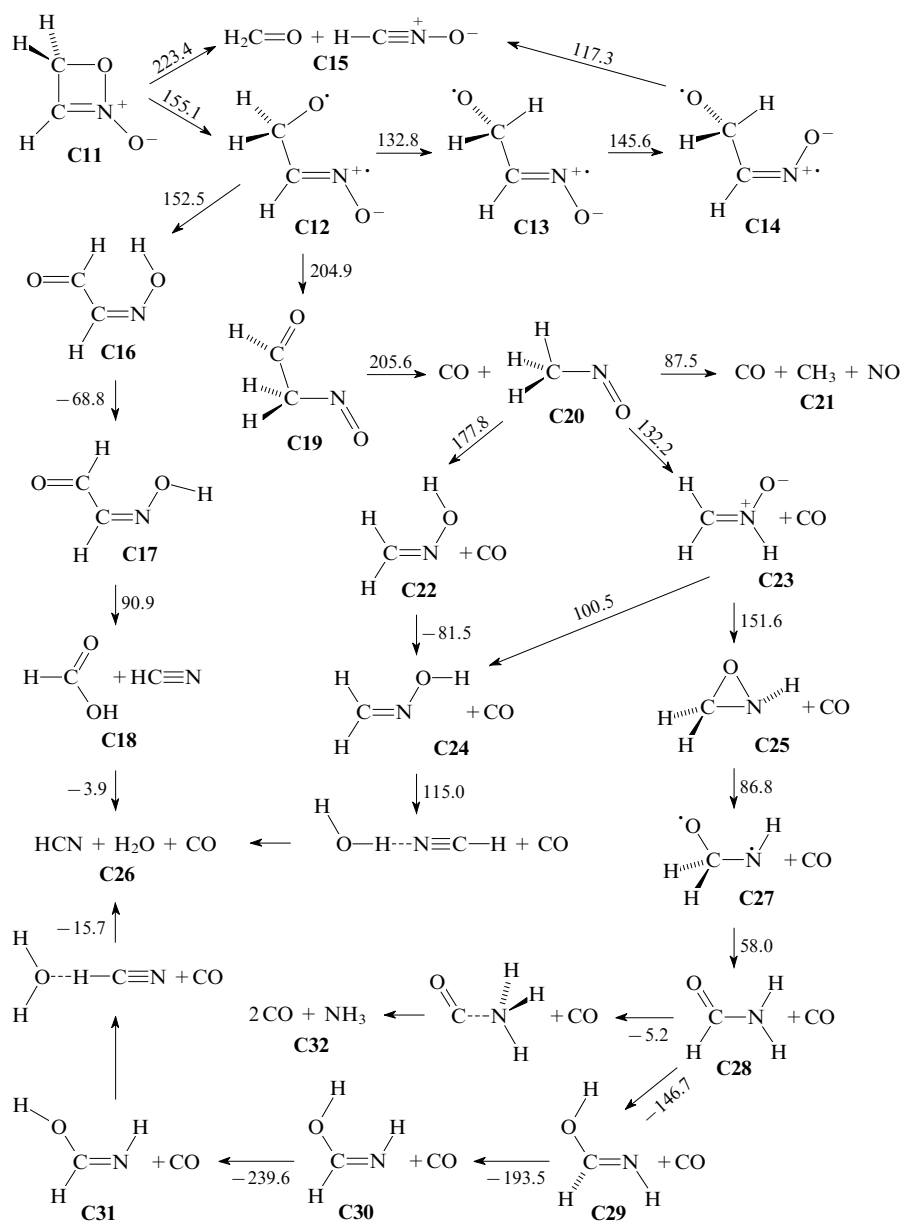


**Figure 8.** A scheme of decomposition of 4H-1,2-oxazete 2-oxide (**C11**) [at the B3LYP/6-311 + + G(df,p) level].<sup>62, 63</sup>

The relative enthalpies of formation of the transition states of the corresponding processes (in kJ mol<sup>-1</sup>) are indicated beside the arrows. The enthalpy of formation of nitroethylene was chosen as zero.

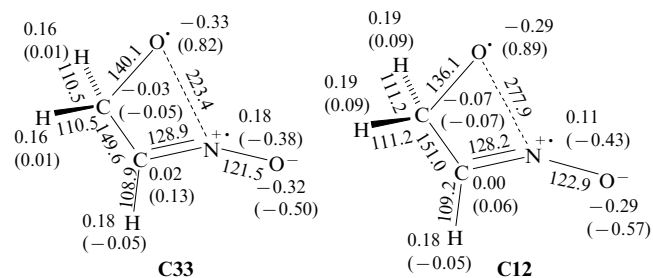
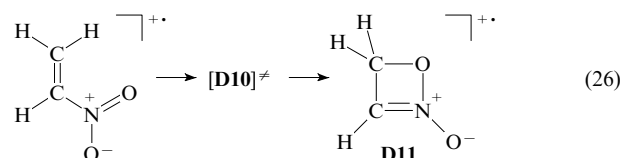
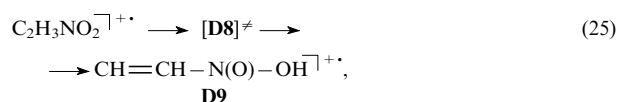
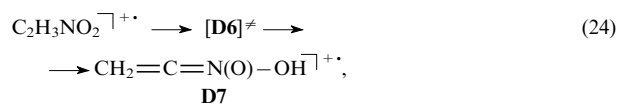
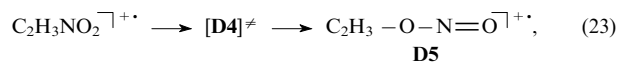
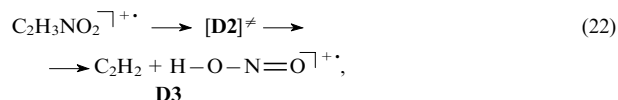
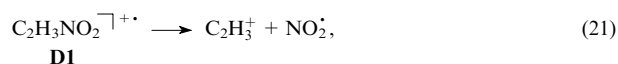


**Figure 9.** Bond lengths (pm) and charges on atoms (spin densities) (in a.u.) for transition state **C33** and reaction product **C12** of the formation of a singlet biradical of 4H-1,2-oxazete 2-oxide [B3LYP/6-31G(d)].<sup>62, 63</sup>

products contain intense peaks of ions with  $m/z$  44 ( $[M-HCO]^+$ ) and  $m/z$  43 ( $[M-H_2CO]^+$ ), which allowed suggesting a mechanism involving the formation of compounds **C11** and **C19**.<sup>74</sup> In addition, in the mass spectra of nitroethylene decomposition products there are peaks corresponding to the ions  $[M-CO]^+$ ,  $[M-CH_3]^+$ ,  $[M-NO]^+$  etc., which provides evidence for the mechanism presented in Fig. 8. However, the recourse to data from mass spectrometric analysis for discussion of a reaction mechanism provokes certain objections, because in the course of such an experiment the corresponding radical cations rather than molecules themselves can decompose. Chemical reactions of the radical cations have activation barriers that differ considerably from those of analogous processes involving molecules, which was proved by calculations of the gas-phase monomolecular decomposition of the nitroethylene radical cation (**D1**) at the B3LYP/6-31G(d) level.<sup>54, 67</sup>



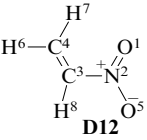
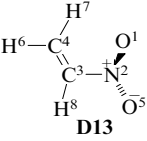
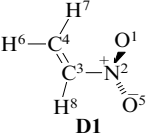
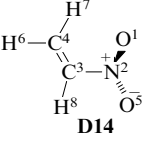
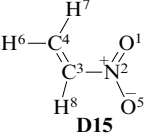
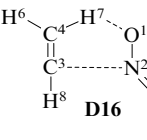
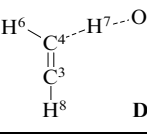
For radical cation **D1**, as for molecule **C1**, six major mechanisms of monomolecular decomposition have been examined [Eqns (21)–(26)]:<sup>54</sup>



An investigation of the structure of radical cation **D1** indicated the existence of two distinct conformations with the rotation angle  $\text{C}^4\text{C}^3\text{N}^2\text{O}^1$  of roughly  $60^\circ$  (**D1**) (its enthalpy of formation was taken as zero) and a planar one (**D12**). Although the structures **D1** and **D12** differ in energy insignificantly, they undergo different processes. Reactions involving an intramolecular hydrogen transfer correspond to conformer **D12**, whereas rearrangements (23) and (26) are characteristic of structure **D1**. Between the two conformations, transition state **D13** was found (Table 9).

A study of process (21) demonstrated that most favourable is cleavage of the C–N bond to yield the cation  $\text{C}_2\text{H}_3^+$  and radical  $\text{NO}_2^{\cdot}$  (Table 10). If positive charge is concen-

**Table 9.** Geometric parameters of intermediates and transition states between them, the relative enthalpy of the C–N bond dissociation in the nitroethylene radical cation.

Structure	Bond length $r/\text{pm}$						Dihedral angle $\text{C}^4\text{C}^3\text{N}^2\text{O}^1/\text{deg}$	$\Delta H/\text{kJ mol}^{-1}$
	$\text{C}^4\text{C}^3$	$\text{C}^3\text{N}^2$	$\text{N}^2\text{O}^1$	$\text{N}^2\text{O}^5$	$\text{C}^3\text{H}^7$	$\text{H}^7\text{O}^1$		
 <p style="text-align: center;"><b>D12</b></p>	135.0	139.9	124.5	125.5	108.8	253.7	0.0	1.6
 <p style="text-align: center;"><b>D13</b></p>	135.3	141.4	127.1	121.6	108.7	253.7	28.5	1.64
 <p style="text-align: center;"><b>D1</b></p>	136.6	145.2	119.0	126.8	108.7	269.5	62.1	0.0
 <p style="text-align: center;"><b>D14</b></p>	129.6	187.6	119.1	119.1	108.7	256.5	–15.3	46.6
 <p style="text-align: center;"><b>D15</b></p>	129.1	194.7	118.7	119.1	108.8	255.9	0.0	48.8
 <p style="text-align: center;"><b>D16</b></p>	126.1	324.1	118.6	120.8	112.3	192.8	0.0	72.8
 <p style="text-align: center;"><b>D17</b></p>	125.4	455.7	118.3	122.5	115.1	174.0	179.5	62.4

**Table 10.** The activation parameters of the primary steps of the monomolecular decomposition of nitroethylene radical cation (**D1**) (the energy for the radical cation is taken relative to the non-planar radical cation **D1**) [B3LYP/6-31G(d)].

Process	Equation	$\Delta H_{298}^\ddagger$ /kJ mol <sup>-1</sup>
C–N bond cleavage	(21)	96.5
The elimination of HO–N=O	(22)	
The nitro–nitrite rearrangement	(23)	58.4
1,3- <i>H</i> -Sigmatropic shift to an <i>aci</i> -form	(24)	158.0
1,4- <i>H</i> -Sigmatropic shift to an <i>aci</i> -form	(25)	94.1
The formation of 4 <i>H</i> -1,2-oxazete 2-oxide	(26)	51.8

trated on the nitro group, the relative enthalpy of formation increases to 222.7 kJ mol<sup>-1</sup>.

Upon stretching of the C–N bond in the radical cation **D1**, several transition states (**D14**, **D16**) and minima (**D15**, **D17**) were located (see Table 9).

From the data on the geometry of complex **D17**, one can assume two variants of further development of the process, *viz.*, decomposition with abstraction of the NO<sub>2</sub> group or with elimination of the HNO<sub>2</sub> molecule. These processes have not been studied so far.

Nevertheless, one can assert that the formation of the C–N bond in the nitroethylene radical cation is not a barrier-free reaction but rather has a sophisticated mechanism involving several stable intermediates.

According to calculations, the elimination of nitrous acid is not a primary step for the nitroethylene radical cation, it can rather represent a secondary process of mechanism (21) or (25). On the contrary, the barrier to the nitro–nitrite rearrangement is considerably lower than the dissociation energy of the C–N bond (see Table 10, TS structures are illustrated in Fig. 10).

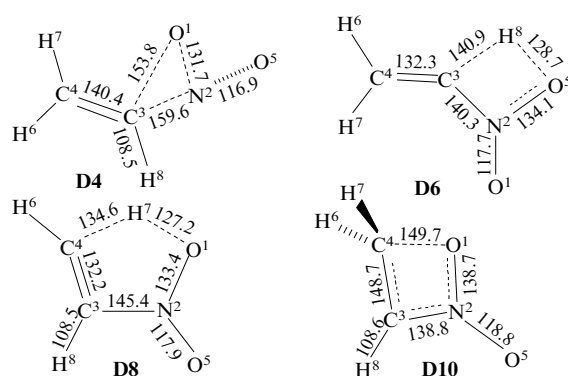


**Figure 10.** Bond lengths (pm) of the transition states of the primary steps of nitroethylene radical cation (**D1**) decomposition [B3LYP/6-31G(d)].<sup>54</sup>

**D4**, for the nitro–nitrite rearrangement; **D6**, for the 1,3-*H*-sigmatropic shift to the *aci*-form; **D8**, for the 1,4-*H*-sigmatropic shift to the *aci*-form; **D10**, for the formation of a cyclic intermediate.

The activation enthalpy of the 1,3-*H*-transfer is significantly higher than that of all the other considered mechanisms (see Table 10), hence the occurrence of this process is unlikely. In contrast, 1,4-sigmatropic shift of a hydrogen atom under certain conditions can compete with other

processes. These results differ fundamentally from those obtained in studying nitroethylene (**C1**)<sup>66</sup> where the barrier to the *aci*-form formation according to reaction (16) is substantially lower than the activation enthalpy of alternative process (17).

As in the case of molecule **C1**, the calculation for radical cation **D1** predicts that the mechanism of the generation of the radical cation **D11** [reaction (26)] is the only possible explanation of the observed products (see Table 10), which is also evidenced by data from mass spectrometry.<sup>74</sup> It can be really rivalled only by the nitro–nitrite rearrangement, the barrier to which is just 6 kJ mol<sup>-1</sup> higher (see Table 10). This inference is also confirmed by the presence of a peak with *m/z* 30 in the mass spectra.<sup>74</sup>

Figure 11 presents a scheme of studied reactions of the gas-phase monomolecular decomposition mechanism of radical cations **D1** and **D12**, including some secondary processes.

The barriers to reactions involving cations and radical cations are significantly lower than the computed activation enthalpies of the thermal decomposition reactions of molecules. Accordingly, mass spectrometry data, without additional theoretical studies, do not allow unambiguous choice of one or another mechanism of gas-phase decomposition, but rather can merely serve as a point of departure for further investigations.

For liquid-phase processes and gas-phase reactions at high pressures, a mechanism of bimolecular thermal decomposition can be observed. Quantum chemical calculations predict<sup>67,75</sup> that a bimolecular scheme of decomposition of compound **C1** is associated with a substantially lesser energy consumption as compared to that for monomolecular processes and can be autocatalytic (Fig. 12, 13).

In the first step, two nitroethylene molecules (**C1**) spatially oriented in a certain fashion interact with one another to produce stable rings just as in the Diels–Alder reaction.<sup>67,75</sup> Depending on possible arrangements of the reactant molecules, there are four distinct transition states and the corresponding products. The latter have ‘boat’ conformations, and the most stable isomers are formed with greater enthalpies of activation (see Fig. 12).

As in the case of the monomolecular decomposition of nitroethylene, in the destruction of dimeric products **C34**, **C35**, **C36** and **C37** (see Fig. 12) an important role is played by biradical processes (see Fig. 13).

Thus for the isomer **C35** the structure of which is portrayed in Fig. 14 energetically most favourable is the process that pertains to the generation of a singlet biradical intermediate **C39** by reaction (31) or *via* an intermediate product **C40** in two steps [(32) and (33)] followed by its decomposition. Compound **C39** derived from rings **C35** or **C40** by homolytic cleavage of the NO bond can give rise to formaldehyde, nitrile oxide or nitroethylene (**C45** or **C47**) through several isomerization steps that are not connected with significant energy consumption [reactions (34)–(41) in Fig. 13]. The molecule **C1** formed undergoes the reaction anew; thus, an autocatalytic scheme is realized.

For the isomer **C36** (see Fig. 12), a rearrangement into a five-membered ring is likely (cleavage of the N–O bond in the ring and recyclization involving the C–O bond, 78.1 kJ mol<sup>-1</sup>) akin to reaction (42) in Fig. 13.

In the gas phase,<sup>56</sup> such a bimolecular decomposition mechanism is unlikely due to low concentration of nitroalkenes.

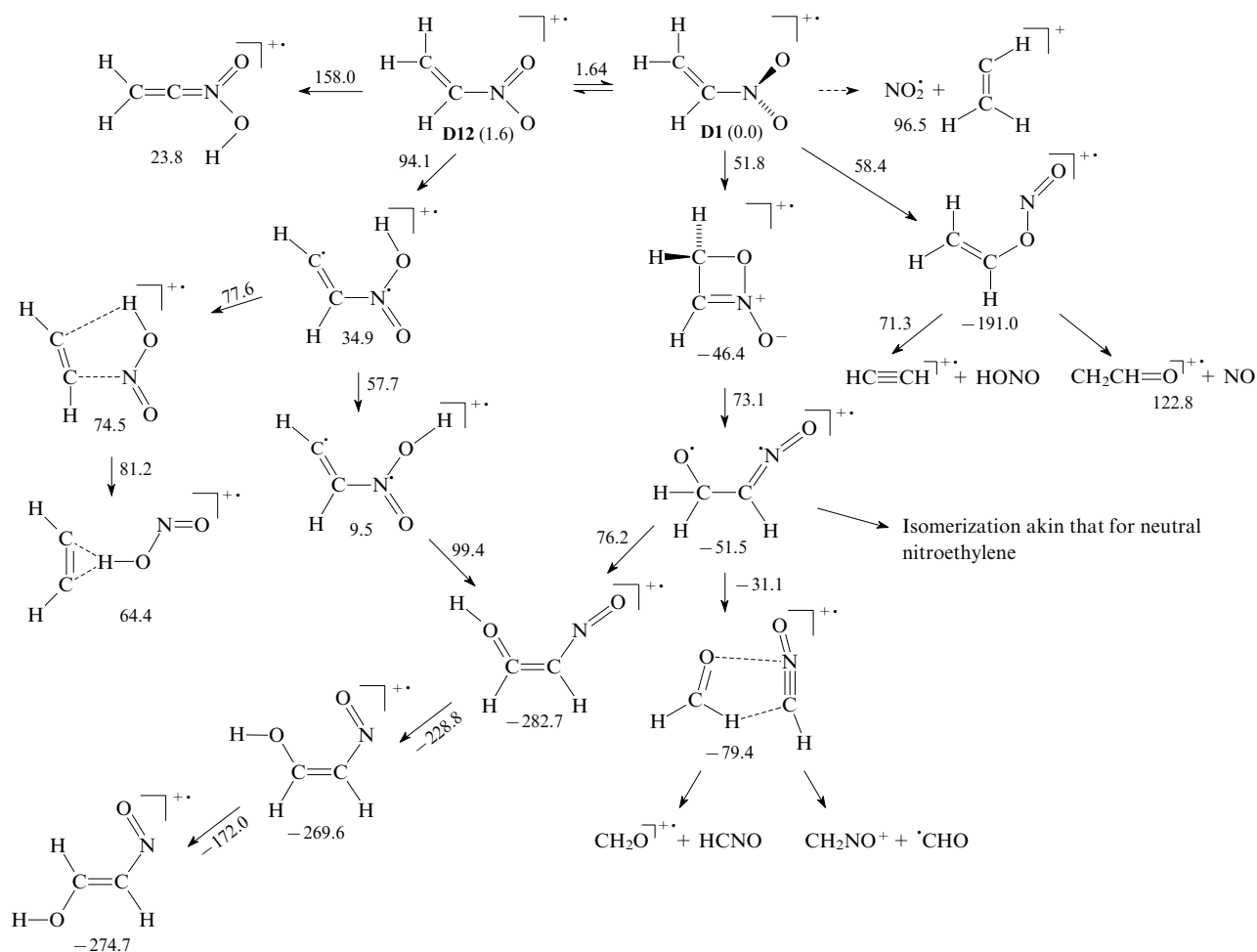


**Figure 11.** A scheme of a mechanism of the gas-phase monomolecular decomposition of the nitroethylene radical cation [at the B3LYP/6-31G(d) level].<sup>54</sup>

Hereinafter, the activation enthalpies (beside the arrows) and reaction enthalpies (under the structures) in  $\text{kJ mol}^{-1}$  are presented. The dashed arrows denote hypothetical processes.

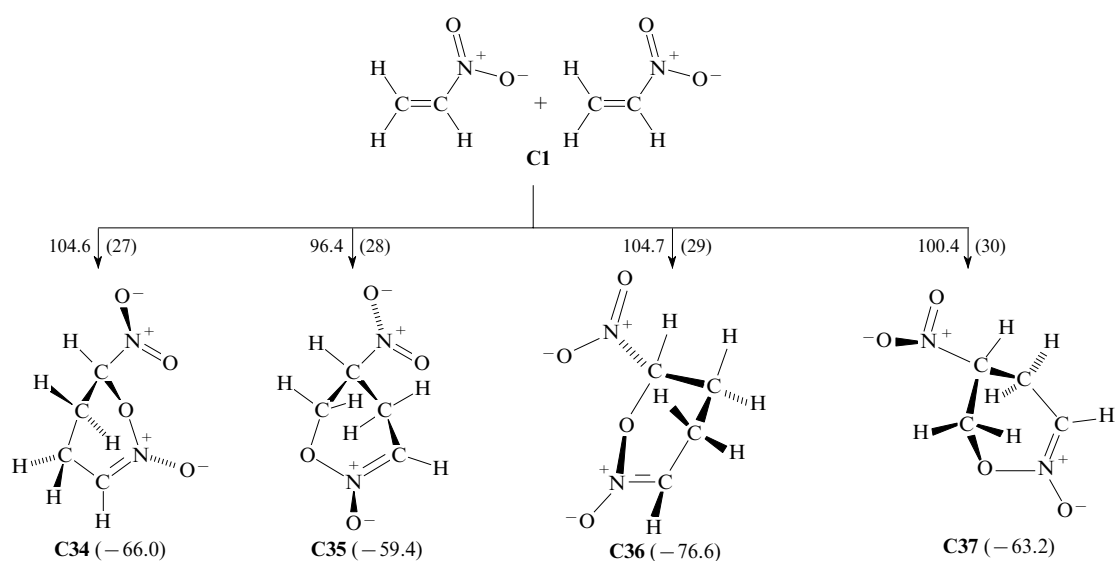


**Figure 12.** The primary stages of the bimolecular decomposition of nitroethylene [by B3LYP/6-31G(d)].<sup>67, 75</sup>

Hereinafter, reaction numbers are indicated in parentheses beside the arrows.

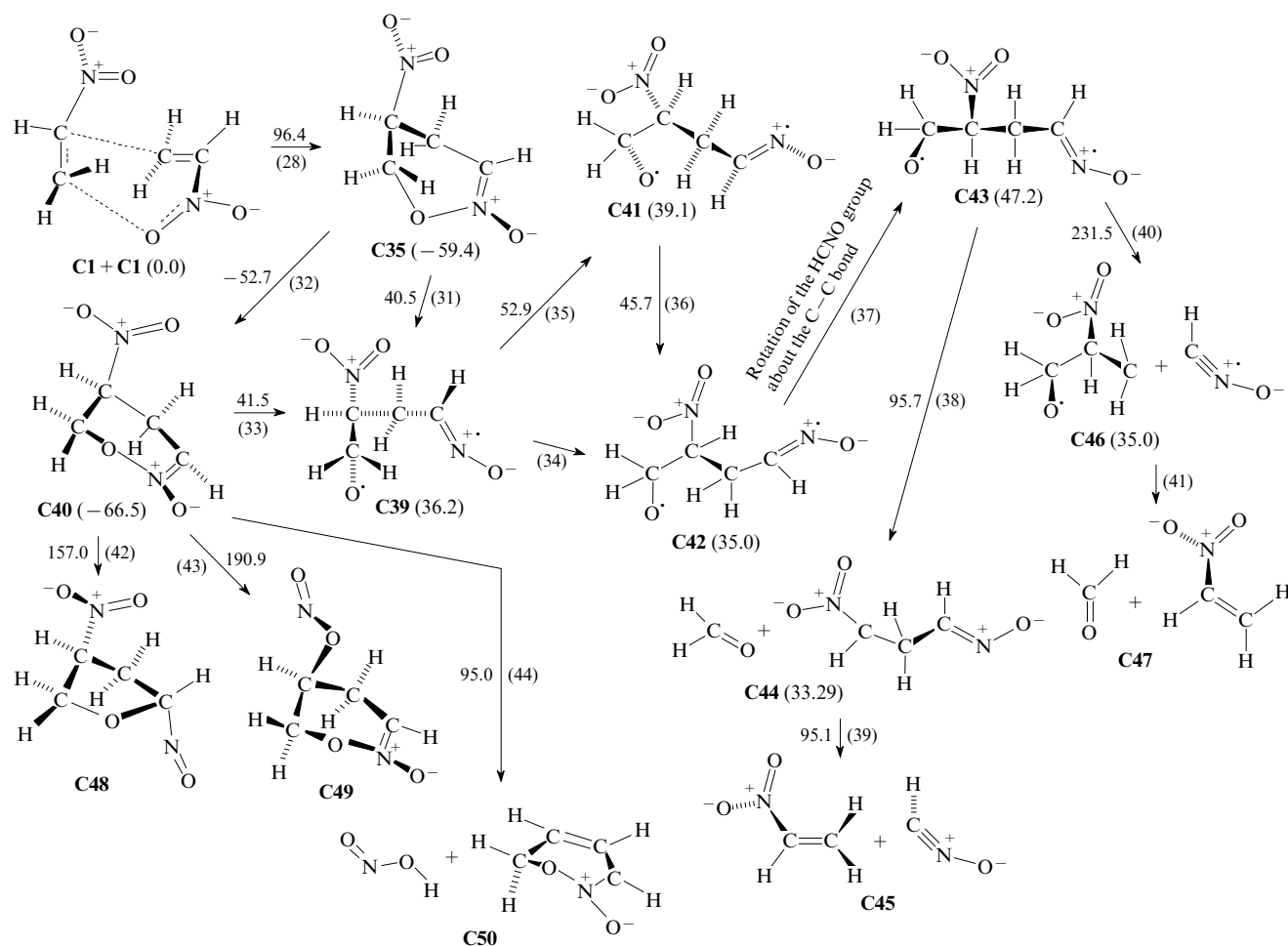


**Figure 13.** A scheme of a mechanism of the bimolecular autocatalytic thermodecomposition of nitroethylene (**C1**) [at the B3LYP/6-31G(d) level].<sup>67, 75</sup>

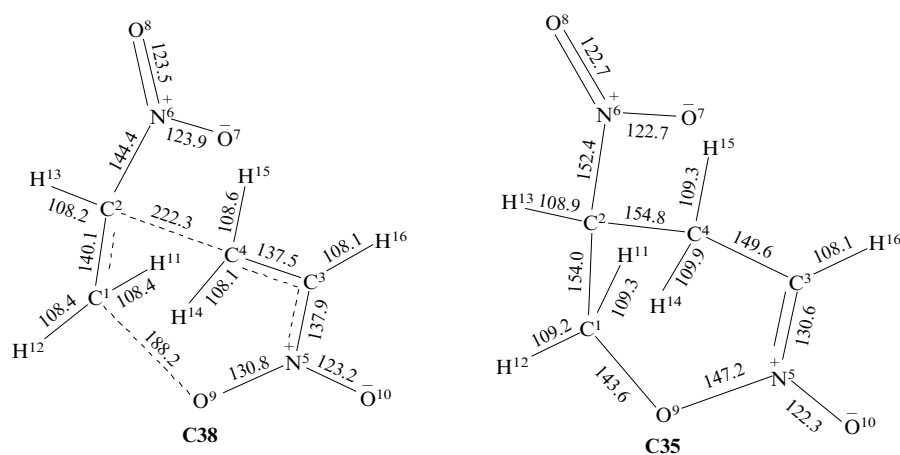
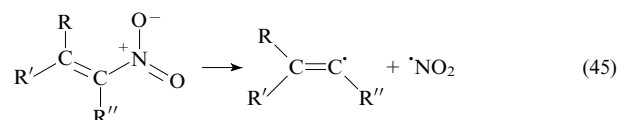


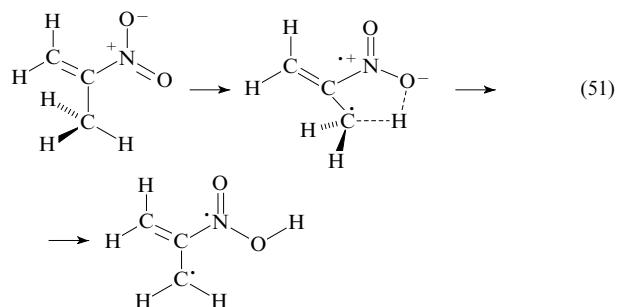
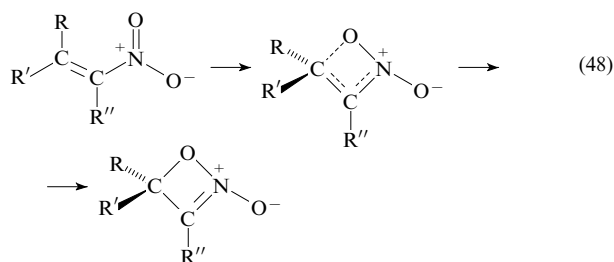
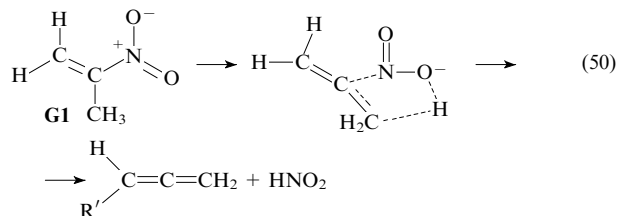
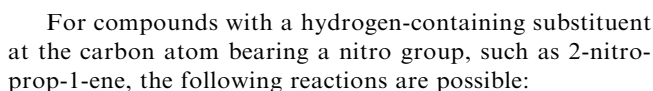
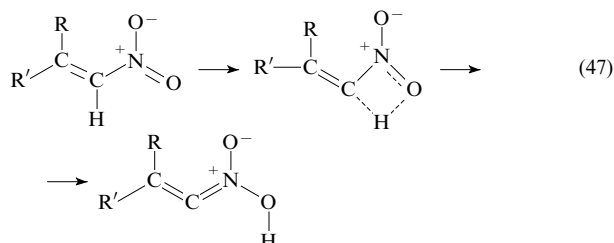
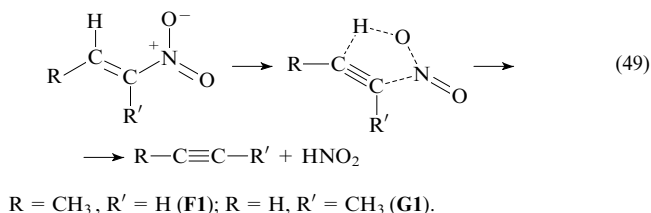
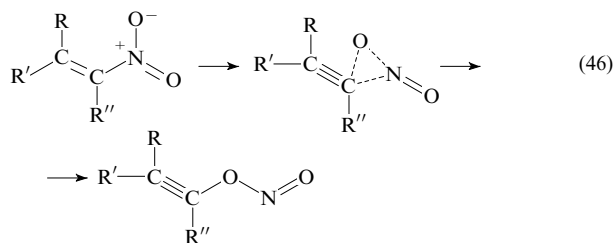
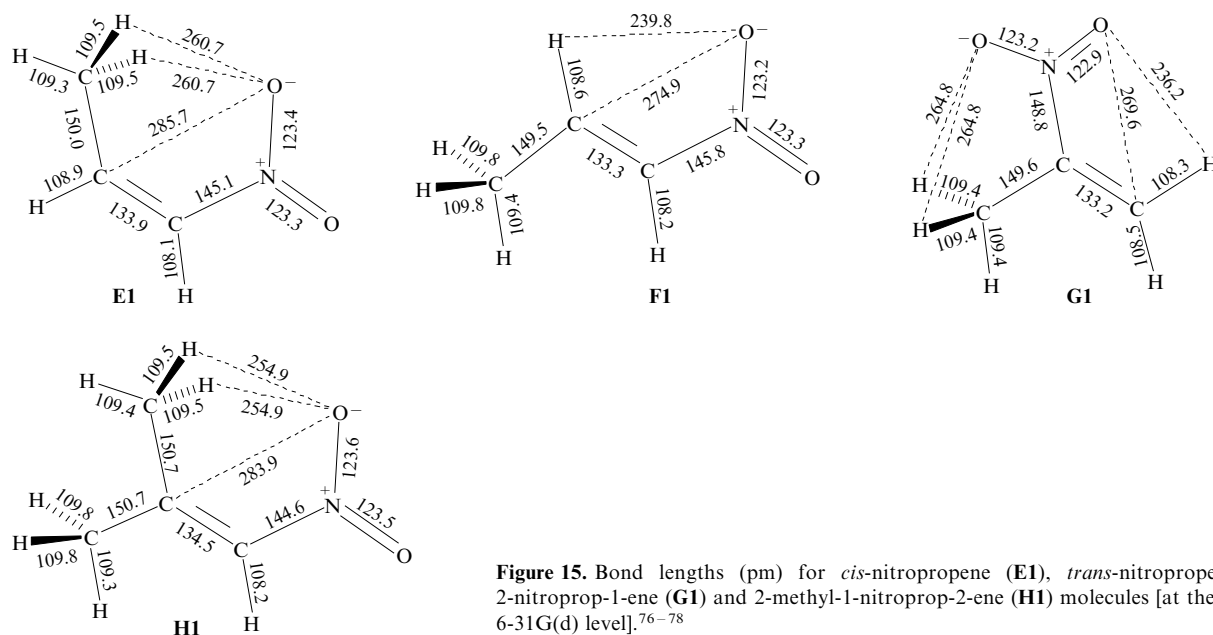
**Figure 14.** Bond lengths (pm) in transition state **C38** and dimer **C35** [B3LYP/6-31G(d)].<sup>67, 75</sup>

## 2. The mechanism of the thermal decomposition of nitropropenes

Calculations of primary steps of the thermal decomposition of nitropropene, namely, of *cis*-nitropropene (**E1**), *trans*-nitropropene (**F1**), 2-nitroprop-1-ene (**G1**) and 2-methyl-1-nitroprop-1-ene (**H1**) have been performed.<sup>76–79</sup> Their structures are illustrated in Fig. 15.

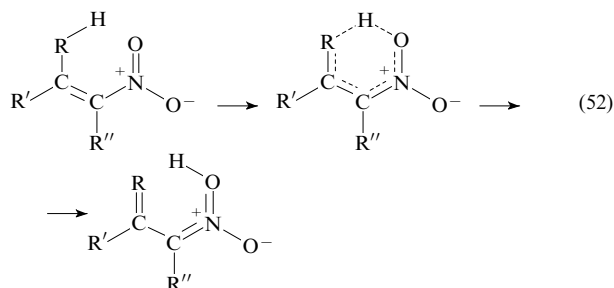
For *cis*- and *trans*-nitropropene and 2-methyl-1-nitroprop-1-ene, the following mechanisms are possible:




$$\begin{aligned} &\text{R} = \text{CH}_3, \text{R}' = \text{R}'' = \text{H} \text{ (E1)}; \text{R} = \text{R}'' = \text{H}, \text{R}' = \text{CH}_3 \text{ (F1)}; \\ &\text{R} = \text{R}' = \text{CH}_3, \text{R}'' = \text{H} \text{ (H1)}. \end{aligned}$$

For *trans*-nitropropene and 2-nitroprop-1-ene, the elimination of HNO<sub>2</sub> is added to the listed reactions [with the exception of process (47), which is impossible for the propene **G1**].

For nitroalkenes with a hydrogen-containing substituent in the *cis*-position with respect to the nitro group (the compounds **E1** and **H1**), there is a possibility of yet another channel of gas-phase decomposition, namely, 1,5-sigmatropic hydrogen shift from RH to the nitro group:



R = CH<sub>2</sub>, R' = R'' = H (**E1**); R = CH<sub>2</sub>, R' = CH<sub>3</sub>, R'' = H (**H1**).

Quantum chemical calculations [B3LYP/6-31G(d) basis set] of primary steps of major alternative mechanisms of the thermal decomposition of compounds **E1**, **F1**, **G1** and **H1** showed that, as in the case of nitroethylene (**C1**), the formation of various oxazetes plays an essential role.

For *trans*-nitropropene (**F1**) and 2-nitroprop-1-ene (**G1**), the thermodecomposition mechanisms associated with the formation of 4-methyl-4*H*-1,2-oxazete 2-oxide (**F2**) and 3-methyl-4*H*-1,2-oxazete 2-oxide (**G2**), respectively, in the primary steps are probably the only possible ones, since the activation enthalpy of the primary step of the formation of these oxazetes has the lowest value among all the studied primary processes of thermal decomposition (Table 11).

**Table 11.** Activation enthalpies (kJ mol<sup>-1</sup>) of processes (45)–(52) for substituted nitropropenes calculated by B3LYP/6-31G(d).<sup>76–78</sup>

Process	<i>cis</i> -Nitropropene ( <b>E1</b> )	<i>trans</i> -Nitropropene ( <b>F1</b> )	2-Nitroprop-1-ene ( <b>G1</b> )	2-Methyl-1-nitroprop-1-ene ( <b>H1</b> )
(45)	281.1 303.3 <sup>a</sup> 266.1 <sup>d</sup>	291.8	270.7 (146.0) <sup>b</sup>	288.4 (~251) <sup>c</sup>
(46)	240.6	251.3	233.9	239.1
(47)	255.3	255.5		252.8
(48)	197.3	186.8 (176.8) <sup>c</sup>	196.7 (155.0) <sup>b</sup>	182.2
(49)		248.2	223.8 (155.0) <sup>b</sup>	
(50)			217.3	
(51)			254.2	
(52)	140.7 ~176.6 <sup>a</sup>			139.8 (151.5) <sup>c</sup>

**Note.** In parentheses, experimental data are given.

<sup>a</sup> Calculation<sup>79</sup> by MP2/6-31G(d); <sup>b</sup> Ref. 80; <sup>c</sup> Ref. 81; <sup>d</sup> calculation<sup>79</sup> by MP4/6-31G(d) + ZPE; <sup>e</sup> Refs 56 and 81.

This is also confirmed by the examination of secondary processes of gas-phase thermodecomposition of *trans*-nitropropene (**F1**) (Fig. 16).<sup>77, 78</sup>

The rate-limiting step of the thermal decomposition of compound **F1** is the cyclization to oxazete **F2** (48), *i.e.*, its primary step. Further development of the process is associated with the generation of the singlet biradical **F3** in an intermediate step, which either isomerizes followed by its decomposition into acetaldehyde and nitrile oxide (**F7**), or rearranges to 2-oxopropanal 1-oxime (**F8**) and eventually decomposes into experimentally observed products (hydrogen cyanide and acetic acid, water, methane, methyl alcoh-

ol, *etc.*). It should be noted that oxime **F8** can result from the bimolecular reaction of nitrile oxide with acetaldehyde.

Examination of secondary reactions of the decomposition of *cis*-nitropropene (**E1**) that occur to yield 4-methyl-4*H*-1,2-oxazete 2-oxide (**E2**) in the rate-limiting step (Fig. 17) demonstrated that this mechanism is analogous to that discussed for nitroethylene (**C1**) and *trans*-nitropropene (**F1**).

Analyzing data in Table 11, one can draw a conclusion that for *cis*-nitropropene and 2-methyl-1-nitroprop-1-ene the decomposition channels associated with the 1,5-sigmatropic hydrogen shift from a hydrogen-containing substituent to an oxygen of the NO<sub>2</sub> group [reaction (52)] are preferable. However, examination of secondary processes refutes the unambiguity of this deduction.

For the first time, this mechanism was studied for compound **E1** by the *ab initio* method MP2/6-31G(d) in 1993.<sup>79</sup> A scheme suggested and calculated for the decomposition of *cis*-nitropropene (**E1**) is illustrated in Fig. 18.

The rate-limiting step of mechanism (52) is the conversion of *aci*-form (**E23**) to 2-hydroxy-2,5-dihydroisoxazole (**E25**) rather than the primary step, *i.e.*, its formation. This conclusion was also justified by a later examination by the density functional method B3LYP/6-31G(d) (Fig. 19),<sup>76–78</sup> albeit the decomposition scheme was somewhat different from that proposed.<sup>79</sup>

In particular, further destruction of isoxazoline **E25** can occur through rearrangements to propanedial (1*E*)-oxime (**E37**), which dissociates into water and 3-oxopropionitrile (**E38**). The latter decomposes into acetonitrile and CO (**E39**). However, this channel is energetically unfavourable because its barrier exceeds the activation enthalpy of the rate-limiting step.

An alternative route of the development of this process is associated with the generation of singlet biradical **E27**, which can isomerize *via* oxirane-2-carbaldehyde oxime (**E28** or **E29**) to biradical (**E30**); the latter affords oxime **E37** in several steps. Oxime **E37** has twelve rotational isomers, *e.g.*, structures **E31**–**E36** (see Fig. 19); others are omitted. The relative activation enthalpy of the most energetically unfavourable reaction of this chain is almost 7 kJ mol<sup>-1</sup> lower than the activation enthalpy of the rate-limiting step of the overall process. The mechanism of the further decomposition of oxime **E37** is analogous to that of its direct formation from isoxazole **E25**, which has been described earlier (see Fig. 19).

Thus, for *cis*-nitropropene the relative enthalpy of formation of the transition state of the rate-limiting step of mechanism (52) associated with a 1,5-sigmatropic shift of hydrogen is merely 14.8 kJ mol<sup>-1</sup> lower than the barrier to the rate-limiting step of process (48). Therefore, these two channels can compete well with each other.

For compound **H1**, the probability of the occurrence of gas-phase decomposition reactions *via* 4,4-dimethyl-4*H*-1,2-oxazete 2-oxide (**H2**) followed by its destruction according to the biradical scheme substantially increases as compared to that for *cis*-nitropropene. The rate-determining step, which is also the formation of 2-hydroxy-4-methyl-2,5-dihydroisoxazole (**H8**), of the alternative mechanism (52) of the formation of *aci*-form as a result of a 1,5-sigmatropic shift of hydrogen to the nitro group has the relative activation enthalpy that is somewhat higher than the barrier to the rate-determining step of cyclization to 4,4-dimethyl-4*H*-1,2-oxazete 2-oxide (see Table 11, Fig. 20).

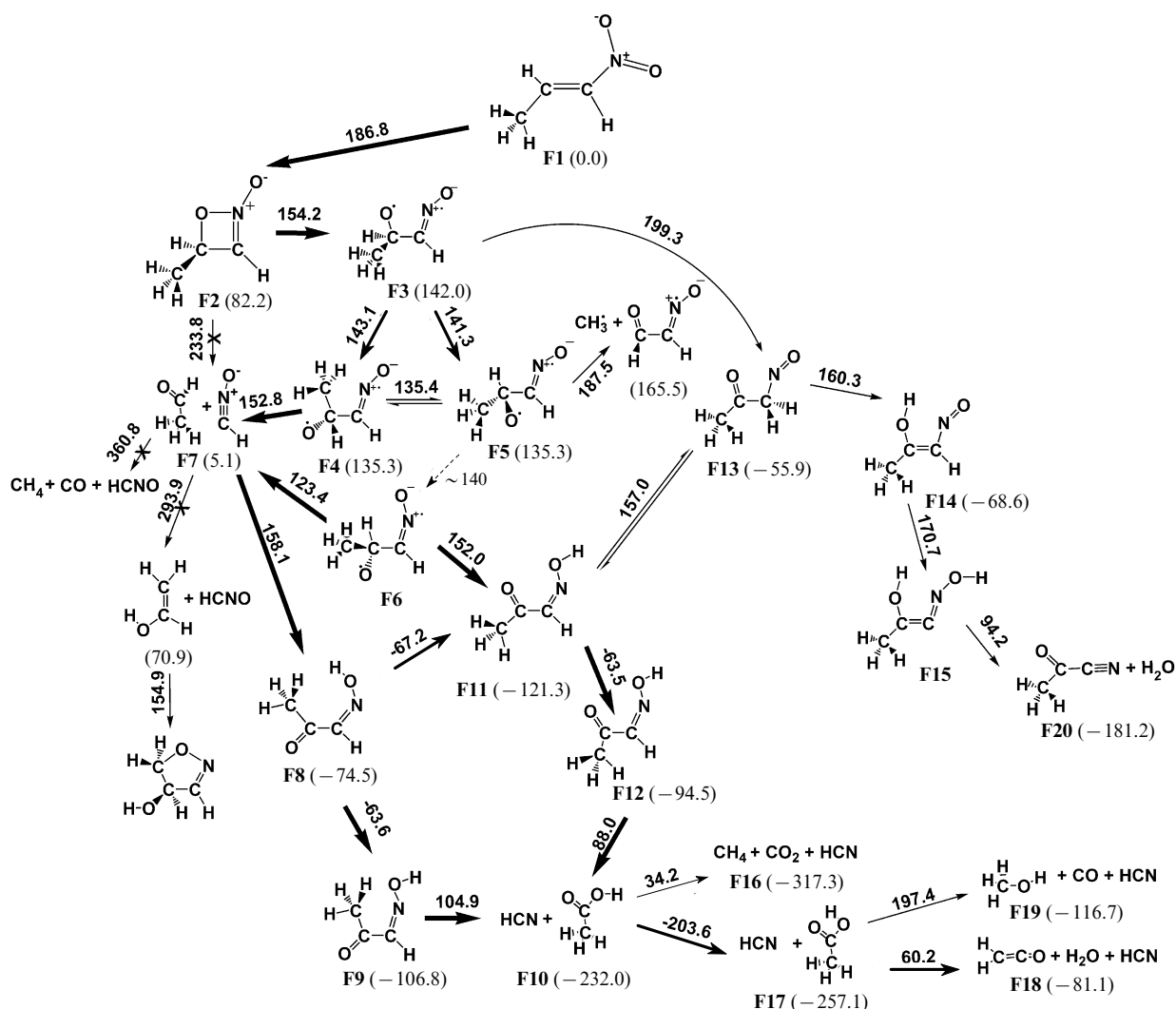


**Figure 16.** A scheme of a mechanism of decomposition of *trans*-nitropropene (**F1**) [B3LYP/6-31G(d)].<sup>77, 78</sup> Hereinafter, thick arrows indicate the most probable, thin arrows indicate a possible and crossed arrows indicate a low probable direction of the process. The enthalpy of formation of *trans*-nitropropene was chosen as zero.

Figures 21–24 illustrate the structures of the transition states and reaction products of the primary steps and rate-limiting steps of major mechanisms of the thermal decomposition of nitropropenes.

Thus, for substituted nitropropenes the major channel of thermodecomposition is the mechanism that pertains to the formation of different oxazetes at the primary step. For nitropropenes bearing a hydrogen-containing substituent in the *cis*-position with respect to the nitro group, this channel can compete with the mechanism where the primary step is a 1,5-sigmatropic shift of hydrogen from the RH group to the NO<sub>2</sub> group.

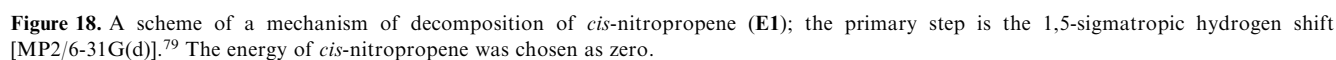
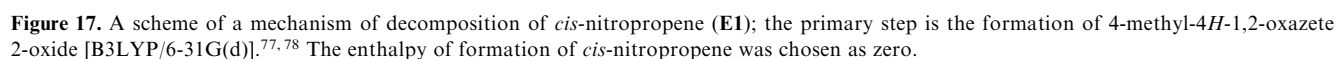
### 3. Mechanism of the thermal decomposition of aminonitroethylenes

Of definite scientific and practical interest is the investigation into the mechanism of thermal decomposition of aminonitroethylenes (*cis*- and *trans*-aminonitroethylenes **II** and **JI**, respectively), 1,1-diamino-2-nitroethylene (**KI**)<sup>82–84</sup> in connection with the prospects of the utilization of one of the representatives of this class of compounds, namely, 1,1-diamino-2,2-dinitroethylene (FOX-7) (**LI**), as

an explosive.<sup>61, 82, 85</sup> The importance of this problem explains numerous works that address the theoretical and experimental study of the synthesis and reactivity,<sup>58, 61, 86–89</sup> chemical and physical properties,<sup>58, 59, 86, 90–97</sup> structure,<sup>59, 61, 98</sup> kinetics and thermodecomposition mechanism<sup>82, 85, 99–101</sup> of compound **L1**.<sup>102</sup>

For compounds **II**, **J1**, **K1** and **L1** the decomposition channels (45), (46) and (48) are likely [ $R = NH_2$ ,  $R' = R'' = H$  (**II**);  $R = R'' = H$ ,  $R' = NH_2$  (**J1**);  $R = R' = NH_2$ ,  $R'' = H$  (**K1**);  $R = R' = NH_2$ ,  $R'' = NO_2$  (**L1**)]. For aminonitroethylenes **II**, **J1** and **K1** reaction (47) is allowed [ $R = NH_2$ ,  $R' = H$  (**II**);  $R = H$ ,  $R' = NH_2$  (**J1**);  $R = R' = NH_2$  (**K1**)]. In addition, for *trans*-aminonitropropene (**J1**) elimination of nitrous acid by reaction (49) is possible ( $R = NH_2$ ,  $R' = H$ ) and the 1,5-sigmatropic shift of a hydrogen atom from  $RH$  to the nitro group [reaction (52)] is feasible for *cis*-aminonitroethylene (**II**), 1,1-diamino-2-nitroethylene (**K1**) and FOX-7 (**L1**) [ $R = NH$ ,  $R' = R'' = H$  (**II**);  $R = NH$ ,  $R' = NH_2$ ,  $R'' = H$  (**K1**);  $R = NH$ ,  $R' = NH_2$ ,  $R'' = NO_2$  (**L1**)].

As evident by inspecting Table 12, the only possible decomposition channel of compound **J1** is the formation





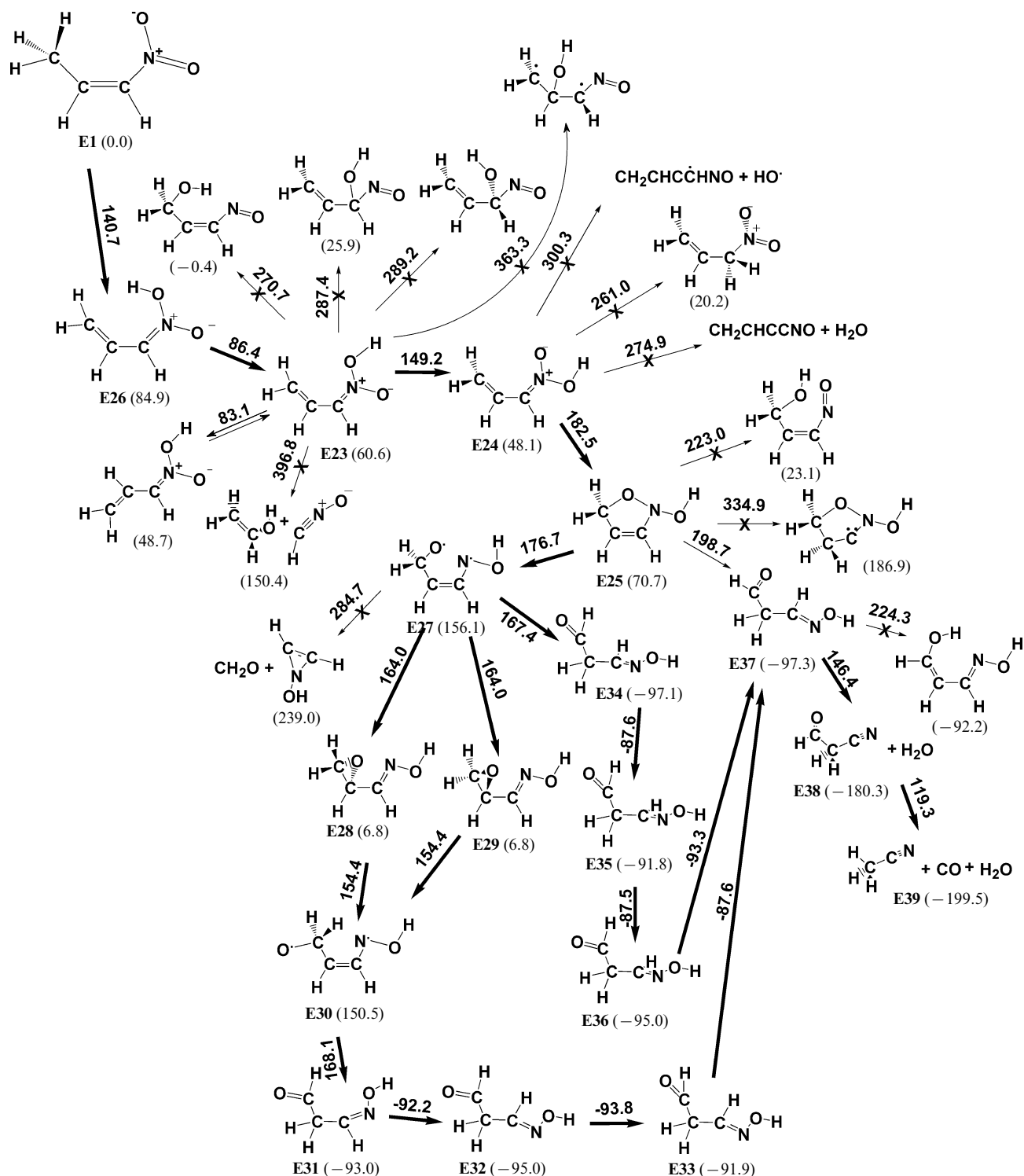


**Figure 19.** A scheme of a mechanism of decomposition of *cis*-nitropropene (E1); the primary step is the 1,5-sigmatropic hydrogen shift [B3LYP/6-31G(d)].<sup>77, 78</sup> The enthalpy of formation of *cis*-nitropropene was chosen as zero.

of 4-amino-4*H*-1,2-oxazete 2-oxide (**J2**). This is also confirmed by a study of secondary processes (Fig. 25). The distinction between the decomposition scheme of *trans*-aminonitroethylene and that of nitroethylene and *trans*-nitropropene is that the rate-limiting step is one of secondary processes (see Fig. 25) rather than the primary step of the generation of oxazete **J2**, as it was in the case of compounds **C1** and **F1**.

The most energetically favourable decomposition channel of oxazete **J2**, as also of the majority of alkenes studied, is the formation of a singlet biradical (**J3**), followed by its isomerization.

Further process can lead to the decomposition of the singlet biradical **J3** into acetaldehyde and formamide, which initially yield a stable complex (**J7**) that lies energetically somewhat lower than infinitely remote molecules (see

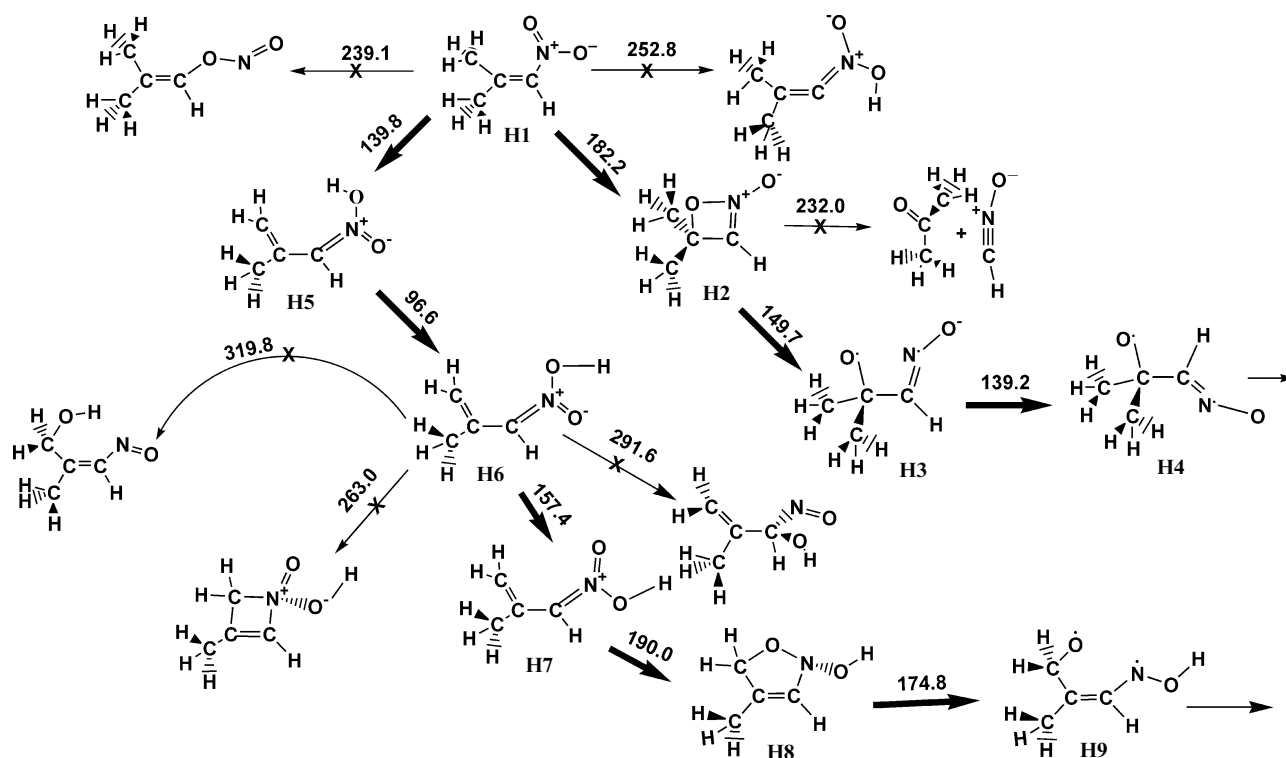


**Figure 20.** A scheme of a mechanism of decomposition of 2-methyl-1-nitroprop-1-ene (**H1**) [B3LYP/6-31G(d)].<sup>78</sup> The enthalpy of formation of 2-methyl-1-nitroprop-1-ene was chosen as zero.

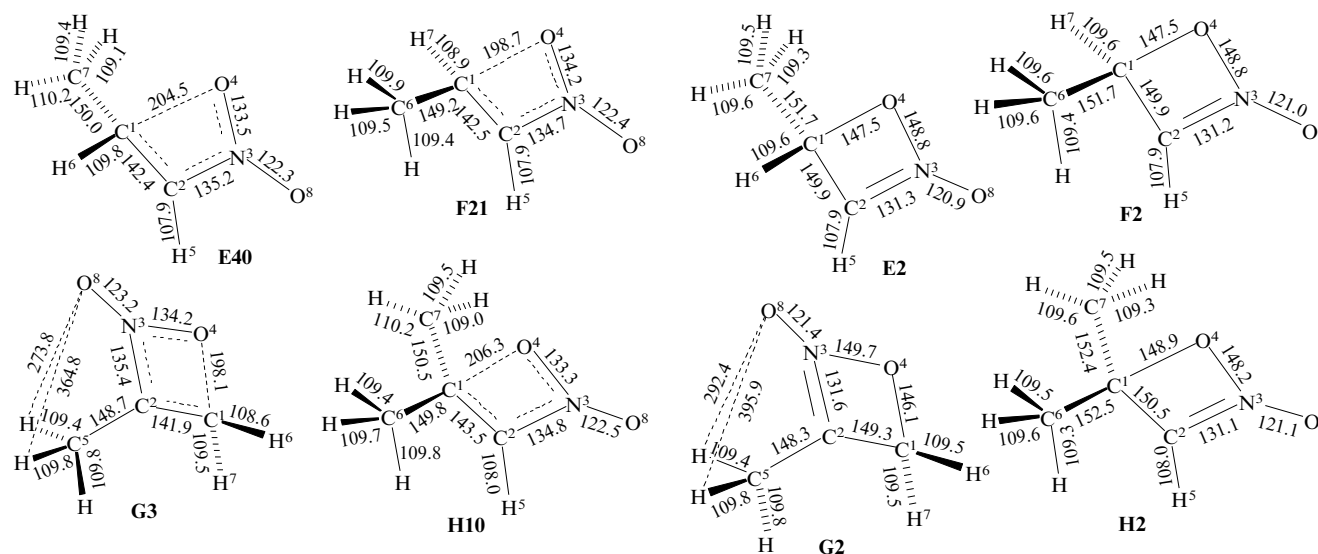


**Figure 21.** Bond lengths (pm) in the transition states of the oxazete formation from substituted and isomeric nitropropenes [at the (B3LYP/6-31G(d) level].<sup>76–78</sup> **E40**, from *cis*-nitropropene; **F21**, from *trans*-nitropropene; **G3**, from 2-nitroprop-1-ene; **H10**, from 2-methyl-1-nitroprop-1-ene.

**Figure 22.** Bond lengths (pm) in the molecules of cyclization products of substituted and isomeric nitropropenes [at the B3LYP/6-31G(d) level].<sup>76–78</sup> **E2** and **F2**, 2-methyl-4*H*-1,2-oxazete 2-oxide; **G2**, 3-methyl-4*H*-1,2-oxazete 2-oxide; **H2**, 4,4-dimethyl-4*H*-1,2-oxazete 2-oxide.

Fig. 25). This complex can isomerize under certain conditions to (*Z*)-2-(hydroxyimino)acetamide (**J8**). Through several isomerization steps, the latter decomposes to elementary products [hydrogen cyanide and carbamic acid (**J15** or **J12**), water, acetic anhydride, ammonia and carbon dioxide]. The second decomposition channel of biradical **J3** (see Fig. 25) is less probable as in the case of *cis*- and *trans*-

nitropropenes.<sup>78</sup> It proceeds through several steps of hydrogen atom transfer and formation of, for instance, carbamoyl cyanide and water (**J19**).

For *cis*-aminonitroethylene (**I1**), the formation of cyclic intermediate (**I2**) and its further decomposition proceed like the corresponding processes for compound **J1** (see Fig. 25).

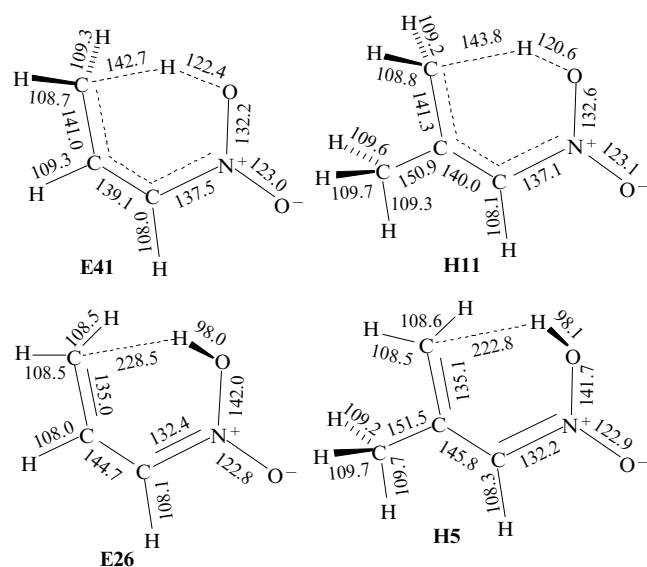


**Figure 23.** Bond lengths (pm) in the transition states and molecules of reaction products of 1,5-sigmatropic hydrogen shift to *aci*-forms for *cis*-nitropropene (**E41** and **E26**) and 2-methyl-1-nitroprop-1-ene (**H11** and **H5**) [by the B3LYP/6-31G(d) method].<sup>76–78</sup>

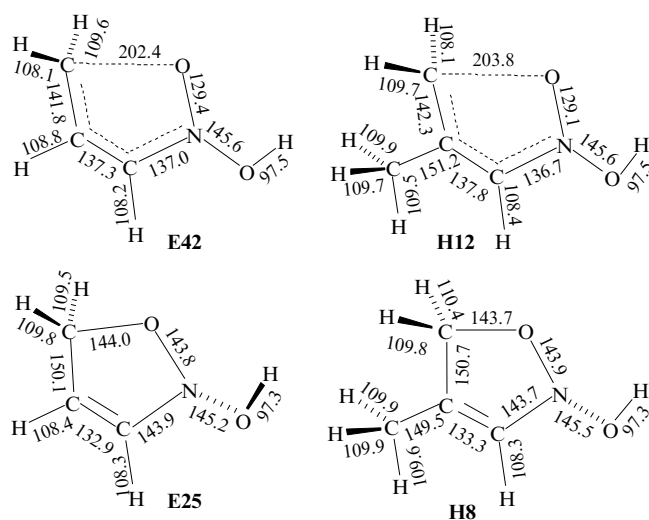


**Figure 24.** Bond lengths (pm) in the transition states and molecules of reaction products of the formation of 2-hydroxy-2,5-dihydroisoxazole (**E42** and **E25**) and 2-hydroxy-4-methyl-2,5-dihydroisoxazole (**H12** and **H8**) [by the B3LYP/6-31G(d) method].<sup>76–78</sup>

The presence of a hydrogen-containing substituent in the *cis*-position with respect to the nitro group results in a possibility, in principle, of another decomposition mechanism that relates to the 1,5-sigmatropic hydrogen shift from the NH<sub>2</sub> group to the NO<sub>2</sub> group for aminonitroethylenes **II**, **K1** and **L1**. The primary steps of these processes for the indicated compounds have activation enthalpies that are significantly lower than the barriers to alternative reactions (see Table 12). It would seem that the results obtained permit an unambiguous conclusion that the gas-phase destruction of the indicated compounds proceeds through the **II**, **K1** and **L1** pathways. Nevertheless, the

**Table 12.** Activation enthalpies (kJ mol<sup>−1</sup>) of processes (45)–(49), (52) for some aminonitroethylenes, calculated by the B3LYP/6-31G(d) method.<sup>82–84</sup>

Process	<i>cis</i> -Amino-nitroethylene ( <b>II</b> )	<i>trans</i> -Amino-nitroethylene ( <b>J1</b> )	1,1-Diamino-2-nitroethylene ( <b>K1</b> )	1,1-Diamino-2,2-nitroethylene ( <b>L1</b> )
(45)	336.5 (348.1) <sup>a</sup> (302.5) <sup>c</sup> (349.8) <sup>b</sup>	321.8 (336.4) <sup>b</sup>	350.6	283.0 (292.9) <sup>b</sup> (267.8) <sup>d</sup> (280.7) <sup>c</sup>
(46)	262.3	266.8	273.1	243.8 (241.3) <sup>c</sup>
(47)	251.5	235.3	230.5	
(48)	183.7	128.0	134.4	124.6
(49)		281.3		
(52)	43.1 (64.0) <sup>a</sup>		31.4	124.2

**Note.** The kinetic estimates of the activation energy (kJ mol<sup>−1</sup>) of thermodecomposition of FOX-7 (**L1**) by different methods are as follows: 338.8 (solid phase),<sup>99</sup> ~250 (amorphous state) and ~290 (crystal),<sup>101</sup> 238.3 (amorphous state) and 322.4 (crystal).<sup>102</sup>

<sup>a</sup> Calculated<sup>79</sup> at the MP2/6-31G(d) level; <sup>b</sup> calculated<sup>61</sup> at the B3P86/6-31G+(d,p) level; <sup>c</sup> calculated<sup>79</sup> at the MP4/6-31G(d)+ZPE level; <sup>d</sup> calculated<sup>85</sup> at the B3LYP/aug-cc-pVDZ level; <sup>e</sup> calculated<sup>60</sup> at the B3LYP/6-31+G(d,p) level.

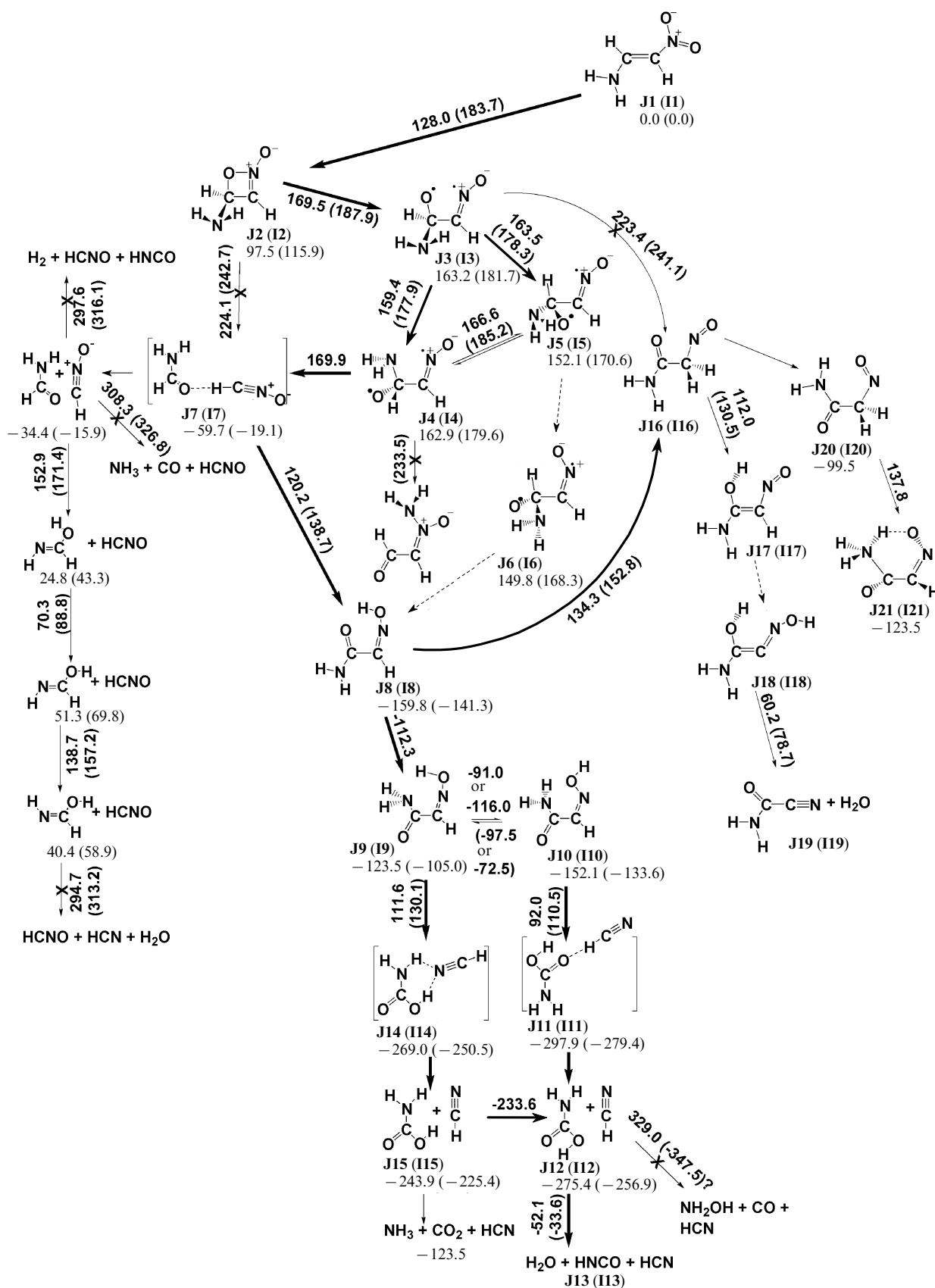
examination of secondary processes of the reaction showed that this is not the case.

Initially, the decomposition scheme of *cis*-aminonitroethylene (**II**) according to mechanism (52) was studied<sup>79</sup> by the MP2/6-31G(d) method (Fig. 26). As in the case of *cis*-nitropropene, the rate-determining step of process (52) is the formation of 1,2,5-oxadiazol-2(5*H*)-ole (**I25**) rather than the primary step. This inference is also verified by the investigation of the decomposition processes of aminonitroethylene (**II**) at the B3LYP/6-31G(d) level.<sup>83, 84</sup> However, unlike that of compound **E1**, the relative activation enthalpy of this stage is substantially (almost 1.5 times) higher than the barrier to the rate-limiting step of the cyclization channel (see Table 12, Fig. 27). All attempts to find a decomposition pathway of the *aci*-form of compound **II** (see Fig. 27) the energy barrier of which would be lower than the activation enthalpy of the rate-determining step of the formation of 4-amino-4*H*-1,2-oxazete 2-oxide proved unsuccessful. Thus, the channel associated with energetically favourable 1,5-sigmatropic shift of a hydrogen atom from the RH group to the NO<sub>2</sub> group is presumably a dead end.

Table 13 lists data on the investigation of the rate-limiting step of process (52) for 1,1-diamino-2-nitroethylene and 1,1-diamino-2,2-dinitroethylene.<sup>82</sup>

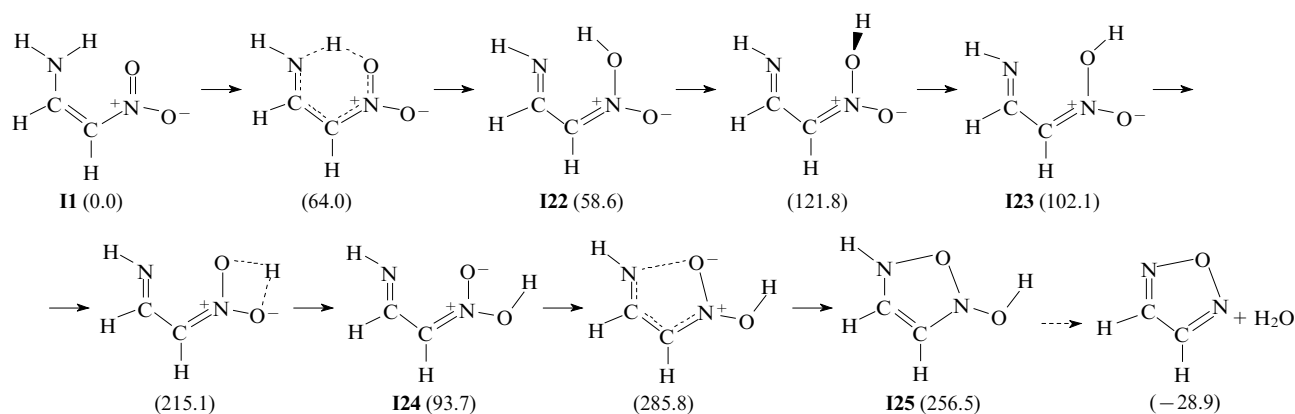
The relative enthalpies of formation of transition states in the reactions that result, after a number of conformational transitions, in 4-amino-2-hydroxy-2,5-dihydro-1,2,5-oxadiazole (**K4**) and 4-amino-2-hydroxy-3-nitro-2,5-dihydro-1,2,5-oxadiazole (**L4**) from the *aci*-forms of compounds **K1** and **L1**, respectively, exceed almost twice the barriers to the rate-limiting steps of the formation of 4,4-diamino-4*H*-1,2-oxazete 2-oxide (**K2**) and 4,4-diamino-3-nitro-4*H*-1,2-oxazete 2-oxide (**L2**).

Figures 28–30 show the structures of the transition states and reaction products of the primary steps and

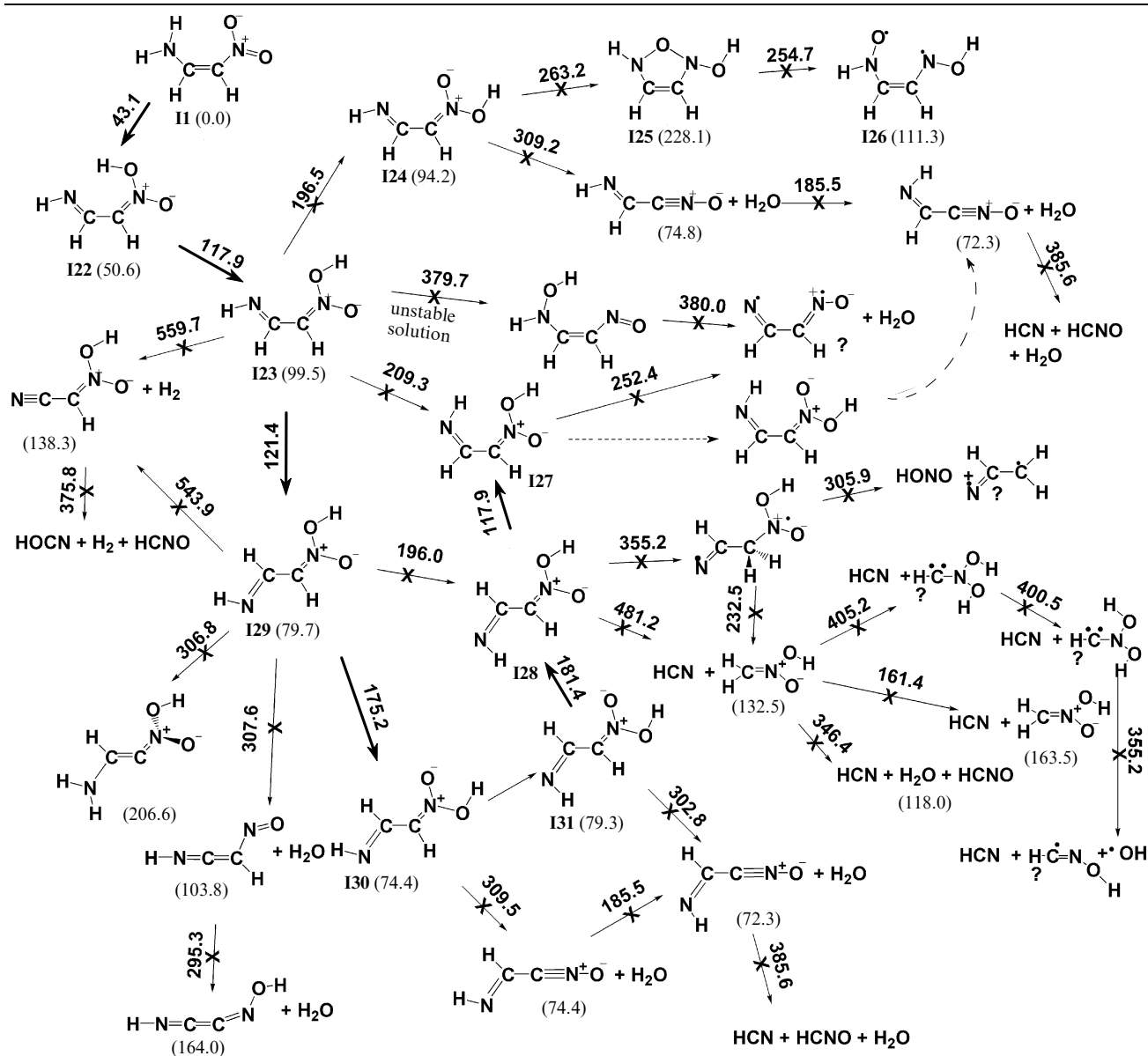


**Figure 25.** A scheme of a mechanism of decomposition of *trans*-aminonitroethylene (J1) and *cis*-aminonitroethylene (II) [by the B3LYP/6-31G(d) method].<sup>82–84</sup>

The enthalpies of formation of compounds J1 and II, respectively, were taken as zeros; the values for the thermodecomposition of *cis*-aminonitroethylene are given in parentheses. The process J9 (19) ⇌ J10 (110) can proceed through two transition states that have different enthalpies of formation. The transition states differ in the rotation angles of the OH group.

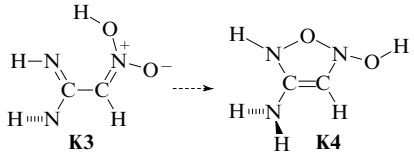
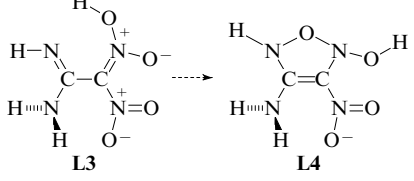


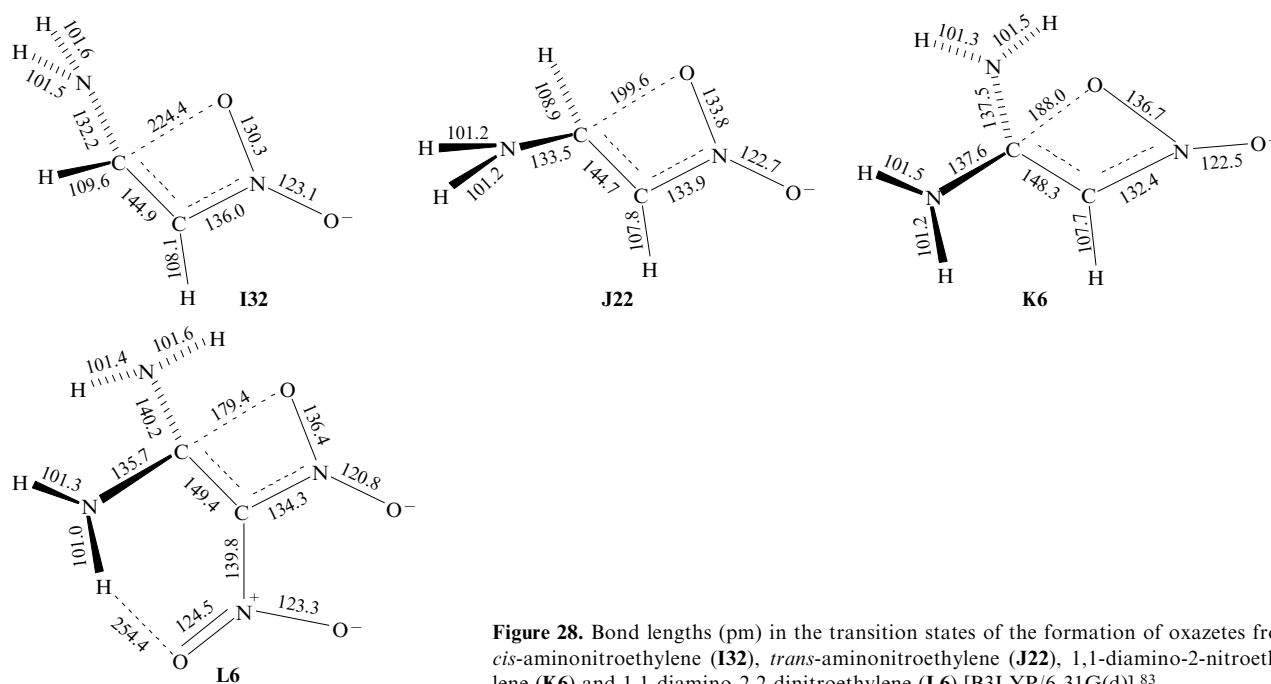
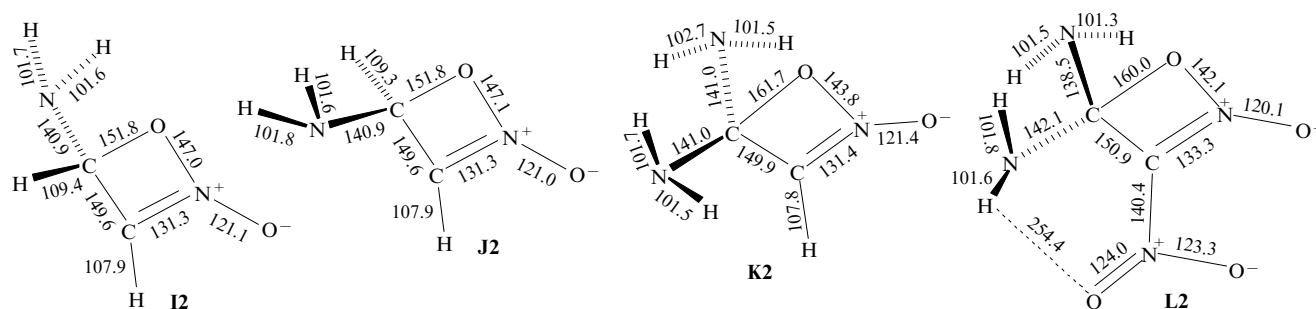
**Figure 26.** A scheme of a mechanism of decomposition of *cis*-aminonitroethylene (II); the primary step is 1,5-sigmatropic hydrogen shift from RH to the NO<sub>2</sub> group [MP2/6-31G(d)].<sup>79</sup> The energy of *cis*-aminonitroethylene was taken as zero.



**Figure 27.** A scheme of a mechanism of decomposition of *cis*-aminonitroethylene (II); the primary step is 1,5-sigmatropic hydrogen shift from RH to the NO<sub>2</sub> group [B3LYP/6-31G(d)].<sup>82–84</sup> The enthalpy of formation of *cis*-aminonitroethylene was taken as zero. The question mark denotes hypothetical structures.

**Table 13.** The rate-limiting steps of the 1,5-sigmatropic hydrogen shift from a hydrogen-containing substituent to the nitro group and their activation enthalpies for different aminonitroethylenes [B3LYP/6-31G(d), the enthalpies of formation of the corresponding compounds were taken as zero].

Compound	Process	$\Delta H_{298}^\ddagger / \text{kJ mol}^{-1}$
1,1-Diamino-2-nitroethylene ( <b>K1</b> )		274.9
1,1-Diamino-2,2-dinitroethylene ( <b>L1</b> )		228.0

**Figure 28.** Bond lengths (pm) in the transition states of the formation of oxazetes from *cis*-aminonitroethylene (**I32**), *trans*-aminonitroethylene (**J22**), 1,1-diamino-2-nitroethylene (**K6**) and 1,1-diamino-2,2-dinitroethylene (**L6**) [B3LYP/6-31G(d)].<sup>83</sup>**Figure 29.** Bond lengths (pm) in the molecules of cyclization products of substituted and isomeric aminonitroethylenes [(B3LYP/6-31G(d)).<sup>83</sup> **I2** and **J2**, 4-amino-4H-1,2-oxazete 2-oxide; **K2**, 4,4-diamino-4H-1,2-oxazete 2-oxide; **L2**, 4,4-diamino-3-nitro-4H-1,2-oxazete 2-oxide.

major mechanisms of the thermal destruction of nitropropenes.

Therefore, the formation of various substituted oxazetes seems to be the most favorable channel for gas-phase

decomposition of aminonitroethylenes as in the case of nitroethylene and nitropropenes. Nevertheless, it is early to put an end to this issue as yet.

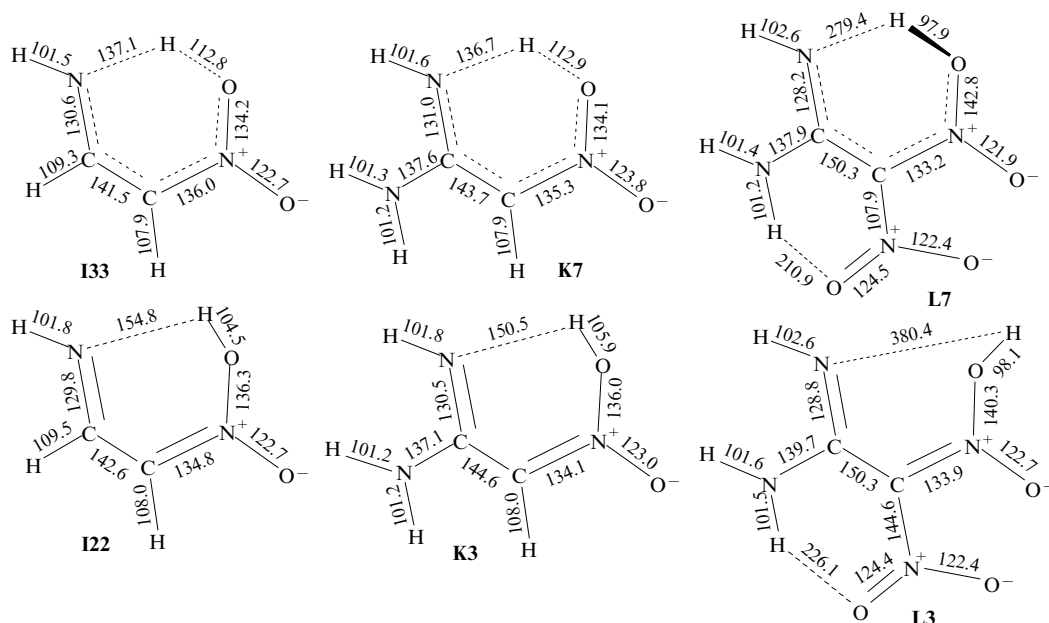


**Figure 30.** Bond lengths (pm) in the transition states and molecules of reaction products of 1,5-sigmatropic hydrogen shift to *aci*-forms for *cis*-aminonitroethylene (I33 and I22), 1,1-diamino-2-nitroethylene (K7 and K3) and 1,1-diamino-2,2-dinitroethylene (L7 and L3) [B3LYP/6-31G(d)].<sup>83</sup>

#### IV. Mechanisms of the gas-phase monomolecular decomposition of nitrobenzene and its derivatives

The thermal decomposition of aromatic nitro compounds in the gaseous state occurs in a very sophisticated manner, which complicates obtaining reliable kinetic data corresponding to the primary reaction steps. A controversial question is also the mechanism of the decomposition, since there is no sufficient body of experimental observations on the barriers to various alternative mechanisms of monomolecular decomposition.<sup>2</sup> Even thermochemical estimates of the enthalpies of formation of compounds and dissociation energies of different bonds in the nitrobenzene series are comparatively few in number, and their accuracies are inferior to those of the data obtained for nitroalkanes.<sup>103, 104</sup> Hence, the use of quantum chemical methods for studying the structures and reactivities of nitroarenes in the gas-phase monomolecular decomposition is of special interest.

On this road, however, there are considerable obstacles. The experimental values of the Arrhenius parameters that are stated to correspond to the primary step of gas-phase decomposition, which were obtained in different research groups, substantially differ.<sup>2</sup> Data on the structures of products at the initial steps of decomposition obtained by using, for the most part, mass spectrometry do not allow unambiguous inferences on the reaction mechanisms to be made.<sup>105–108</sup> There are also problems in obtaining and interpreting information on low-frequency vibrations of molecules, which is required for the calculation of the pre-exponential factors of reactions. The situation regarding the structures of free molecules of nitroarenes is somewhat better. By microwave spectroscopy and gas electron diffraction, a sufficiently large body of data was obtained.<sup>109, 110</sup> At the same time, in this case, too, there are certain problems, particularly in studying the rotation barriers of functional groups. Another serious hurdle on the route of the research of the gas-phase decomposition mechanism of nitrobenzenes is relatively large sizes of molecules, which

limits the application of most powerful and reliable *ab initio* methods.

The chemistry of aromatic compounds is rich and diverse, and the number of different development pathways of thermal decomposition reactions is enormous. At the beginning we shall consider various alternative mechanisms of gas-phase decomposition by the example of nitrobenzene (M1), and then we shall discuss characteristics of the influence of the molecular structure on the competition of these processes. The theoretical investigation of the gas-phase decomposition of nitrobenzene was carried out by various methods.<sup>12, 111, 112</sup> All the principal mechanisms of the monomolecular decomposition of nitrobenzene were calculated<sup>112</sup> by PBE/L1 with the use of the 'Priroda' ('Nature') computer programme<sup>113</sup> and the hybrid DFT method B3LYP/6-31G(d,p) with the aid of the Gaussian03 software.<sup>114</sup> The estimates of the value of  $D(\text{C}-\text{N})$ , 284.7 and 292.6 kJ mol<sup>-1</sup> obtained by these methods, are close enough to each other and agree well with the most reliable value of the activation energy of the gas-phase decomposition of nitrobenzene equal to 291.6 kJ mol<sup>-1</sup> (Ref. 81). The value of  $D(\text{C}-\text{N})$  for nitrobenzene derived from experimental data by Eqn (2) and equal to 285.8 kJ mol<sup>-1</sup> lies between the two calculated theoretical values quoted above. Let us note that good estimates of  $D(\text{C}-\text{N})$  are provided by the majority of quantum chemical methods including semi-empirical ones.<sup>12</sup>

Structures of transition states and activation barriers of studied reactions of the non-radical decomposition of nitrobenzene are illustrated in Fig. 31. Based on these data, one can make a conclusion that two processes can compete with the homolytic dissociation of the C-NO<sub>2</sub> bond: NNR and the formation of a bicyclic intermediate, (6S)-7-oxa-8-azabicyclo[4.2.0]octa-1(8),2,4-triene N-oxide (M7), which has not been studied earlier in the aromatic compound series. Analogous cyclization reactions were discussed in Section III.1 for the gas-phase decomposition of nitroethylene. The activation barriers to NNR and cyclization are similar and lower than  $D(\text{C}-\text{N})$ .<sup>112</sup>

The pre-exponential factor of radical decomposition [from experimental estimates,<sup>115</sup>  $\log A = 17.3$  (s<sup>-1</sup>)] is sub-

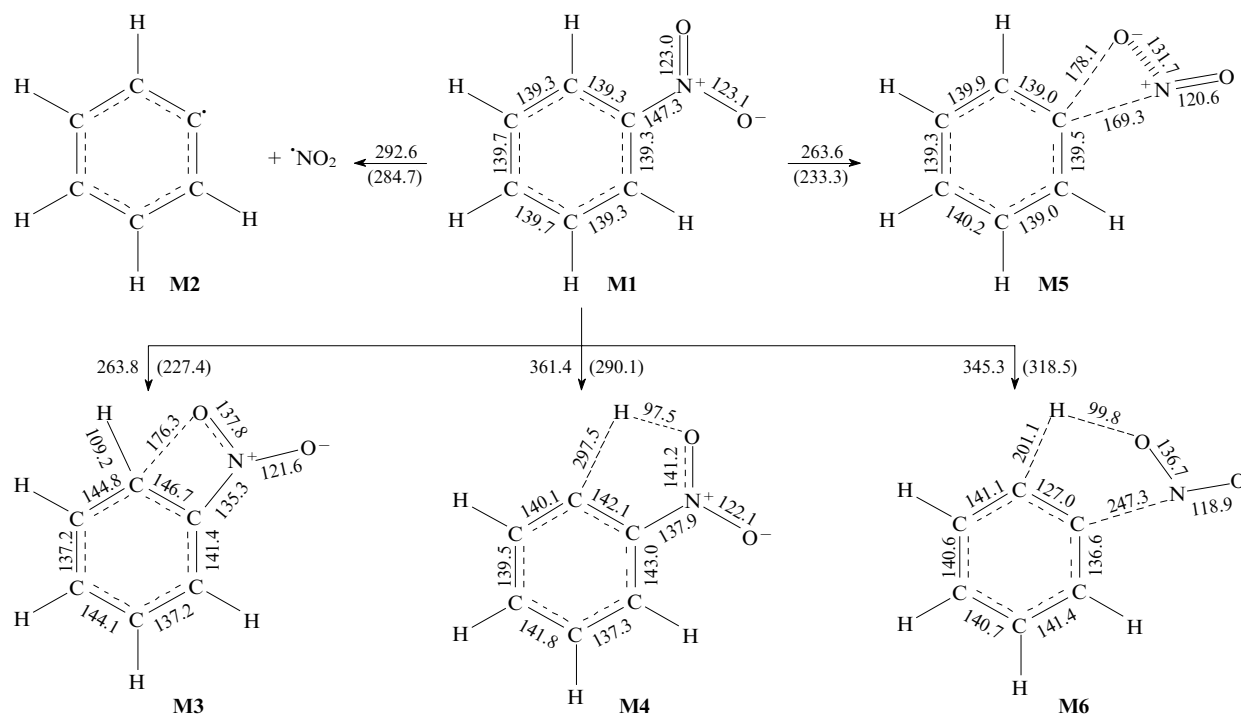


**Figure 31.** Bond lengths (pm) in the transition states and activation enthalpies [by the B3LYP/6-31G(d,p) and by PBE/L1 methods (in parentheses); kJ mol<sup>-1</sup>] of the primary steps of the monomolecular decomposition reaction of nitrobenzene.<sup>112</sup> **M2** is the radical decomposition, **M3** is the cyclization, **M4** is the formation of an *aci*-form, **M5** is the nitro-nitrite rearrangement, **M6** is the elimination of HNO<sub>2</sub>.

stantially higher than those of the molecular mechanisms involved. However, lower activation barriers permit the NNR and cyclization to compete with the radical decomposition at relatively low temperatures. A rigorous theoretical calculation allowing for the hindered rotation of functional groups has not been conducted for the non-radical decomposition of nitrobenzene. At the PBE/L1 level, the estimated<sup>112</sup> values of  $\log A$  for NNR and cyclization are 13.0 and 12.1 (s<sup>-1</sup>), respectively; B3LYP/6-31G(d,p) provides similar values: 13.05 and 12.1 (s<sup>-1</sup>) (the estimates were obtained for  $T = 298.15$  K). According to recent data,<sup>31</sup> the value of  $\log A$  in the reactions of non-radical decomposition depends on temperature comparatively weakly, and for rough estimates this dependence can be ignored. Considering the above-listed assumptions, at  $T = 600$  K the NNR rate assessed by PBE/L1 is  $\sim 1.4$  times that of radical decomposition, while cyclization proceeds approximately two times slower than the homolytic cleavage of the C-NO<sub>2</sub> bond. At 700 K, the situation changes, and the rate of radical decomposition becomes 2.5 times higher than that of NNR. According to B3LYP, the rate of radical decomposition is higher than those of alternative molecular processes even at 600 K. However, these outcomes do not exclude a possibility of competition at lower temperatures.

The peculiarities of the gas-phase decomposition mechanism should be taken into account when developing a procedure for predicting the margin of chemical stability of explosives based on a high-temperature experiment. For the mechanistic schemes of the gas-phase radical decomposition of nitrobenzene discussed in the literature, there are no reliable experimental data.<sup>2</sup> Somewhat better matters stand with secondary decomposition reactions of phenyl nitrite (**M8**). Beyond any doubt is the fact that the dissociation

energy of the O-NO bond in this compound is considerably lower than the value of  $D(\text{C}-\text{N})$  for nitrobenzene.<sup>116</sup> However, the mechanism of further development of the decomposition process was not studied in detail. All the steps of the formation of a bicyclic intermediate (see Fig. 31) have barriers that are lower than  $D(\text{C}-\text{N})$  for nitrobenzene. This mechanism is sufficiently sophisticated, there is a large number of alternative channels. For the appreciation of the further development, the following processes are essential (Fig. 32).

1. The opening of the four-membered ring in the bicycle **M7** to generate the singlet biradical **M12**.

2. The opening of the benzene ring of the biradical **M12** to yield (2*E*,4*E*)-5-formylpenta-2,4-dienonitrile *N*-oxide (**M13**). This chain of transformations demonstrates that the intramolecular oxidation of nitrobenzene can compete with the cleavage of the C-N bond.

3. The 1,2-sigmatropic hydrogen shift in biradical **M12** to the adjacent CH group to afford 2-nitrosocyclohexa-2,4-dienone (**M14**).

4. The 1,3-sigmatropic hydrogen shift synchronized with abstraction of the NO group in compound **M14** to produce a complex of 6-oxocyclohexa-2,4-dienyl and NO (**M15**), in which the group N=O is located 195 pm above the benzene ring. It attracts attention that the most important steps of decomposition of nitrobenzene by this mechanism are akin to those of the gas-phase decomposition of nitroethylene.

One can assume at least three possible alternative mechanisms of the gas-phase decomposition of nitrobenzene that stem from the theoretical study: the homolytic dissociation of the C-NO<sub>2</sub> bond, the nitro-nitrite rearrangement and the formation of a bicyclic intermediate. For the first two of them we shall discuss the influence of the



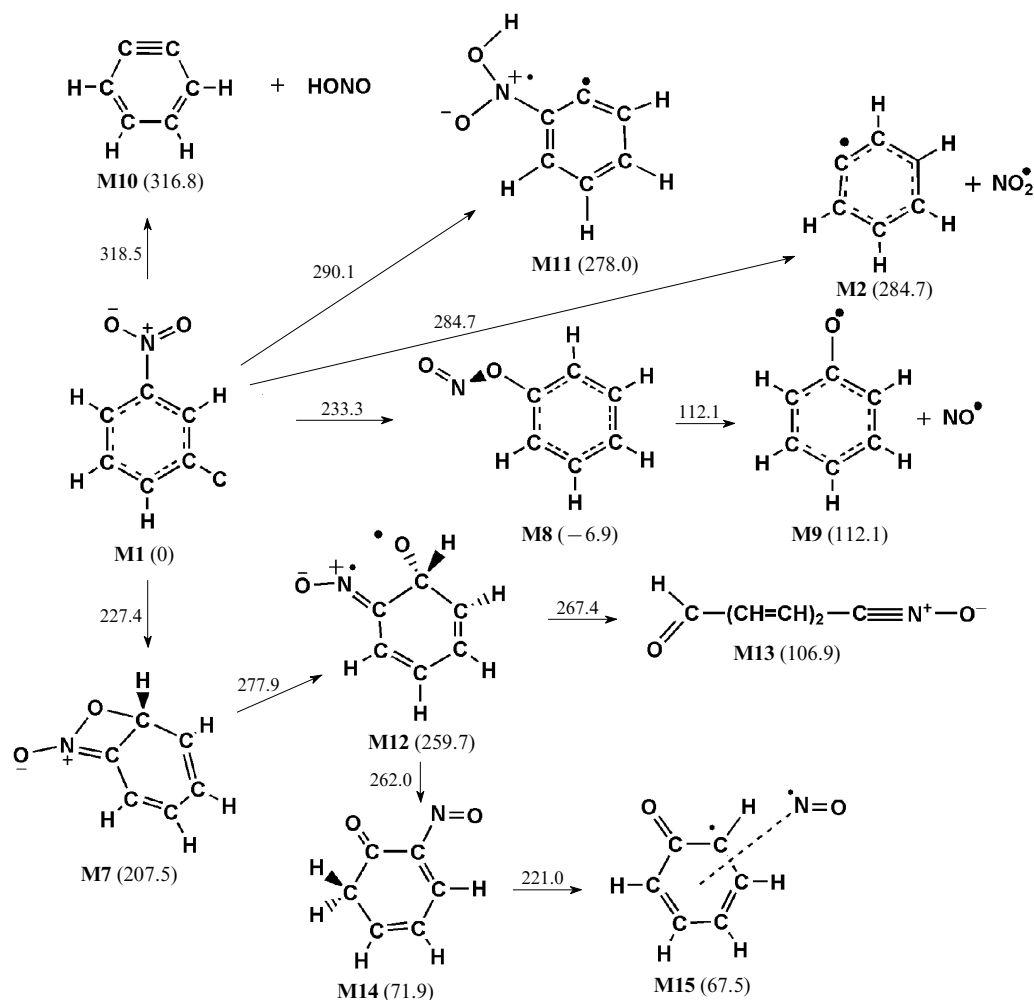


**Figure 32.** A scheme of a mechanism of decomposition of nitrobenzene (**M1**) (PBE/L1).<sup>112</sup> The enthalpy of formation of nitrobenzene was taken as zero.

molecular structure on changes in the reaction barriers. High activation enthalpy of the second step of the biradical opening of the four-membered ring in the bicyclic compound does not allow this mechanism to compete with NNR for nitrobenzene; however, electron-withdrawing substituents can alter the situation as it will be shown when considering the thermodecomposition of *o*-dinitrobenzene.

### 1. Radical decomposition of nitroarenes

What is presently regarded as firmly established is that nitrobenzene as well as the majority of its monofunctional derivatives: halonitrobenzenes, *m*- and *p*-nitroanilines, nitrotoluenes, and nitrophenols decompose by a radical mechanism at relatively high temperatures ( $\sim 700$ – $800$  K).<sup>8</sup> Apparently, the gas-phase decomposition of *m*- and *p*-dinitrobenzene, 1,3,5-trinitrobenzene and some other nitroarenes with electron-withdrawing substituents occur predominantly by this mechanism. The experimentally determined kinetic features of the gas-phase decomposition of nitroarenes as well as similarity of the obtained values of the dissociation energy of the C–N bond suggest the radical mechanism. This fact has been noted even in the first publications that addressed the quantum chemical calculations of the value of  $D(\text{C–N})$  for nitrobenzene.<sup>117</sup> Later, more detailed data were obtained that made it

possible to establish the fact that the strength and the length of the C–N bond in the nitroarene series change in parallel. It was demonstrated<sup>117,118</sup> that such dependences can be employed for the evaluation of the reliability of experimental results and the correspondence of the values of activation energy obtained to the radical mechanism. For instance, it was established that the experimental values of the activation energy of the gas-phase decomposition of *m*- and *p*-nitrotoluenes are underestimated. They fall out of a correlation that describes other monofunctional derivatives of nitrobenzene. The validity of this conclusion was confirmed by semi-empirical calculations<sup>119,120</sup> as well as by estimates of  $D(\text{C–N})$  made by density functional methods.<sup>116</sup>

Based on the analysis of experimental data, studies of molecular structures and calculations of  $D(\text{C–N})$ , it was established that in the nitroarene series most significant alterations in the  $r(\text{C–N})$  and  $D(\text{C–N})$  parameters take place upon the introduction of electron-donating substituents (halogen atoms, the  $\text{CH}_3$ ,  $\text{NH}_2$ ,  $\text{OH}$  groups) in *para*- and *ortho*-positions. In this case, the dissociation energy of the C–N bond and the barrier to the  $\text{NO}_2$  group rotations about the C–N bond increase.<sup>121</sup> The observed changes in the nitroarene series can be explained by a direct polar conjugation of the electron-donating substituents with the

electron acceptor (the NO<sub>2</sub> group).<sup>117</sup> In the presence of *meta* electron-donating substituents, the direct polar conjugation is absent, and, as a consequence, the calculation predicts considerably lesser alterations of  $r(\text{C}-\text{N})$ ,  $D(\text{C}-\text{N})$  and the rotational barriers of the nitro groups as compared with nitrobenzene. In the presence of *ortho* bulky groups that force rotation of the NO<sub>2</sub> groups relative to the benzene ring plane, the direct polar conjugation is distorted, which is accompanied by an increase in  $r(\text{C}-\text{N})$  and decrease in  $D(\text{C}-\text{N})$  and the rotational barriers of the NO<sub>2</sub> group. A correlation between the changes in the rotational barrier of the nitro group and the length of the C–N bond has been established.<sup>121</sup>

The trends indicated above are exemplified by calculations presented in Table 14 and Figures 33 and 34. Analogous factors, obviously, are also manifested in more complex aromatic nitro compounds containing several nitro groups and electron-donating substituents. Electron-withdrawing substituents, in particular, the NO<sub>2</sub> group, aldehyde and carboxyl groups bring about an increase in  $r(\text{C}-\text{N})$  and reduction in rotational barriers of the NO<sub>2</sub> groups.<sup>15</sup> It was shown<sup>117</sup> that using resonance substituent constants and a quantitative assessment of steric effects for *ortho*-substituted nitrobenzenes it is possible to determine with high accuracy the activation energies of virtually all the nitroarenes studied that decompose by the radical mechanism. The root-mean-square deviation of the calculated and experimental values for 14 compounds studied is 7.3 kJ mol<sup>−1</sup>. If we exclude *m*- and *p*-nitrotoluenes for which the experimental values of activation energy are evidently underestimated, the root-mean-square deviation will lower to 3.7 kJ mol<sup>−1</sup>.

Within the framework of this approach, one can estimate the activation energy of the radical decomposition of mono- and polyfunctional derivatives of nitrobenzene,

**Table 14.** Bond lengths (pm), dissociation energies [ $D(\text{C}-\text{N})/\text{kJ mol}^{-1}$ ] and rotation barriers of the NO<sub>2</sub> group ( $V_{\text{NO}_2}/\text{kJ mol}^{-1}$ ) in nitroarenes [calculated by B3LYP/6-31G(d)].

Compound	$r(\text{CN})$	$r(\text{NO})$	$D(\text{CN})$	$V_{\text{NO}_2}$
C <sub>6</sub> H <sub>5</sub> NO <sub>2</sub>	147.3	123.1	292.6	31.4
<i>o</i> -(CH <sub>3</sub> )C <sub>6</sub> H <sub>4</sub> NO <sub>2</sub>	147.5	123.1	281.9	18.0
<i>m</i> -(CH <sub>3</sub> )C <sub>6</sub> H <sub>4</sub> NO <sub>2</sub>	147.3	123.1	293.3	31.4
<i>p</i> -(CH <sub>3</sub> )C <sub>6</sub> H <sub>4</sub> NO <sub>2</sub>	146.9	123.2	296.8	33.1
<i>o</i> -(NH <sub>2</sub> )C <sub>6</sub> H <sub>4</sub> NO <sub>2</sub>	144.9	124.7	310.6	46.1
<i>m</i> -(NH <sub>2</sub> )C <sub>6</sub> H <sub>4</sub> NO <sub>2</sub>	147.4	123.2	294.6	31.4
<i>p</i> -(NH <sub>2</sub> )C <sub>6</sub> H <sub>4</sub> NO <sub>2</sub>	145.6	123.4	310.5	41.4
<i>o</i> -(OH)C <sub>6</sub> H <sub>4</sub> NO <sub>2</sub>	144.7	125.3	326.1	63.6
<i>m</i> -(OH)C <sub>6</sub> H <sub>4</sub> NO <sub>2</sub>	146.7	123.1	290.2	30.1
<i>p</i> -(OH)C <sub>6</sub> H <sub>4</sub> NO <sub>2</sub>	146.2	123.3	303.1	37.7
<i>o</i> -(NO <sub>2</sub> )C <sub>6</sub> H <sub>4</sub> NO <sub>2</sub>	147.5	122.8	244.8	5.0
<i>m</i> -(NO <sub>2</sub> )C <sub>6</sub> H <sub>4</sub> NO <sub>2</sub>	147.7	122.9	280.8	30.1
<i>p</i> -(NO <sub>2</sub> )C <sub>6</sub> H <sub>4</sub> NO <sub>2</sub>	147.8	122.9	279.7	27.6
C <sub>6</sub> H <sub>3</sub> (NO <sub>2</sub> ) <sub>3-1,3,5</sub>	147.9	122.7	271.0	28.9
<i>o</i> -FC <sub>6</sub> H <sub>4</sub> NO <sub>2</sub>	146.9	123.3	275.0	17.6
<i>m</i> -FC <sub>6</sub> H <sub>4</sub> NO <sub>2</sub>	147.5	123.0	287.3	30.5
<i>p</i> -FC <sub>6</sub> H <sub>4</sub> NO <sub>2</sub>	146.8	123.1	295.0	34.3
<i>o</i> -ClC <sub>6</sub> H <sub>4</sub> NO <sub>2</sub>	147.5	123.1	261.3	9.6
<i>m</i> -ClC <sub>6</sub> H <sub>4</sub> NO <sub>2</sub>	147.6	123.0	285.2	31.0
<i>p</i> -ClC <sub>6</sub> H <sub>4</sub> NO <sub>2</sub>	147.1	123.1	291.2	32.6
<i>o</i> -BrC <sub>6</sub> H <sub>4</sub> NO <sub>2</sub>	147.5	123.1	263.4	10.5
<i>m</i> -BrC <sub>6</sub> H <sub>4</sub> NO <sub>2</sub>	147.5	123.0	285.1	31.0
<i>p</i> -BrC <sub>6</sub> H <sub>4</sub> NO <sub>2</sub>	147.0	123.2	290.8	32.6

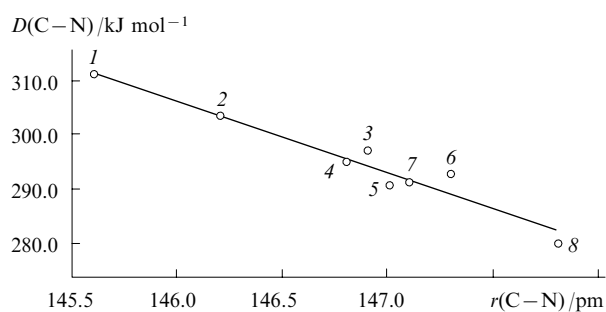


**Figure 33.** A correlation of the dissociation energy of the C–N bond with its length (the correlation coefficient is 0.94).

(1) *p*-(NH<sub>2</sub>)C<sub>6</sub>H<sub>4</sub>NO<sub>2</sub>, (2) *p*-(OH)C<sub>6</sub>H<sub>4</sub>NO<sub>2</sub>, (3) *p*-(CH<sub>3</sub>)C<sub>6</sub>H<sub>4</sub>NO<sub>2</sub>, (4) *p*-FC<sub>6</sub>H<sub>4</sub>NO<sub>2</sub>, (5) *p*-BrC<sub>6</sub>H<sub>4</sub>NO<sub>2</sub>, (6) C<sub>6</sub>H<sub>5</sub>NO<sub>2</sub>, (7) *p*-ClC<sub>6</sub>H<sub>4</sub>NO<sub>2</sub>, (8) *p*-C<sub>6</sub>H<sub>4</sub>(NO<sub>2</sub>)<sub>2</sub>.<sup>15</sup>

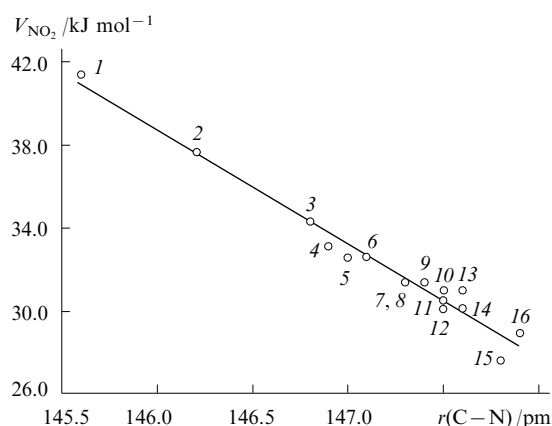


**Figure 34.** A correlation of the rotational barrier of nitro group with the length of the C–N bond (the correlation coefficient is 0.97).

(1) *p*-(NH<sub>2</sub>)C<sub>6</sub>H<sub>4</sub>NO<sub>2</sub>, (2) *p*-(OH)C<sub>6</sub>H<sub>4</sub>NO<sub>2</sub>, (3) *p*-FC<sub>6</sub>H<sub>4</sub>NO<sub>2</sub>, (4) *p*-(CH<sub>3</sub>)C<sub>6</sub>H<sub>4</sub>NO<sub>2</sub>, (5) *p*-BrC<sub>6</sub>H<sub>4</sub>NO<sub>2</sub>, (6) *p*-ClC<sub>6</sub>H<sub>4</sub>NO<sub>2</sub>, (7) C<sub>6</sub>H<sub>5</sub>NO<sub>2</sub>, (8) *m*-(CH<sub>3</sub>)C<sub>6</sub>H<sub>4</sub>NO<sub>2</sub>, (9) *m*-(NH<sub>2</sub>)C<sub>6</sub>H<sub>4</sub>NO<sub>2</sub>, (10) *m*-BrC<sub>6</sub>H<sub>4</sub>NO<sub>2</sub>, (11) *m*-FC<sub>6</sub>H<sub>4</sub>NO<sub>2</sub>, (12) *m*-(OH)C<sub>6</sub>H<sub>4</sub>NO<sub>2</sub>, (13) *m*-ClC<sub>6</sub>H<sub>4</sub>NO<sub>2</sub>, (14) *m*-C<sub>6</sub>H<sub>4</sub>(NO<sub>2</sub>)<sub>2</sub>, (15) *p*-C<sub>6</sub>H<sub>4</sub>(NO<sub>2</sub>)<sub>2</sub>, (16) C<sub>6</sub>H<sub>3</sub>(NO<sub>2</sub>)<sub>3-1,3,5</sub>.<sup>15</sup>

which enables the control and, if necessary, correction of possible experimental errors. Of certain interest is the possibility of calculation of the activation energy of radical decomposition and the value of  $D(\text{C}-\text{N})$  for compounds that decompose under experimental conditions by various non-radical mechanisms (*o*-nitrotoluene, *o*-nitroaniline, *o*-nitrophenol, *o*-dinitrobenzene and their derivatives). These data are important for studying the competition of different mechanisms of the primary step of the gas-phase decomposition of nitroarenes on changes in temperature. The calculated values of  $D(\text{C}-\text{N})$  obtained with the use of quantum chemical methods can also be utilized for examining the reliability of experimental data. In most cases, the calculated estimates of the activation energy of radical decomposition that rely on the value of  $D(\text{C}-\text{N})$  and Eqn (2) are in good agreement with the experimental values. In this case, the root-mean-square error of calculated and experimental data does not exceed 4–5 kJ mol<sup>−1</sup> (Ref. 119). Correlations of the energies  $E_a$  and  $D(\text{C}-\text{N})$  with the length of the bond being broken, ionization potential<sup>117</sup> and other geometric and energetic character-

istics of molecules can be of certain interest for examining substituent effects. They confirm the dominating influence of a direct polar conjugation on alterations in the listed parameters in the series of aromatic nitro compounds. In a number of instances, steric factors leading to a disruption of the conjugation of electron-donating substituents with the benzene ring should also be taken into account.

The pre-exponential factor of radical decomposition in the nitroarene series alters negligibly.<sup>8</sup> For monofunctional nitrobenzene derivatives as well as for 1,3,5-trinitrobenzene, the observed change in  $\log A$  does not exceed 0.6, which is comparable with the error of its experimental determination. Such a situation practically excludes the possibility of an analysis of substituent effects on the magnitude of the  $A$ -factor of the reaction. Several sufficiently evident tendencies can only be noted. A slight augmentation in  $\log A$  is observed in the series of monofunctional nitrobenzene derivatives in the presence of electron-donating substituents in a molecule. This effect is stronger for *para*-substituted compounds. Nitro groups in *m*- and *p*-dinitrobenzenes (as well as in 1,3,5-trinitrobenzene) bring about an insignificant decrease in  $\log A$  as compared to that of nitrobenzene.

Reliable evidence of the location of the radical decomposition TS in the nitrobenzene series is absent. The values of  $\log A$  obtained in calculations performed for model fragments with stretching of the C–N bond in the range 280 to 350 pm are consistent with experimental values for nitrobenzene.<sup>15</sup> It was noted<sup>121</sup> that if we neglect the rotational barrier of the NO<sub>2</sub> group in the TS due to its small value, then the observed alterations in  $\log A$  in the series of monofunctional nitrobenzene derivatives can be accounted for by differences in rotational barriers in the molecules. The higher the value of a rotational barrier the greater  $\log A$ . Although this approach is a gross oversimplification,

it permits the attainment of satisfactory agreement between the calculated and experimental estimates of  $\log A$  for a large number of nitroarenes. Relying on calculated estimates of  $\log A$ ,  $D(\text{C}–\text{N})$  and  $E_a$ , an assumption was made<sup>15</sup> that there is a compensatory effect in the radical gas-phase decomposition reactions of nitroarenes. This suggestion appears quite probable, however, it needs additional substantiation with involvement of experimental and calculated data. Of special interest is the performance of rigorous theoretical calculations of the pre-exponential factors of the reactions.

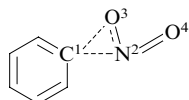
## 2. The nitro–nitrite rearrangement

As demonstrated above by the example of nitrobenzene, the NNR barrier is considerably lower than  $D(\text{C}–\text{N})$ , which opens up in principle a possibility of competition between this mechanism and the radical decomposition. The study of the NNR mechanism in the nitroarene series was carried out using various *ab initio* and DFT methods,<sup>111, 112, 116, 119</sup> the results of which are in fair agreement with each other. The largest number of reactions has been studied by the present authors.<sup>41</sup> Data on geometric parameters, TS and activation enthalpies for nitrobenzene, its numerous monofunctional derivatives as well as 1,3,5-trinitrobenzene are presented in Table 15.

For all the examined compounds, the activation enthalpy of the nitro–nitrite rearrangement is lower than the dissociation energy of the C–N bond, which suggests a possibility of a contribution of this process to the net rate constant of gas-phase thermal decomposition. For most investigated compounds, the indicated characteristics change in parallel (Fig. 35).

The lowest values of energy barriers to this reaction were noted for *o*-dinitrobenzene and *o*-nitrotoluene. It is these

**Table 15.** Geometric parameters of the transition state and the activation enthalpy of the nitro–nitrite rearrangement for some nitroarenes [calculated by B3LYP/6-31G(d)].



Compound	Distances /pm				Angles /deg			$\Delta H_{298}^\ddagger$ /kJ mol <sup>−1</sup>
	C <sup>1</sup> N <sup>2</sup>	N <sup>2</sup> O <sup>3</sup>	C <sup>1</sup> O <sup>3</sup>	N <sup>2</sup> O <sup>4</sup>	O <sup>3</sup> C <sup>1</sup> N <sup>2</sup>	C <sup>1</sup> N <sup>2</sup> O <sup>3</sup>	O <sup>3</sup> N <sup>2</sup> O <sup>4</sup>	
C <sub>6</sub> H <sub>5</sub> NO <sub>2</sub>	169.2	131.7	178.2	120.7	44.5	71.4	120.9	263.6
<i>o</i> -(CH <sub>3</sub> )C <sub>6</sub> H <sub>4</sub> NO <sub>2</sub>	168.0	131.9	178.8	120.8	44.6	72.1	120.8	243.5
<i>m</i> -(CH <sub>3</sub> )C <sub>6</sub> H <sub>4</sub> NO <sub>2</sub>	169.4	131.7	178.4	120.8	44.4	71.5	120.8	263.2
<i>p</i> -(CH <sub>3</sub> )C <sub>6</sub> H <sub>4</sub> NO <sub>2</sub>	167.8	132.0	177.9	120.9	44.8	71.6	120.7	266.5
<i>o</i> -(NH <sub>2</sub> )C <sub>6</sub> H <sub>4</sub> NO <sub>2</sub>	159.0	132.9	180.4	123.5	45.6	75.7	119.3	264.9
<i>m</i> -(NH <sub>2</sub> )C <sub>6</sub> H <sub>4</sub> NO <sub>2</sub>	169.4	131.7	178.0	120.7	44.5	71.2	120.9	263.2
<i>p</i> -(NH <sub>2</sub> )C <sub>6</sub> H <sub>4</sub> NO <sub>2</sub>	163.6	132.9	177.5	121.6	45.6	72.7	120.3	276.1
<i>o</i> -(OH)C <sub>6</sub> H <sub>4</sub> NO <sub>2</sub>	166.3	133.3	181.5	121.0	44.8	73.7	120.1	282.9
<i>m</i> -(OH)C <sub>6</sub> H <sub>4</sub> NO <sub>2</sub>	169.4	131.6	177.6	120.6	44.5	71.1	121.0	261.9
<i>p</i> -(OH)C <sub>6</sub> H <sub>4</sub> NO <sub>2</sub>	165.2	132.6	177.5	121.2	45.3	72.2	120.6	273.2
<i>o</i> -(NO <sub>2</sub> )C <sub>6</sub> H <sub>4</sub> NO <sub>2</sub>	164.8	131.9	169.5	119.4	46.4	68.7	122.9	223.0
<i>m</i> -(NO <sub>2</sub> )C <sub>6</sub> H <sub>4</sub> NO <sub>2</sub>	168.8	131.6	176.5	120.1	44.8	70.7	121.5	261.1
<i>p</i> -(NO <sub>2</sub> )C <sub>6</sub> H <sub>4</sub> NO <sub>2</sub>	168.2	131.3	174.9	120.0	44.9	70.2	122.2	251.5
C <sub>6</sub> H <sub>3</sub> (NO <sub>2</sub> ) <sub>3</sub> -1,3,5	168.7	131.5	175.1	119.7	44.9	70.1	122.3	256.9
<i>o</i> -FC <sub>6</sub> H <sub>4</sub> NO <sub>2</sub>	165.2	132.6	175.7	120.5	45.7	71.3	121.2	283.3
<i>m</i> -FC <sub>6</sub> H <sub>4</sub> NO <sub>2</sub>	169.0	131.6	177.2	120.4	44.6	71.0	121.2	262.3
<i>p</i> -FC <sub>6</sub> H <sub>4</sub> NO <sub>2</sub>	167.1	132.1	177.4	120.8	45.0	71.7	120.8	269.5
<i>o</i> -ClC <sub>6</sub> H <sub>4</sub> NO <sub>2</sub>	166.4	132.2	175.9	120.3	45.3	71.1	121.5	245.9
<i>m</i> -ClC <sub>6</sub> H <sub>4</sub> NO <sub>2</sub>	168.9	131.7	177.2	120.4	44.7	71.0	121.2	262.4
<i>p</i> -ClC <sub>6</sub> H <sub>4</sub> NO <sub>2</sub>	167.2	132.0	176.8	120.6	45.0	71.3	121.1	265.2

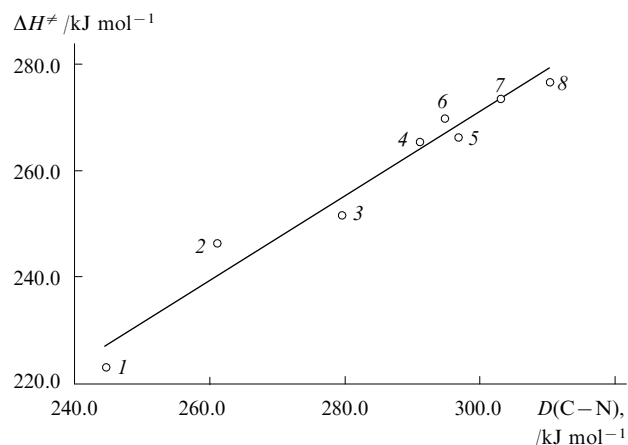


**Figure 35.** A correlation between  $\Delta H^\ddagger$  and  $D(\text{C}-\text{N})$  (the correlation coefficient is 0.964).<sup>15</sup>

(1)  $o\text{-C}_6\text{H}_4(\text{NO}_2)_2$ , (2)  $o\text{-ClC}_6\text{H}_4\text{NO}_2$ , (3)  $p\text{-C}_6\text{H}_4(\text{NO}_2)_2$ ,  
(4)  $p\text{-ClC}_6\text{H}_4\text{NO}_2$ , (5)  $p\text{-(CH}_3\text{)C}_6\text{H}_4\text{NO}_2$ , (6)  $p\text{-FC}_6\text{H}_4\text{NO}_2$ ,  
(7)  $p\text{-(OH)C}_6\text{H}_4\text{NO}_2$ , (8)  $p\text{-(NH}_2\text{)C}_6\text{H}_4\text{NO}_2$ .

compounds for which the least alterations in bond lengths ( $\Delta r$ ) in the transition state in the course of the reaction as compared to a starting molecule are observed. Thus for  $o$ -dinitrobenzene and  $o$ -nitrotoluene  $\Delta r(\text{C}-\text{N})$  are equal to 17.3 and 20.5 pm, respectively, whereas for nitrobenzene it is 30 pm. A comparison of nitrobenzene,  $m$ -dinitrobenzene and 1,3,5-trinitrobenzene shows that an increase in the number of  $\text{NO}_2$  groups results in an insignificant lowering of the reaction barrier (by 6.7 kJ mol<sup>−1</sup>). The values of  $\Delta r(\text{C}-\text{N})$  in this series are equal to 21.9, 21.1 and 20.8 pm, respectively. The decrease in the energy barrier of the nitro–nitrite rearrangement with an increase in the number of nitro groups, according to B3LYP/6-31G(d), is even more weakly pronounced than the lowering of the C–N bond strength. Based on these data, one can suppose that the contribution of the nitro–nitrite rearrangement to the net rate constant for gas-phase decomposition of mononitrobenzenes should be greater than that for their polynitro derivatives.

### 3. Gas-phase decomposition of nitroarenes with hydrogen-containing *ortho*-substituents relative to the nitro group

Studies on the kinetics of the thermal decomposition of  $o$ -nitrotoluene (**N1**),  $o$ -nitroaniline (**O1**) and  $o$ -nitrophenol (**P1**) as well as a number of their nitro derivatives demonstrated<sup>7,81</sup> that the Arrhenius parameters for these compounds substantially differ from those obtained for other nitroarenes with the same number of nitro groups. Activation energies and pre-exponential factors for the former are significantly lower (Table 16).

The mass spectra of decomposition products of these compounds contain intense peaks corresponding to elimination of the OH radical, which are absent from the mass spectra of other aromatic compounds.<sup>105, 106, 108, 122</sup> It was thus assumed that the gas-phase decomposition of the indicated aromatic nitro compounds starts with isomerization (Fig. 36) accompanied by the loss of the OH radical. For the first time, a theoretical study of alternative mechanisms of the gas-phase decomposition of 2,4,6-TNT was conducted<sup>123</sup> using 1-nitropropene as the model compound. It was established that the geometric structures of the reaction centres of *cis*-nitropropene and 2,4,6-TNT are similar. The major alternative mechanisms of the primary

**Table 16.** Kinetic parameters of the gas-phase decomposition of aromatic compounds by a molecular mechanism.<sup>7</sup>

Compound	$T/\text{K}$	$E_a/\text{kJ mol}^{-1}$	$\log A (\text{s}^{-1})$
<i>o</i> -Nitrotoluene ( <b>N1</b> )	623–693	$207 \pm 5$	$12.4 \pm 0.4$
<i>o</i> -Nitroaniline ( <b>O1</b> )	693–763	$241 \pm 8$	$13.5 \pm 0.4$
<i>o</i> -Dinitrobenzene ( <b>Q1</b> )	623–723	$205 \pm 10$	$12.3 \pm 0.7$
<i>o</i> -Nitrophenol ( <b>P1</b> )	663–733	$220 \pm 8$	$12.6 \pm 0.2$
2,4,6-Trinitrotoluene	593–663	$197 \pm 10$	$12.4 \pm 0.8$
2,4,6-Trinitroaniline	673–743	$207 \pm 8$	$12.6 \pm 0.5$

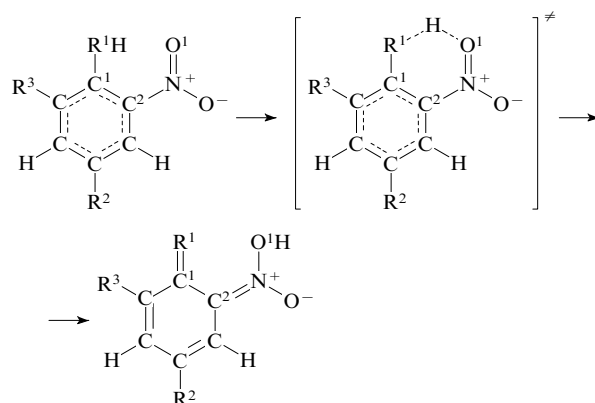


**Figure 36.** A scheme of the formation mechanisms of the *aci*-forms of nitroarenes with hydrogen-containing *ortho* substituents.<sup>122</sup>

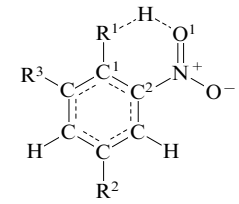
reaction steps, *viz.*, radical decomposition, NNR, inter- and intramolecular transfer of hydrogen and oxygen atoms, were examined employing the semi-empirical methods MINDO/3 and MNDO. The activation enthalpies of non-radical decomposition reactions<sup>123</sup> are listed in Table 17.

**Table 17.** Activation enthalpies of 1-nitropropene decomposition reactions calculated by different methods.<sup>123</sup>

Reactions	$\Delta H^\ddagger / \text{kJ mol}^{-1}$	
	MNDO	MINDO/3
Intramolecular transfer of a hydrogen atom	249	182
Intermolecular transfer of a hydrogen atom	211	166
Intramolecular transfer of an oxygen atom	534	209
Intermolecular transfer of an oxygen atom	435	186
Nitro–nitrite rearrangement	216	147

Among monomolecular decomposition processes that occur in the gaseous state, the lowest barrier, according to MNDO, is that of NNR. MINDO/3 predicts that the reaction barrier to the intramolecular hydrogen transfer is lower than that of NNR. Subsequently, this process was intensively examined<sup>79</sup> for compounds **N1**, **O1** and **P1** as well as for 2,4- and 2,6-dinitro and 2,4,6-trinitro derivatives of toluene, aniline and phenol. The investigation was carried out by the *ab initio* method HF/6-31G(d). In later publications,<sup>41, 111, 124, 125</sup> this reaction was thoroughly studied with the aid of various semi-empirical, *ab initio* and DFT methods.

A theoretical study<sup>15</sup> confirms that the reaction barrier to the intramolecular hydrogen transfer is substantially lower than the value of  $D(\text{C}-\text{N})$  for  $o$ -nitrotoluene,  $o$ -nitroaniline,  $o$ -nitrophenol (Table 18). In the series of com-

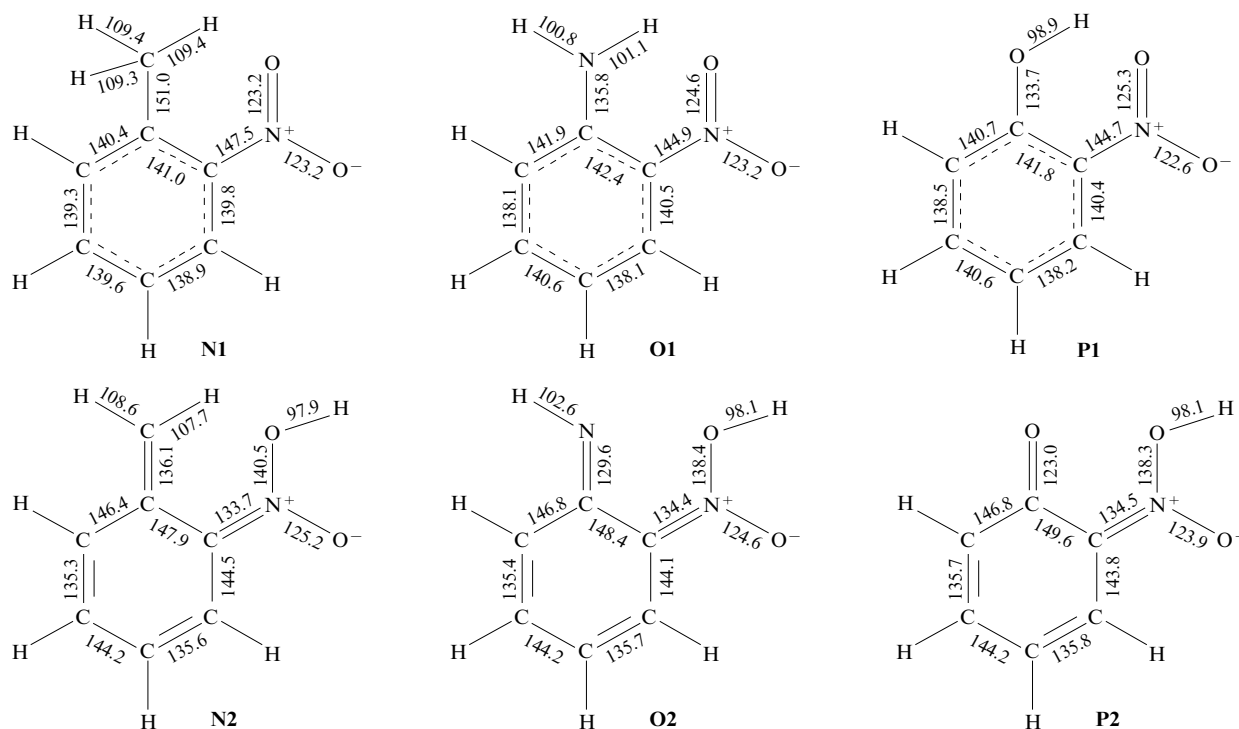
**Table 18.** Bond lengths in the transition state, the activation enthalpy and entropy for the hydrogen transfer in some nitroarenes [calculated by B3LYP/6-31G(d)].


R <sup>1</sup>	R <sup>2</sup>	R <sup>3</sup>	Bond lengths /pm						$\Delta H^\ddagger$ /kJ mol <sup>-1</sup>	$\Delta S^\ddagger$ , /J mol <sup>-1</sup> K <sup>-1</sup>
			C <sup>1</sup> C <sup>2</sup>	C <sup>2</sup> N	NO <sup>1</sup>	O <sup>1</sup> H	HR <sup>1</sup>	R <sup>1</sup> C <sup>1</sup>		
CH <sub>3</sub>	H	H	144.6	138.6	133.4	112.6	153.4	141.4	184.9	-22.89
CH <sub>3</sub>	NO <sub>2</sub>	H	144.7	139.6	132.6	114.0	151.8	141.0	179.0	-22.71
CH <sub>3</sub>	H	NO <sub>2</sub>	145.4	139.7	132.5	114.0	151.0	140.8	174.1	-22.37
CH <sub>3</sub>	NO <sub>2</sub>	NO <sub>2</sub>	144.7	139.8	132.3	113.9	151.7	140.8	171.0	-19.17
NH <sub>2</sub>	H	H	148.7	134.3	140.3	97.6	286.9	129.5	178.8	-4.29
NH <sub>2</sub>	NO <sub>2</sub>	H	148.8	135.0	139.8	97.7	282.8	129.2	182.8	-2.49
NH <sub>2</sub>	H	NO <sub>2</sub>	149.4	134.7	139.8	97.7	284.8	128.5	191.1	4.09
NH <sub>2</sub>	NO <sub>2</sub>	NO <sub>2</sub>	149.6	135.4	139.3	97.8	280.1	128.3	192.6	4.50
OH	H	H	150.0	134.5	140.5	97.7	277.2	123.1	135.1	6.45
OH	NO <sub>2</sub>	H	150.2	135.1	140.0	97.8	273.6	122.8	134.7	6.87
OH	H	NO <sub>2</sub>	150.1	134.8	140.1	97.8	271.9	122.3	129.1	26.02
OH	NO <sub>2</sub>	NO <sub>2</sub>	150.2	135.5	139.6	97.8	268.7	122.1	127.3	26.30

pounds **N1**, **O1**, **P1**, *ab initio* and DFT methods predict a decrease in the activation enthalpy. For *o*-nitrophenol, the activation enthalpy is more than twice as low as  $D(C-N)$ . Data on geometric parameters of the reaction centres of the first representatives of the series, which are illustrated in Fig. 37, allow an explanation of the indicated tendency.

The transition states in the reactions of *o*-nitrophenol (**P1**) and *o*-nitroaniline (**O1**) coincide with the reaction

product structures (except for the torsional angle  $HO^1NC^2$ , which is close to  $90^\circ$  in the TS), whereas the TS for *o*-nitrotoluene (**N1**) is shifted to a greater degree toward the starting compound. The reduction in the activation enthalpy in the series *o*-nitrotoluene, *o*-nitroaniline, *o*-nitrophenol, which is especially strongly pronounced for the last compound, is mainly governed by the degree of unfavourability of the quinonoid structure formed.

**Figure 37.** Bond lengths (pm) in the starting molecules and transition states of the hydrogen transfer for *o*-nitrotoluene (**N1** and **N2**), *o*-nitroaniline (**O1** and **O2**) and *o*-nitrophenol (**P1** and **P2**) [B3LYP/6-31G(d)].<sup>15</sup>

An increase in the number of nitro groups in *o*-nitrotoluenes and *o*-nitrophenols brings about a small decrease in the activation enthalpy, while in *o*-nitroaniline, conversely, its increase.

In the series *o*-nitrotoluene, *o*-nitroaniline, *o*-nitrophenol, according to B3LYP/6-31G(d), the increase in the activation entropy takes place. An increase in the number of nitro groups also produces an increase in the activation entropy.

It should be noted that the data from calculation and experimental results appreciably differ: the experimental values of the activation energy in all instances exceed the calculated ones. The observed differences (most significant for the nitroaniline reactions) are much higher than  $RT$  (at  $T = 600$  and  $700$  K 5 and  $5.8 \text{ kJ mol}^{-1}$ , respectively). Taking into account that the B3LYP/6-31G(d) method sufficiently well reproduces values of  $D(\text{C}-\text{N})$  for nitroalkanes, nitroalkenes, nitroarenes as well as the activation enthalpies of the molecular decomposition of nitroalkanes, the observed considerable divergence from experimental data can be explained by the fact that, under experimental conditions, several reactions with close rate constants of rate-determining steps occur in parallel.

The kinetics of the gas-phase decomposition of *o*-nitrotoluene, *o*-nitroaniline and *o*-nitrophenol was studied<sup>7</sup> in the temperature interval 623–733 K. The corresponding *para*- and *meta*-isomers, which decompose predominantly by the radical mechanism and have the values of  $D(\text{C}-\text{N})$  close to those of *ortho*-isomers, were examined in an analogous temperature range.<sup>8</sup> Hence, it is possible to suggest that radical decomposition can also contribute to an experimentally measured rate constant for the thermal decomposition of aromatic nitro compounds with hydrogen-containing substituents in the *ortho*-position relative to the nitro group, which ultimately results in an overestimation of the experimentally measured activation enthalpy of the gas-phase decomposition of *ortho*-isomers as compared with theoretical estimates of the activation enthalpy of rearrangements of the corresponding compounds to *aci*-forms. An assumption was made<sup>41</sup> that as experimental temperature drops, the possibility of competition with NNR cannot be excluded. A comparison of the calculated and experimental values of the reaction pre-exponential factors also suggest a possibility of the contribution of several parallel elementary processes to the experimentally measured rate constants for the thermal decomposition of *o*-nitrotoluene, *o*-nitroaniline, and *o*-nitrophenol and their derivatives. If we assess the reaction  $A$ -factor based on the activation entropy values provided in Table 18, then for *o*-nitrotoluene we shall obtain the calculated value  $\log A \approx 11.6 \text{ (s}^{-1}\text{)}$ , which is considerably lower than the experimental one (for  $T = 298.15 \text{ K}$ ). Consideration of the temperature dependence does not change the situation.

Thus, the analysis of calculated and experimental data indicates that for aromatic nitro compounds with hydrogen-containing *ortho*-substituents relative to the nitro group, the most favourable channel of decomposition is an intramolecular transfer of a hydrogen atom to the nitro group. All the studied alternative mechanisms of the primary step of monomolecular decomposition have lower values of the rate constants.<sup>2, 15</sup>

#### 4. Formation of bicyclic intermediates

*o*-Dinitrobenzene (**Q1**) decomposes by a non-radical mechanism, this is suggested by both experimental values

of the Arrhenius parameters [ $E_a = 205 \text{ kJ mol}^{-1}$ ,  $\log A = 12.3 \text{ (s}^{-1}\text{)}$ ] and results of mass spectrometric studies.<sup>105, 106, 108</sup> In the literature, several mechanisms of the non-radical decomposition of *o*-dinitrobenzene are discussed including elimination of an oxygen atom or a molecule as well as a number of other schemes.<sup>2</sup> All of them, however, have no serious theoretical substantiation. A theoretical study of the mechanism of the gas-phase decomposition of *o*-dinitrobenzene at the PBE/L1 and B3LYP/6-31G(d,p) levels was reported.<sup>112</sup> The results of both methods agree well with each other (Fig. 38). Real contributors to the rate constant for the thermal decomposition of *o*-dinitrobenzene can be the NNR and the formation of a bicyclic intermediate. Judging by the calculations, the contribution of isomerization to (6*S*)-6-nitro-7-oxa-8-azabicyclo[4.2.0]octa-1(8),2,4-triene *N*-oxide (**Q2**) prevails. Unlike that of nitrobenzene, the second step is a concerted process of opening the four-membered ring in bicycle **Q2** and the elimination of the nitro group, which proceeds with a lower activation enthalpy than does the cyclization (see Fig. 38).

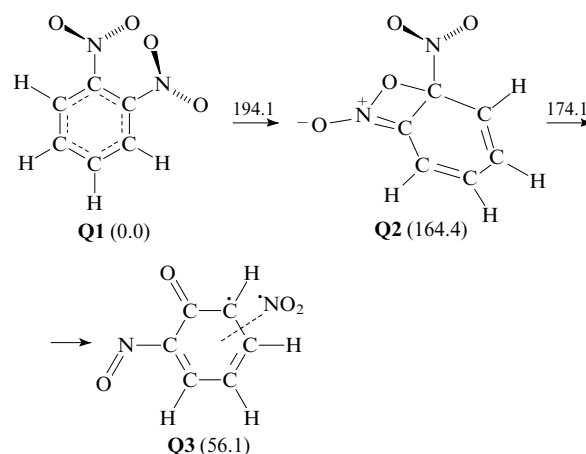


**Figure 38.** A scheme of a mechanism of decomposition of *o*-dinitrobenzene (**Q1**) (PBE/L1).<sup>112</sup>

The enthalpy of formation of *o*-dinitrobenzene was taken as zero.

By an analogous mechanism, 1,2,3- and 1,2,4-trinitrobenzene, hexanitrobenzene and other polynitrobenzenes bearing nitro groups at vicinal carbon atoms decompose in the gaseous state.<sup>112</sup>

Thus, theoretical studies with the aid of state-of-the-art quantum chemical methods make it possible to explain all the available experimental data from the ground of four major mechanisms of the gas-phase monomolecular decomposition of aromatic nitro compounds: the homolytic cleavage of the C–N bond, NNR, formation of a bicyclic intermediate and intramolecular transfer of a hydrogen atom. This does not imply that the possibility of other mechanisms of the primary reaction step is completely excluded, however, for them there are no reliable theoretical or experimental data required for discussion.

For understanding the mechanism of the gas-phase decomposition of nitroarenes, of major significance are the results of mass spectrometric studies. As has already been noted in other sections of this review, their interpretation pertains to the theoretical examination of the destruction mechanism of radical cations.<sup>54</sup> The dissociation energies

( $\Delta E$ ) of some radical cations of aromatic nitro compounds (on the assumption that the barriers to the reversed reactions are absent) [calculated by the B3LYP/6-31G(d) method] and activation enthalpies of some decomposition processes of aromatic nitro compound radical cations [B3LYP/6-31G(d)] are listed below.

Process	$\Delta E/\text{kJ mol}^{-1}$
$\text{C}_6\text{H}_5\text{NO}_2^{+\bullet} \rightarrow \text{C}_6\text{H}_5^+ + \text{NO}_2^\bullet$	148.5
$\text{C}_6\text{H}_5\text{NO}_2^{+\bullet} \rightarrow \text{C}_6\text{H}_5^+ + \text{NO}_2^+$	320.8
$p\text{-NO}_2\text{C}_6\text{H}_4\text{NO}_2^{+\bullet} \rightarrow p\text{-C}_6\text{H}_4\text{NO}_2^+ + \text{NO}_2^\bullet$	167.2
$p\text{-NO}_2\text{C}_6\text{H}_4\text{NO}_2^{+\bullet} \rightarrow p\text{-C}_6\text{H}_4\text{NO}_2^+ + \text{NO}_2^+$	265.4
$o\text{-CH}_3\text{C}_6\text{H}_4\text{NO}_2^{+\bullet} \rightarrow o\text{-C}_6\text{H}_4\text{CH}_3^+ + \text{NO}_2^\bullet$	156.2
$o\text{-CH}_3\text{C}_6\text{H}_4\text{NO}_2^{+\bullet} \rightarrow o\text{-C}_6\text{H}_4\text{CH}_3^+ + \text{NO}_2^+$	355.2
$m\text{-CH}_3\text{C}_6\text{H}_4\text{NO}_2^{+\bullet} \rightarrow m\text{-C}_6\text{H}_4\text{CH}_3^+ + \text{NO}_2^\bullet$	174.0
$m\text{-CH}_3\text{C}_6\text{H}_4\text{NO}_2^{+\bullet} \rightarrow m\text{-C}_6\text{H}_4\text{CH}_3^+ + \text{NO}_2^+$	366.3
$p\text{-CH}_3\text{C}_6\text{H}_4\text{NO}_2^{+\bullet} \rightarrow p\text{-C}_6\text{H}_4\text{CH}_3^+ + \text{NO}_2^\bullet$	185.6
$p\text{-CH}_3\text{C}_6\text{H}_4\text{NO}_2^{+\bullet} \rightarrow p\text{-C}_6\text{H}_4\text{CH}_3^+ + \text{NO}_2^+$	370.9

Process	$\Delta H^\ddagger/\text{kJ mol}^{-1}$
$\text{C}_6\text{H}_5\text{NO}_2^{+\bullet} \rightarrow \text{C}_6\text{H}_5\text{ONO}^{+\bullet}$	114..2
$p\text{-NO}_2\text{C}_6\text{H}_4\text{NO}_2^{+\bullet} \rightarrow p\text{-NO}_2\text{C}_6\text{H}_4\text{ONO}^{+\bullet}$	115.6
$o\text{-CH}_3\text{C}_6\text{H}_4\text{NO}_2^{+\bullet} \rightarrow o\text{-CH}_3\text{C}_6\text{H}_4\text{ONO}^{+\bullet}$	117.8
$m\text{-CH}_3\text{C}_6\text{H}_4\text{NO}_2^{+\bullet} \rightarrow m\text{-CH}_3\text{C}_6\text{H}_4\text{ONO}^{+\bullet}$	134.4
$p\text{-CH}_3\text{C}_6\text{H}_4\text{NO}_2^{+\bullet} \rightarrow p\text{-CH}_3\text{C}_6\text{H}_4\text{ONO}^{+\bullet}$	129.1
$o\text{-CH}_3\text{C}_6\text{H}_4\text{NO}_2^{+\bullet} \rightarrow o\text{-CH}_2\text{C}_6\text{H}_4\text{N(O)OH}^{+\bullet}$	40.7

The presented data permit some general inferences to be drawn about the decomposition mechanism of the molecules and radical cations of the simplest aromatic nitro compounds. In most cases, the major decomposition channels of molecules and radical cations coincide. Thus for the studied compounds (with the exception of *o*-nitrotoluene and *o*-nitroaniline) the minimum barrier corresponds to the nitro–nitrite rearrangement. For the molecules and radical cations of *o*-nitrotoluene and *o*-nitroaniline, the intramolecular transfer of a hydrogen atom is energetically more favourable. However, the barriers to radical cation reactions are significantly (2–8 times) lower than those of the corresponding molecules. This peculiarity should be taken into consideration when interpreting data from mass spectrometry.

## V. Conclusion

The material presented in the review clearly demonstrates that state-of-the-art quantum chemical methods have become an essential tool in examining the gas-phase monomolecular decomposition of major classes of C-nitro compounds. The theoretical studies allowed a substantial increase in the amount of mechanisms being considered, and in a number of cases (for example, for nitroethylenes and nitrobenzenes) permitted more accurate interpretations of experimental observations.

One should also mark appreciable progress achieved in the understanding of the basic regularities of the influence of molecular structure on the change in the Arrhenius parameters of the primary reaction step in a series of related compounds. At the same time, a whole set of inadequately studied problems both in the appreciation of the competition of various mechanisms of gas-phase monomolecular decomposition and in elucidation of peculiarities of reaction pathways leading to experimentally observed products still

persists. Hence, beyond any doubt is the necessity for further insight into the mechanism of gas-phase decomposition reactions with the use of experimental and theoretical methods. Of great interest is, in particular, the study of the monomolecular decompositions of nitro compounds by employing quantum chemical methods of high level (G3, G3B3, CBS-QB3, QCISD, *etc.*).

Despite all the progress in theoretical studies associated with the development of modern *ab initio* methods and computational hardware, experimental investigations retain in full measure their leading position. In addition, it should be borne in mind that advances reached in the theoretical study of the mechanisms of the thermal destruction of nitro compounds became possible owing to the availability of a large number of reliable experimental values of the Arrhenius parameters of the primary steps of gas-phase decomposition reactions as well as data on product compositions in initial stages of decomposition. This information enables the control of the reliability of obtained calculation results and conclusions based on them.

## References

1. G M Nazin, G B Manelis, F I Dubovitskii *Usp. Khim.* **37** 1443 (1968) [*Russ. Chem. Rev.* **37** 603 (1968)]
2. T B Brill, K J James *Chem. Rev.* **93** 2667 (1993)
3. G M Nazin, G B Manelis *Usp. Khim.* **63** 327 (1994) [*Russ. Chem. Rev.* **63** 313 (1994)]
4. G M Nazin *Usp. Khim.* **41** 1537 (1972) [*Russ. Chem. Rev.* **41** 711 (1972)]
5. G M Nazin, G B Manelis *Izv. Akad. Nauk, Ser. Khim.* 811 (1972)<sup>a</sup>
6. R Shaw *Int. J. Chem. Kinet.* **5** 261 (1973)
7. V G Matveev, V V Dubikhin, G M Nazin *Izv. Akad. Nauk, Ser. Khim.* 474 (1978)<sup>a</sup>
8. V G Matveev, V V Dubikhin, G M Nazin *Izv. Akad. Nauk, Ser. Khim.* 783 (1978)<sup>a</sup>
9. V G Kiselev, N P Gritsan *J. Phys. Chem. A* **112** 4458 (2008)
10. V G Kiselev, V E Zarko, N P Gritsan *Kinet. Katal.* **47** 357 (2006)<sup>b</sup>
11. G M Khrapkovskii, A G Shamov, G A Shamov, V A Shlyapochnikov *Ros. Khim. Zh.* **41** (4) 14 (1997)<sup>c</sup>
12. G M Khrapkovskii, A G Shamov, G A Shamov, V A Shlyapochnikov *Zh. Org. Khim.* **35** 29 (1999)<sup>d</sup>
13. I S Zaslonko, Yu P Petrov, V N Smirnov *Kinet. Katal.* **38** 353 (1997)<sup>b</sup>
14. A G Shamov, G M Khrapkovskii, G A Shamov, in *Struktura i Dinamika Molekulyarnykh Sistem (Sb. Statei V Vseros. Konf.)*, Ioshkar-Ola, 1998 [Structure and Dynamics of Molecular Systems (Collection of Articles of Vth All-Russian Conference), Ioshkar-Ola, 1998] Pt. 3, p. 347
15. D V Chachkov, Candidate Thesis in Chemical Sciences, Kasan State Technological University, Kazan, 2005
16. G G Garifzianova, R V Tsyshevskii, A G Shamov, G M Khrapkovskii *Int. J. Quantum Chem.* **107** 2489 (2007)
17. E V Nikolaeva, A G Shamov, G M Khrapkovskii, Kh E Kharlampidi *Zh. Obshch. Khim.* **72** 802 (2002)<sup>e</sup>
18. B C Garrett, D G Truhlar *J. Chem. Phys.* **70** 1593 (1979)
19. V A Shlyapochnikov, G M Khrapkovskii, A G Shamov *Izv. Akad. Nauk, Ser. Khim.* 863 (2002)<sup>a</sup>
20. Yu I Tarasov, I V Kochikov, N Vogt, A V Stepanova, B K Novosadov, R Z Deyanov, D M Kovtun, J Vogt *J. Mol. Struct.* **872** 150 (2008)
21. G M Khrapkovskii, D V Chachkov, A G Shamov *Zh. Obshch. Khim.* **71** 1530 (2001)<sup>e</sup>
22. G M Khrapkovskii, D V Chachkov, A G Shamov *Zh. Obshch. Khim.* **74** 1835 (2004)<sup>e</sup>

23. V A Shlyapochnikov, in *Kolebatel'nye Spektry Alifaticeskikh Nitrosoedinenii* (Vibrational Spectra of Aliphatic Nitro-Compounds) (Ioshkar-Ola: Mariisk. State University, 2007) p. 17
24. M A Tafipolsky, I V Tokmakov, V A Shlyapochnikov *J. Mol. Struct.* **510** 149 (1999)
25. V I Faustov, S A Shevelev, N A Anikin *Izv. Akad. Nauk, Ser. Khim.* 2800 (1979)<sup>a</sup>
26. V I Faustov, S A Shevelev, N A Anikin *Izv. Akad. Nauk, Ser. Khim.* 2200 (1980)<sup>a</sup>
27. P A Denis, O N Ventura, H T Le, M T Ngyen *Phys. Chem. Chem. Phys.* **5** 1730 (2003)
28. T F Shamsutdinov, D V Chachkov, E V Nikolaeva, A G Shamov, G M Khrapkovskii *Vest. Kazan. Tekhnol. Univ.* (2) 27 (2003)
29. A G Shamov, E V Nikolaeva, D V Chachkov, G M Khrapkovskii, in *Proceedings of the 35th International Annual Conference of ICT, Karlsruhe, 2004* p. 127:1
30. G M Khrapkovskii, E A Ermakova, V A Zakharov, A G Shamov, V A Tikhomirov *Zh. Fiz. Khim.* **64** 2247 (1990)<sup>f</sup>
31. A F Shamsutdinov, T F Shamsutdinov, D V Chachkov, A G Shamov, G M Khrapkovskii *Int. J. Quantum Chem.* **107** 2343 (2007)
32. G M Khrapkovskii, E V Nikolaeva, D V Chachkov, A G Shamov, in *Proceedings of the IVth Seminar 'New Trends in Research of Energetic Materials', University of Pardubice Czech Republic, 2001* p. 162
33. A M Wodtke, E J Hints, Y T Lee *J. Phys. Chem.* **90** 3549 (1986)
34. M J S Dewar, P J Ritchie, J Alster *J. Org. Chem.* **50** 1031 (1985)
35. M L McKee *J. Am. Chem. Soc.* **108** 5784 (1986)
36. M T Nguyen, H T Le, B Hajtag, T Veszpremi, M C Lin *J. Phys. Chem.* **107** 4286 (2003)
37. M R Manaa, L E Fried *J. Phys. Chem.* **102** 9884 (1998)
38. E Martinez-Nunez, S A Vasquez *J. Phys. Chem.* **109** 8907 (1998)
39. E Martinez-Nunez, S A Vasquez *J. Phys. Chem.* **111** 10501 (1998)
40. A Fernandez-Ramos, E Martinez-Nunez, M A Rios, J Rodriguez-Otero, S A Vasquez, C M Estevez *J. Am. Chem. Soc.* **120** 7594 (1998)
41. G M Khrapkovskii, E V Nikolaeva, D V Chachkov, A G Shamov *Zh. Obshch. Khim.* **74** 983 (2004)<sup>e</sup>
42. E Martinez-Nunez, I Borgez Jr, S A Vasquez *J. Phys. Org. Chem.* **15** 123 (2002)
43. W F Hu, T J He, D M Chen, F C Liu *J. Phys. Chem. A* **106** 7294 (2002)
44. E V Nikolaeva, A G Shamov, D V Chachkov, G M Khrapkovskii, in *Struktura i Dinamika Molekulyarnykh Sistem (Sb. Statei X Vseros. Konf.)*, Kazan, 2003 [Structure and Dynamics of Molecular Systems (Collection of Articles of Xth All-Russian Conference), Kazan, 2003] Pt. 3, p. 241
45. M L McKee *J. Phys. Chem.* **93** 7365 (1989)
46. C Lifshitz, M Rejwan, I Levin, T Peres *Int. J. Mass Spectrom. Ion Processes* **84** 271 (1988)
47. M Siroes, J L Holmes, C E C A Hop *Org. Mass Spectrom.* **25** 167 (1990)
48. E E Ferguson *Chem. Rev. Lett.* **138** 450 (1987)
49. H Egsgaard, L Carlsen *Chem. Phys. Lett.* **147** 30 (1988)
50. G M Khrapkovskii, A M Rozin, V A Tikhomirov, A G Shamov, G N Marchenko *Dokl. Akad. Nauk SSSR* **298** 921 (1988)<sup>g</sup>
51. G M Khrapkovskii, A G Shamov, G A Shamov, V A Shlyapochnikov *Mendeleev Commun.* 169 (1997)
52. G M Khrapkovskii, A G Shamov, G A Shamov, V A Shlyapochnikov *Izv. Akad. Nauk, Ser. Khim.* 913 (2001)<sup>a</sup>
53. J Ottis, Z Jalov, F Liška *J. Energ. Mater.* **26** 220 (2008)
54. E V Nikolaeva, Candidate Thesis in Chemical Sciences, Kazan State Technological University, Kazan, 2002
55. E V Nikolaeva, A G Shamov, G M Khrapkovskii, in *Struktura i Dinamika Molekulyarnykh Sistem (Sb. Statei VI Vseros. Konf.)*, Ufa, 2002 [Structure and Dynamics of Molecular Systems (Collection of Articles of VIth All-Russian Conference), Ufa, 2002] Vol. 2, p. 75
56. G B Manelis, G M Nazin, Yu I Rubtsov, V A Strunin, in *Termicheskoe Razlozhenie i Gorenje Vzryvchatykh Veshchestv i Porokhov* (Thermal Decomposition and Combustion of Explosives and Powders) (Moscow: Nauka, 1996) p. 35
57. T H Cottrell, T E Crahm, T J Reid *Trans. Faraday Soc.* **47** 584 (1951)
58. N V Latypov, J Bergman, A Langlet, U Wellmar, U Bemm *Tetrahedron* **54** 11525 (1998)
59. H Östmark, A Langlet, H Bergman, N Wingborg, U Wellmar, U Bemm, in *Proceedings of the 11th (International) Symposium on Detonation, Snow Mass, CO, 1998* p. 18
60. A Gindulyte, L Massa, L Huang, J Karle *J. Phys. Chem. A* **103** 11045 (1999)
61. P Politzer, M C Concha, M E Grice, J S Murray, P Lane, D Habibollahzadeh *J. Mol. Struct. (THEOCHEM)* **452** 75 (1998)
62. A G Shamov, G M Khrapkovskii, in *Proceedings of the 30th International Annual Conference of ICT, Karlsruhe, 1999* p. 60:1
63. A G Shamov, G M Khrapkovskii, in *Struktura i Dinamika Molekulyarnykh Sistem (Sb. Statei VI Vseros. Konf.)*, Kazan, 1999 [Structure and Dynamics of Molecular Systems (Collection of Articles of VIth All-Russian Conference), Kazan, 1999] Pt. 3, p. 347
64. A G Shamov, G M Khrapkovskii, G A Shamov, in *Struktura i Dinamika Molekulyarnykh Sistem (Sb. Statei V Vseros. Konf.)*, Ioshkar-Ola, 1998 [Structure and Dynamics of Molecular Systems (Collection of Articles of Vth All-Russian Conference), Ioshkar-Ola, 1998] Pt. 3, p. 183
65. A Gindulyte, L Massa, L Huang, J Karle *J. Phys. Chem. A* **103** 11040 (1999)
66. A G Shamov, G M Khrapkovskii *Mendeleev Commun.* 163 (2001)
67. A G Shamov, E V Nikolaeva, G M Khrapkovskii *Zh. Obshch. Khim.* **74** 1327 (2004)<sup>e</sup>
68. T H Kinstle, J G Stam *J. Org. Chem.* **35** 1771 (1970)
69. J T Pinhey, E Rizzardo *Tetrahedron Lett.* **41** 4057 (1973)
70. A Berndt *Angew. Chem.* **80** 666 (1968)
71. K Wieser, A Berndt *Angew. Chem.* **87** 72 (1975)
72. K Wieser, A Berndt *Angew. Chem.* **87** 73 (1975)
73. T Sheradsky, U Reichman, M Frankel *J. Org. Chem.* **33** 3619 (1968)
74. H Egsgaard, L Carlsen *Org. Mass Spectrom.* **24** 1031 (1989)
75. E V Nikolaeva, A G Shamov, G M Khrapkovskii, in *Struktura i Dinamika Molekulyarnykh Sistem (Sb. Statei VIII Vseros. Konf.)*, Ioshkar-Ola, 2001 [Structure and Dynamics of Molecular Systems (Collection of Articles of VIIIth All-Russian Conference), Ioshkar-Ola, 2001] Pt. 2, p. 190
76. A G Shamov, E V Nikolaeva, D V Chachkov, G M Khrapkovskii *Vest. Kazan. Tekhnol. Univ.* (2) 36 (2003)
77. A G Shamov, E V Nikolaeva, D V Chachkov, G M Khrapkovskii, in *Struktura i Dinamika Molekulyarnykh Sistem (Sb. Statei XI Vseros. Konf.)*, Kazan, 2004 [Structure and Dynamics of Molecular Systems (Collection of Articles of XIth All-Russian Conference), Kazan, 2004] Pt. 3, p. 82
78. A G Shamov, E V Nikolaeva, D V Chachkov, G M Khrapkovskii, in *Proceedings of the 36th International Annual Conference of ICT, Karlsruhe, 2005* p. 50:1
79. K Lammertsma *On the Viability of Nitronic Acids in the Decomposition of Nitroaromatics: a Theoretical Study of Nitronic Acids*, Alabama University, Birmingham Department of Chemistry, 1993 p. 70. Contract F08635-90-K-0204. Rep. A495372 (1993)
80. Y-X Zhang, S H Bauer *J. Phys. Chem. A* **104** 1217 (2000)
81. V G Matveev, V V Dubikhin, G M Nazin *Kinet. Katal.* **7** 280 (1976)<sup>b</sup>
82. A G Shamov, E V Nikolaeva, D V Chachkov, G M Khrapkovskii, in *Struktura i Dinamika Molekulyarnykh Sistem (Sb. Statei X Vseros. Konf.)*, Kazan, 2003 [Structure and Dynamics of Molecular Systems (Collection of Articles of Xth All-Russian Conference), Kazan, 2003] Pt. 3, p. 233



83. G A Shamov, E V Nikolaeva, D V Chachkov, T F Shamsutdinov, in *Fundamental'nye i Prikladnye Nauki (Sb. Statei 'Otechety Konkursa Proektov 2002 AN RT')* [Fundamental and Applied Sciences (Collection of Articles 'Reports on Competition of Projects 2002 AN RT')] (Kazan: FEN, 2004) p. 437
84. A G Shamov, E V Nikolaeva, F I Vorob'eva, G M Khrapkovskii *Vest. Kazan. Tekhnol. Univ.* (2) 5 (2007)
85. H Dorset *Computational Studies of FOX-7, a New Insensitive Explosive, Salisbury, South Australia, 2000* DSTO-TR-1054 AR-011-596 (2000)
86. I J Lochert *Fox-7 — a New Insensitive Explosive, Salisbury, South Australia, 2001* DSTO-TR-1238 AR-012-065 (2001)
87. A J Bellamy, P Goede, C Sandberg, N V Latypov, in *Proceedings of the 33th International Annual Conference of ICT, Karlsruhe, 2002* p. 3:1
88. G Herve, G Jacob, N V Latypov *Tetrahedron* **61** 6743 (2005)
89. G Herve, G Jacob *Tetrahedron* **63** 953 (2007)
90. E Holmgren, P Goede, N V Latypov, in *Proceedings of the 32th International Annual Conference of ICT, Karlsruhe, 2001* p. 119:1
91. A J Bellamy, N V Latypov, P Goede *J. Chem. Res. (S)* 257 (2002)
92. C Eldsiter, H Edvinsson, M Johansson, Å Pettersson, C Sandberg, in *Proceedings of the 33th International Annual Conference of ICT, Karlsruhe, 2002* p. 63:1
93. S Ye, K Tonokura, M Koshi *Combust. Flame* **132** 240 (2003)
94. A Kretschmer, P Gerber, A Happ, in *Proceedings of the 35th International Annual Conference of ICT, Karlsruhe, 2004* p. 172:1
95. P B Kempa, M Herrman, F J M Metzger, V Thome, A Kjellström, N V Latypov, in *Proceedings of the 35th International Annual Conference of ICT, Karlsruhe, 2004* p. 71:1
96. U Teipel, I Fuhr, K Hartlieb, A Kjellström, C Elsäter, in *Proceedings of the 35th International Annual Conference of ICT, Karlsruhe, 2004* p. 51:1
97. R Wild, U Teipel, in *Proceedings of the 35th International Annual Conference of ICT, Karlsruhe, 2004* p. 69:1
98. I Fuhr, U Teipel, J Ulrich, in *Proceedings of the 35th International Annual Conference of ICT, Karlsruhe, 2004* p. 49:1
99. W P C de Klerk, C Popescu, A E D M van der Heijden *J. Therm. Anal. Cal.* **72** 955 (2003)
100. A Pettersson, P Goede, A Kjellström, S Wallin *Mass Spectrometric Study on FOX-7 Decomposition, Tumba, Sweden, 2004* Project No. E2004 ISRN FOI-R-319-SE (2004)
101. U Ticmanis, M Kaiser, G Pantel, I Fuhr, U Teipel, in *Proceedings of the 35th International Annual Conference of ICT, Karlsruhe, 2004* p. 70:1
102. A J Bellamy *Struct. Bond* **125** 1 (2007)
103. Yu A Lebedev, E A Miroshnichenko, Yu K Knobel' *Termokhimiya Nitrosoedinenii* (Thermochemistry of Nitro Compounds) (Moscow: Nauka, 1970)
104. L V Gurvich, G V Karachevtsev, V I Kondrat'ev, Yu A Lebedev, V A Medvedev, V A Potapov, Yu S Khodeev, in *Energii Razryva Khimicheskikh Syvazei, Potentsialy Ionizatsii i Srodstvo k Elektronu* (Energies of Rupture of Chemical Bonds, Ionization Potentials and Electron Affinity) (Moscow: Nauka, 1974) p. 69
105. E K Fields, S Meyerson *J. Org. Chem.* **37** 3861 (1972)
106. S Meyerson, I Puskas, E K Fields *J. Am. Chem. Soc.* **88** 4974 (1966)
107. B L Korsunskii, G M Nazin, V R Stepanov, A A Fedotov *Kinet. Katal.* **34** 775 (1993)<sup>b</sup>
108. G M Khrapkovskii, G N Marchenko, A G Shamov, in *Vliyanie Stroeniya Molekul na Kineticheskie Parametry Monomolekulyarnogo Raspada S- i O-nitrosoedinenii* (Influence of Structure of Molecules on Kinetic Parameters of Monomolecular Decay of S- and O-Nitro Compounds) (Kazan: FEN, 1997) p. 139
109. N I Sadova, L V Vil'kov *Usp. Khim.* **51** 153 (1982) [*Russ. Chem. Rev.* **51** 87 (1982)]
110. N I Sadova, L S Khaikin, L V Vil'kov *Usp. Khim.* **61** 2129 (1992) [*Russ. Chem. Rev.* **61** 1169 (1992)]
111. G Fayet, L Joubert, P Rotureau, C Adamo *J. Phys. Chem. A* **112** 4054 (2008)
112. A G Shamov, E V Nikolaeva, D V Chachkov, G M Khrapkovskii *Vest. Kazan. Tekhnol. Univ.* (1) 5 (2009)
113. D N Laikov, Yu A Ustynuk *Izv. Akad. Nauk, Ser. Khim.* 804 (2005)<sup>a</sup>
114. M J Frisch, G W Trucks, H B Schlegel, G E Scuseria, M A Robb, J R Cheeseman, J A Montgomery Jr., T Vreven, K N Kudin, J C Burant, J M Millam, S S Iyengar, J Tomasi, V Barone, B Mennucci, M Cossi, G Scalmani, N Rega, G A Petersson, H Nakatsuji, M Hada, M Ehara, K Toyota, R Fukuda, J Hasegawa, M Ishida, T Nakajima, Y Honda, O Kitao, H Nakai, M Klene, X Li, J E Knox, H P Hratchian, J B Cross, C Adamo, J Jaramillo, R Gomperts, R E Stratmann, O Yazyev, A J Austin, R Cammi, C Pomelli, J W Ochterski, P Y Ayala, K Morokuma, G A Voth, P Salvador, J J Dannenberg, V G Zakrzewski, S Dapprich, A D Daniels, M C Strain, O Farkas, D K Malick, A D Rabuck, K Raghavachari, J B Foresman, J V Ortiz, Q Cui, A G Baboul, S Clifford, J Cioslowski, B B Stefanov, G Liu, A Liashenko, P Piskorz, I Komaromi, R L Martin, D J Fox, T Keith, M A Al-Laham, C Y Peng, A Nanayakkara, M Challacombe, P M W Gill, B Johnson, W Chen, M W Wong, C Gonzalez, J A Pople Gaussian Inc., Pittsburgh, PA, 2003
115. V G Matveev, G M Nazin *Izv. Akad. Nauk, Ser. Khim.* 774 (1975)<sup>a</sup>
116. D V Chachkov, E V Nikolaeva, A G Shamov, G M Khrapkovskii, in *Struktura i Dinamika Molekulyarnykh Sistem (Sb. Statei VIII Vseros. Konf.)*, Ioshkar-Ola, 2001 [Structure and Dynamics of Molecular Systems (Collection of Articles of VIIIth All-Russian Conference), Ioshkar-Ola, 2001] Pt. 2, p. 198
117. G M Khrapkovskii, E A Ermakova, V A Rafeev *Izv. Akad. Nauk, Ser. Khim.* 2118 (1994)<sup>a</sup>
118. M Fang, Z Li, Y Fu *Chin. J. Chem.* **26** 1122 (2008)
119. D V Chachkov, E V Nikolaeva, A G Shamov, G M Khrapkovskii, in *Struktura i Dinamika Molekulyarnykh Sistem (Sb. Statei VIII Vseros. Konf.)*, Ioshkar-Ola, 2001 [Structure and Dynamics of Molecular Systems (Collection of Articles of VIIIth All-Russian Conference), Ioshkar-Ola, 2001] Pt. 2, p. 202
120. A G Shamov, E V Nikolaeva, D V Chachkov, G M Khrapkovskii, in *Proceedings of the 34th International Annual Conference of ICT, Karlsruhe, 2003* p. 137:1
121. G M Khrapkovskii, D V Chachkov, A G Shamov, in *Struktura i Dinamika Molekulyarnykh Sistem (Sb. Statei IX Vseros. Konf.)*, Ufa, 2002 [Structure and Dynamics of Molecular Systems (Collection of Articles of IXth All-Russian Conference), Ufa, 2002] Pt. 2, p. 234
122. J H Beynon, G R Lester, A E Williams *J. Phys. Chem.* **63** 1861 (1959)
123. A G Turner, L P Davis *J. Am. Chem. Soc.* **106** 5447 (1984)
124. T Glenewinkel-Meyer, F F Crim *J. Mol. Struct. (THEOCHEM)* **337** 209 (1995)
125. R Sabbah, M Gouali *Aust. J. Chem.* **47** 1651 (1994)
- <sup>a</sup> — *Russ. Chem. Bull., Int. Ed. (Engl. Transl.)*  
<sup>b</sup> — *Kinet. Catal. (Engl. Transl.)*  
<sup>c</sup> — *Mendeleev Chem. J. (Engl. Transl.)*  
<sup>d</sup> — *Russ. J. Org. Chem. (Engl. Transl.)*  
<sup>e</sup> — *Russ. J. Gen. Chem. (Engl. Transl.)*  
<sup>f</sup> — *Russ. J. Phys. Chem. (Engl. Transl.)*  
<sup>g</sup> — *Dokl. Chem. (Engl. Transl.)*